PhD

PROGRAM IN TRANSLATIONAL AND MOLECULAR MEDICINE

DIMET

UNIVERSITY OF MILANO-BICOCCA
SCHOOL OF MEDICINE AND SCHOOL OF SCIENCE

Identification and characterization of a BPIFB4 functional variant associated with human exceptional longevity

Coordinator: Prof. Andrea Biondi
Tutor: Dr. Silvia Brunelli
Co-Tutor: Dr. Annibale A. Puca

Dr. Francesco VILLA

Matr. No. 038200

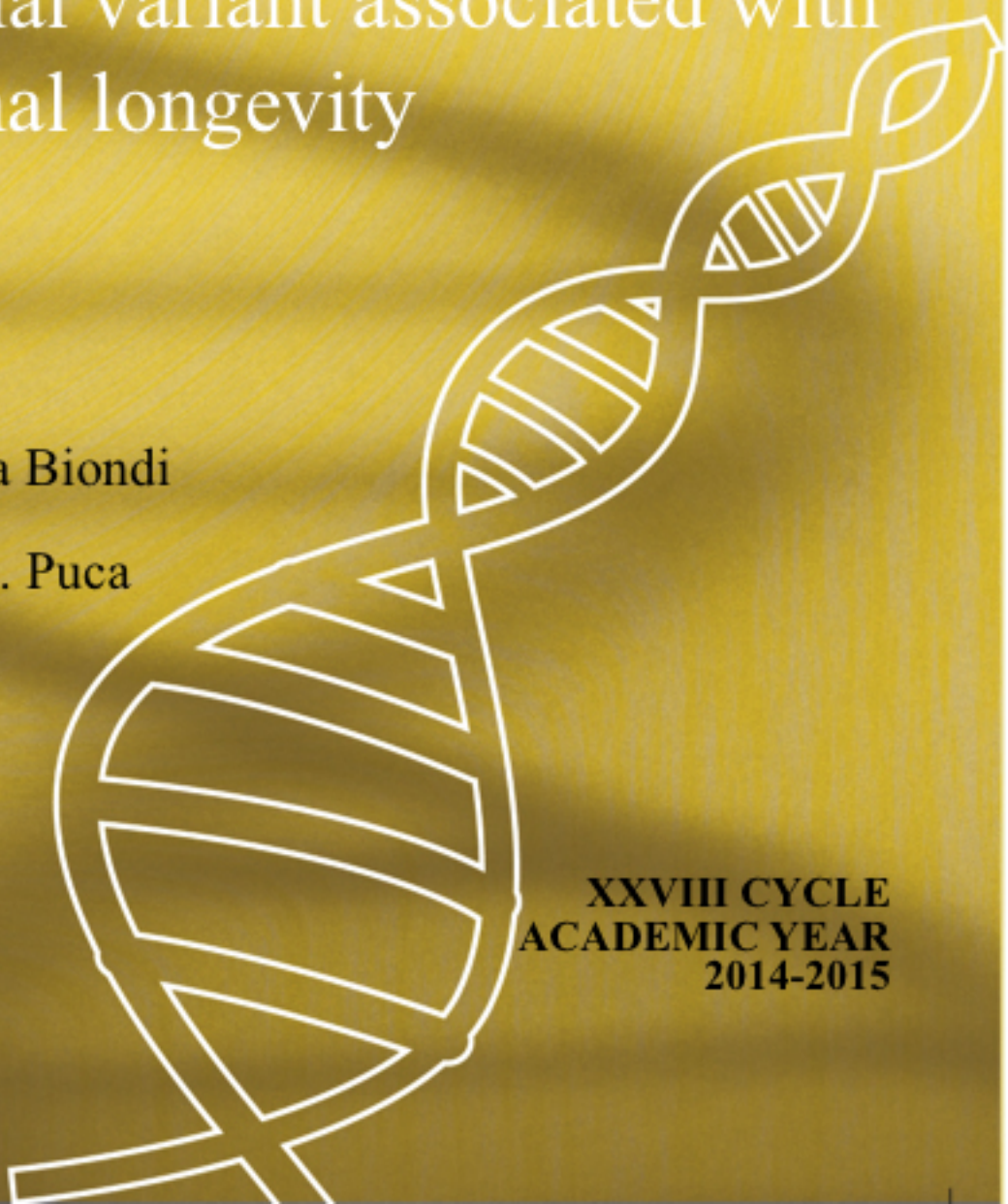

XXVIII CYCLE
ACADEMIC YEAR
2014-2015

Table of contents

Chapter 1. General Introduction

1.1 Definition of aging

Aging is a complex process ruled by stimuli of different nature and belonging to several field of life. Stochastic events contribute to this process by producing casual damages to essential molecules, the external environment interfere through the life style (diet and/or caloric restriction), while the genetic asset provides a background of intrinsic alterations that are protective or detrimental for the onset of aging related pathologies. The attention on this latter point increased in the last years, promoting the search for genetic variations connected with protective features against typical age-related disease like hypertension, diabetes and cancer.

Therefore, longevity is defined as that phenotype of long-living subjects that approach old age under the effects of these several factors.

1.2 The longevity phenotype

The Birth Cohort Study found that in the United State at the beginning of twentieth century life expectancy was 51.5 years for males and 58.3 years for females; currently 1 person each 10,000 reach 100 years of age, and this prevalence is quickly changing and will probably soon approach 1 person each 5,000.[1] It was estimated that the increased ability to reach 100 years old in industrialized countries over the last 160 years reflects a rise in life expectancy — quantified as 3 months

per year for females — subsequent to improvements in diet and a reduced exposure to infection and inflammation.[2] The improvement of healthy care and the attention to a balanced and quality food intake speedup the process towards a diffused longevity. In favor of diet as a modulator of longevity, the Elderly Prospective Cohort Study (EPIC) identified a reduced overall mortality among the elderly consuming a modified Mediterranean diet in which saturated fatty acids were substituted for monounsaturated ones.[3]

Centenarians, despite being exposed to the same environmental conditions as members of the average population, manage to live much longer. Long-living individuals (LLIs), i.e. those that approach 100 years of age, are a model of successful aging: most of them have a compression of disability and morbidity towards the end of their life and tend not to show changes normally observed during aging, such as a decrease in insulin sensitivity and in heart rate variability (HRV).[4-6] The exceptional longevity of LLIs is to some extent genetically driven, as underlined by the familial clustering effect for extreme longevity and the reduced mortality of centenarians' siblings compared to those of non-centenarians. Under a genetic point of view, the compression in morbidity and mortality is correlated with the enrichment of protective alleles and the depletion of detrimental ones. It has been estimated that genetic variants account for at least 25% of human life-span, and for even a larger proportion in individuals living to extreme age.[7, 8]

Ultimately, aging is an independent risk factor associated with endothelial dysfunction, impaired angiogenesis and loss of protein homeostasis, or proteostasis, the decline of which is contrasted by

adaptive cellular responses.[9] The mechanisms that help cells adapt and survive under stressful conditions include the activation of heat shock factor protein 1 (HSF1)-controlled heat shock proteins (HSPs), ribosomal biogenesis and protein synthesis, and are at least in part orchestrated by growth factors, as observed in *Caenorhabditis elegans*, in which HSF-1 is under the control of insulin/IGF-1-like signaling (IIS).[10]

1.3 Genome-Wide Association Studies

In our studies on longevity phenotype, we follow the genetic trait by trying to characterize the functional aspects of the genetic background that make a person a centenarian. Genome Wide Association Studies (GWASs), that analyze the differences in the frequencies of presence of common genetic variants in two population - cases and controls - generate findings that need to be replicated in independent populations. In the case of exceptional longevity, success in replicating initial findings is negatively influenced by the differences in participant ages, gender and disease status distribution across the analyzed populations. Furthermore, the GWAS approach suffers from the multiple-testing statistical penalty that forces the adoption of very low p-values of significance, hence favouring the phenomenon of the winning course, i.e. the enrichment of false-positive associations among the dozens of top findings.[11] Other potential problems that generate false positive and false negative results include the low power of studies using small sample sizes, and a lack of a suitable control for the genetic admixture. On the first point, an extremely instructive review has been written by Altshuler, Daly and Lender,

who calculate the power of a study based on the number of individuals genotyped, the number of tested hypotheses, and the frequency of the allele tested for a specific OR.[12] From the graph given in their review (**Figure 1.1**), it is clear that for the OR expected in human exceptional longevity (between 1.2 and 2), the power of a study is highly dependent upon the number of hypotheses tested.

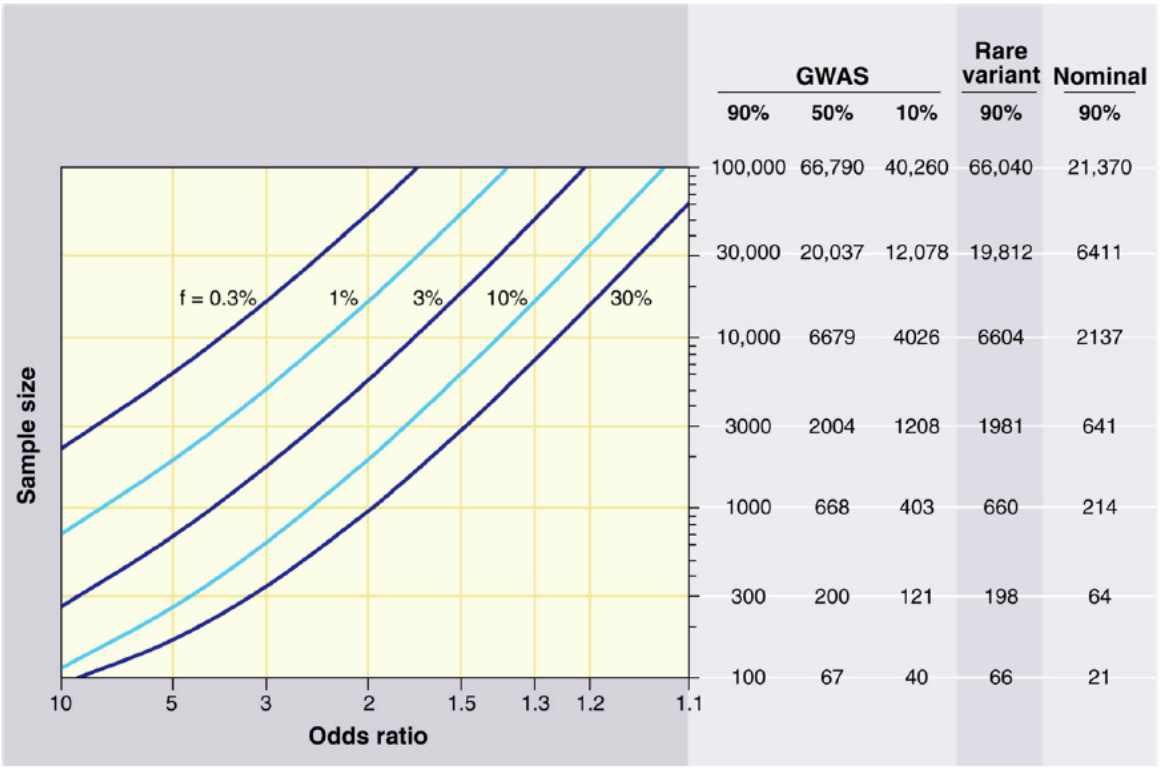

GWAS			Rare variant	Nominal
90%	50%	10%	90%	90%
100,000	66,790	40,260	66,040	21,370
30,000	20,037	12,078	19,812	6411
10,000	6679	4026	6604	2137
3000	2004	1208	1981	641
1000	668	403	660	214
300	200	121	198	64
100	67	40	66	21

Figure 1.1 Sample sizes required for genetic association studies.
The graph shows the total number N of samples (consisting of N/2 cases and N/2 controls) required to map a genetic variant as a function of the increased risk due to the disease-causing allele (x axis) and the frequency of the disease-causing allele (various curves). The required sample size is shown in the table on the right for various different kinds of association studies.[12] Reproduced with permission from The American Association for the Advancement of Science.

For these reasons, recent GWASs have failed to find variants that cross-validate across populations — with the exception of few cases — pointing to the need of much larger studies or alternative study designs in order to discover common polymorphisms with smaller genetic effects and rare variants with high penetrance that influence exceptional longevity.[13, 14] Thus, a GWAS on exceptional longevity can be considered only a hypothesis-generating effort to be used in conjunction with other studies.

To date, the most remarkable genetic findings for exceptional longevity observed in the genome of centenarians are the decreased frequency of detrimental alleles of apolipoprotein E (*APOE*) and the increase of protective alleles of forkhead box O3A (*FOXO3A)*.[15-20] Recently, we found associated with longevity three more variants in *CAMKIV*, *ATXN1* and *DCAMKL1* (**Table 1.1**).[21]

APOE is involved in lipid transport to the lymph system and was the first gene to be successfully replicated as a gene important in exceptional longevity.[22] FOXO3A mediates a pro-survival activity by regulating the cellular response to stimuli ranging from radical stress to growth factors [Insulin growth factor 1 (IGF1)], and by acting on the transcription of genes involved in radical stress response, cell cycle arrest, proliferation, and apoptosis.[23, 24] Protein Kinase B (AKT)-dependent phosphorylation and sirtuin 1 (SIRT1)-dependent deacetylation of FOXO3A induce pro-survival activity by activating genes linked to the stress response and cell cycle arrest and by inhibiting pro-apoptotic genes.[25] In humans, genetic alterations of the IGF1 receptor that alter the IGF signaling pathway confer an

increase in propensity for longevity.[26] *AKT* polymorphisms have also been associated with human longevity.[20]

Table 1.1 Genes and variants found correlated with longevity in humans

Gene	Variant	Occurrence in centenarians	Previous disease correlations	Potential role in longevity
APOE	ε4	reduced	Alzheimer's and cardiovascular diseases	Maintenance of vascular integrity
FOXO3A	rs2802292*	more present	none	Control of cell homeostasis
CAMK4	rs10491334†	more present	hypertension	Modulation of CREB, SIRT and FOXO3A
ATXN1	rs697739	more present	amyotrophic lateral sclerosis (age of onset)	Modulation of CREB
DCAMKL1	rs9315385	more present	heart rate variability	Modulation of CREB

**, result obtained by a candidate gene approach and replicated in other studies; †, result obtained from a GWAS and confirmed in a replication cohort.*

For the above reasons, in our recently published GWAS on individuals enrolled in the Southern Italian Centenarian Study (SICS), we identified CAMK4 rs10491334, a variant that had been already established among the top 5 SNPs in the Framingham Heart Study on diastolic high blood pressure.[27] The fact that CAMK4 rs10491334 associates also with hypertension is reassuring in that hypertension and longevity are regulated by common pathways. In fact, mice with genetic ablation of the angiotensin II type1 receptor — the key regulator of blood pressure — had increased expression of the longevity gene Sirt3 and improved survival.[28]

Interestingly, rs10491334 correlated with CAMK4 protein expression, and functional studies revealed the ability of CAMK4 protein to modulate SIRT1 and FOXO3A (**Figure 1.2**).

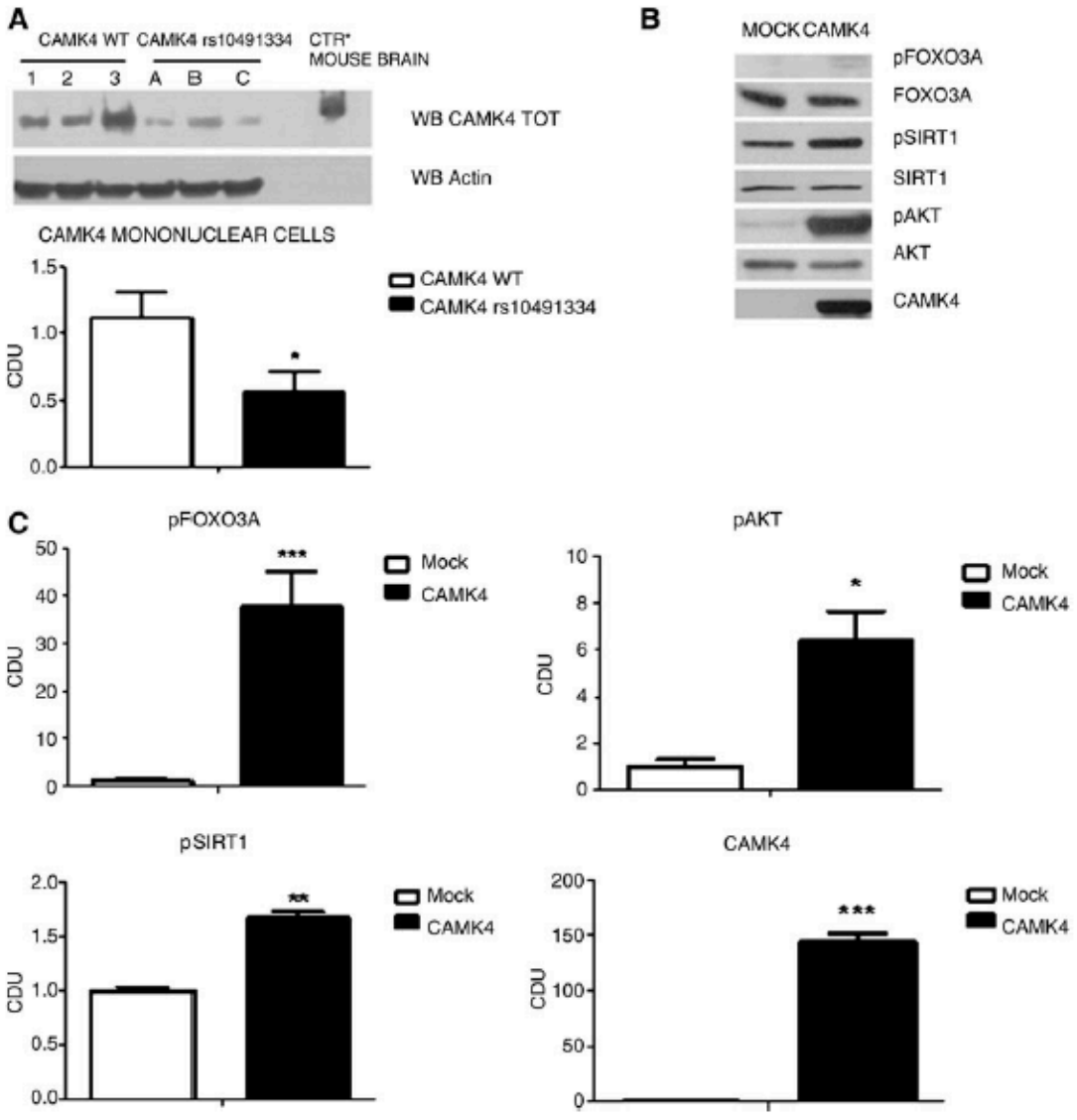

Figure 1.2 Western blot analysis of calcium/calmodulin-dependent protein kinase IV (CAMKIV).
(A) Western blot analysis of CAMKIV revealing higher CAMKIV levels in mononuclear cells of subjects expressing wild-type CAMKIV

(CAMKIV WT) compared to subjects homozygous for the CAMKIV minor allele (CAMKIV rs10491334). CAMKIV levels were normalized to actin (corrected densitometry units, CDU; n=10). (B and C) Western blot analyses of HT29 cells expressing CAMKIV revealing a significant increase of phosphorylated FOXO3A, AKT, and SIRT1 compared with cells infected with empty vector (MOCK). Data from immunoblots were quantified by densitometric analysis. Statistics were performed with analysis of variance (ANOVA). (*) p<0.05; (**) p<0.005; (***) p<0.0005.

The ataxin-1 (ATXN1) rs697739 allele was another variant found among the top findings of our GWAS on SICS individuals. This polymorphism had been previously associated with the age of onset of sporadic amyotrophic lateral sclerosis, a disease of unknown cause characterized by slowly progressive degeneration of motor neurons and that usually occurs in patients aged 40–60 years.[29] ATXN1 is the gene responsible for spinocerebellar ataxia type 1 andantagonizes the neuronal survival function of myocyte enhancer factor-2 (MEF2).[30] MEF2 transcription repression by cabin1-HDAC4 is removed by CAMKIV activation, and this suggests that MEF2 is a common downstream target of CAMKIV and ATXN1.[31, 32]

In addition to CAMKIV rs10491334 and ATXN1 rs697739, the rs9315385 allele of doublecortin and Ca^{2+}/calmodulin-dependent kinase-like-1 (DCAMKL1) was a third top finding of our study. DCAMKL1 has structural similarity with CAMKIV, but despite this, it represses CAMKIV-induced activation of cAMP response element-binding (CREB) protein via phosphorylation of transducer of regulated CREB activity 2 (TORC2) at Ser171.[33] DCAMKL1 rs9315385 was previously associated with total power of HRV[34]. A

reduced HRV is a marker of autonomic dysfunction and is associated with an increased risk of cardiovascular morbidity and mortality.[35] HRV-parasympathetic function decreases up to the eighth decade of life, followed by an increase to higher levels — similar to those found in a younger population — in nonagenarians and centenarians[6]. Similarly to CAMKIV, DCAMKL1 and ATXN1 are expressed mainly in brain. These data support the importance of the CAMKIV/CREB pathway in regulating the aging process.

A brief mention needs to be made here on the cutting edge, genetic signature paper by Sebastiani et al. that very elegantly proved that a complex analysis on 281 SNPs allowed to define clusters of individuals that aged differently based on their genetic signature.[36]

The identification and the study of genetic variants that influence exceptional longevity in humans are important, since novel targets for prevention and therapy of a large spectrum of age-related diseases could be discovered.[37] Genome-wide association studies (GWAS) are hypothesis-generating studies that can be used to this end.

1.4 Aging process theories

1.4.1 Free radicals theory

One of the theory that tempts to explain the aging process is the free radicals theory. Responsible for oxidative stress, free radicals are defined as atoms or molecules that contain one or more unpaired electrons. Biological systems depend on these kind of molecules: the most important are the reactive oxygen species (ROS) superoxide anion radical ($O_2^{\cdot-}$), hydrogen peroxide (H_2O_2), alkoxyl ($RO^{\cdot}$), peroxyl ($ROO^{\cdot}$) and hydroxyl ($^{\cdot}OH$) radicals, and hypochlorous acid

(HOCl).[38] In 1956 Denham Harman proposed the "free-radical theory of aging" (FRTA)[39] that postulated that accumulation of free radicals was the prime cause of the sequential alterations characterizing advancing age and the progressive increase in disease and death rates.[40] This hypothesis was based on the "rate of living" theory formulated by Raymond Pearl explaining longevity variation within species in terms of combined mass-specific resting metabolic rate and the "lifetime energy potential": it held that the pace of life is inversely related to the length of life.[41]

In the oxygen managing system of the cell, mitochondria play an important role and physiological or pathological dysfunctions of them are associated with aging or age-related diseases.[42] The aging process, indeed, is associated with the improvement of the mitochondrial production of ROS, specially in heart and in the vasculature system. In the heart, the last evidences are cardiac hypertrophy, fibrosis and apoptosis. In the vasculature system the mitochondrial oxidative stress and the presence of ROS contribute to the development of chronic low-grade vascular inflammation in aging[43] by activating redox signaling pathways. In addition, the ROS activation of Akt pathway increases the development of the senescent phenotype in endothelial cells characterized by an impairment in the ability of regeneration and angiogenesis, and a general reduction in vascular reactivity and increasing in atherosclerosis events due to less cytokines vessel production.[44]

A proved way to overcome to the rapid aging of mitochondria and consequently of cardiovascular system, is exercise. It's clear that the physical activity brings to a stress–induced NO production able to

restore vascular activity and endothelial cells protein homeostasis.[45] A similar effect is achieved by a caloric restriction lifestyle or by the administration of caloric restriction mimetics, in which the energy sensor AMPK upregulates SIRT activity restoring the vessels activity.

1.4.2 Lipid metabolism and aging

In apparent contrast with the FRTA is the finding that the cell membranes of offspring of nonagenarians have an accumulated amount of endogenous *trans* fatty acids.[46] The peroxidation index of erythrocyte membrane lipids was significantly lower in nonagenarians' offspring than in a group of matched controls.[46] It is of particular interest that we found significantly increased levels of palmitoleic acid (C16:1n-7) in the nonagenarians' offspring, similarly to what was later observed in genetically modified long-living worms.[47] Because these worms were genetically modified in homologue genes of the insulin-like growth factor 1 (IGF1)/forkhead box O3 (FOXO3A) axis, a possible explanation for this finding is that IGF-1 signalling modulates, or is modulated by, the membrane fatty-acid composition.[48] Moreover, it was reported that after chronic thermal or saline stress of yeast, the induced increase in the level of membrane palmitoleic acid was responsible for a reset of heat shock protein (Hsp) release to higher levels.[49] Thus, the high C16:1n-7 detected in the offspring of nonagenarians could be correlated to the low serum level of Hsp70 detected in centenarians' offspring.[50] Endogenous *trans* fatty acids are an index of endogenous free-radical cellular stress and are produced by endothelial nitric oxide synthase (eNOS)-generated nitrates ($NO_2^{\cdot}$), as shown by the lack of *trans*-

arachidonic acids in the retinas of $eNOS^{-/-}$ mice.[51] Moreover, calorie restriction, which is known to increase longevity, induces the expression of eNOS, the activation of telomerase and the biogenesis of mitochondria. Thus, the increase in ROS observed with calorie restriction suggest a role for free-radical stress: the induction of endogenous defense mechanisms, maybe through *trans* fatty acids participation, that culminate in increased resistance to stress and longevity. This adaptive response was named hormesis.[52] From this point of view, the FRTA formulated by Harman doesn't appear consistent and these findings, taken together, suggest that ROS can act as essential signaling molecules for the promotion of metabolic health and longevity.

The degree of oxidative stress could possibly explain this apparent paradox: a low stress situation results protective for organism, while massive stress becomes deleterious. In support of this hypothesis, deletion in worms of mitochondrial proteins, such as ISP-1 and NUO-6, induces the oxidative stress necessary and sufficient for promoting longevity: in fact, this effect is abolished by antioxidants and is induced by mild treatment with oxidants (**Figure 1.3**).[53]

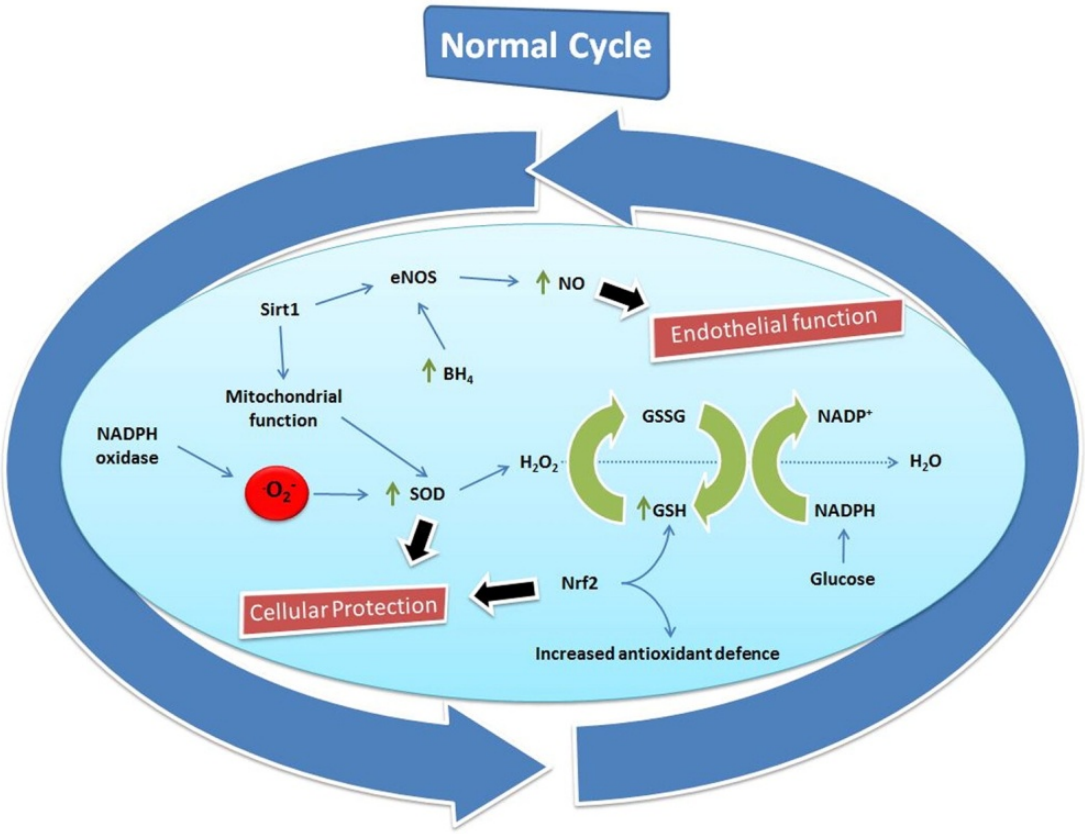

Figure 1.3 Schematic of vascular physiological function

1.5 Nitric Oxide and its prevalent role in the vascular system

The beneficial effects of calorie restriction are multiple: it reduces the incidence of tumors and diabetes and the age-related decline in T-lymphocyte proliferation.[54] The effects of calorie restriction can be explained by increased IGF1-insulin signal (IIS) efficiency: in fact, findings on patients with growth hormone receptor deficiency suggest that their high insulin sensitivity could account for the absence of diabetes and very low incidence of cancer seen in these individuals.[55]

Furthermore, calorie restriction can be mimicked by genetic manipulation aimed at blocking IIS (i.e., the IGF1/PI3K/AKT/FOXO3A axis): for example, the FIRKO mouse − a carrier of a fat-specific insulin receptor knockout − and *C. elegans* models carrying null mutations of daf-2 − an IGF1 homologue − and age-1 − a homologue of the catalytic subunit of mammalian PI3K− all live longer than wild-type animals.[56, 57] To be noted, the beneficial effects of daf-2 and age-1 null mutations are antagonized by null mutation of daf-16, which encoder three members of the FOXO family of transcription factors.[57] Thus, via AKT the IIS is important for controlling eNOS and, hence, human longevity.[58]

Exercise is inversely correlated with total mortality.[59] An elegant report on athletes undergoing marathon training identified a combination of metabolites (i.e., glycerol, niacinamide, glucose-6-phosphate, pantothenate and succinate) that increased in the plasma in response to exercise; in vitro, these metabolites were able to up-regulate the expression of NUR77, a transcriptional regulator of glucose utilization and lipid metabolism genes.[60] NUR77 is under the control of Ca^{2+}/calmodulin-dependent protein kinase (CAMKIV), which is activated by AMPK and has been associated with human exceptional longevity.[21, 32] Furthermore, AMPK controls eNOS phosphorylation, which explains the potentiation of eNOS activity by both calorie restriction and physical exercise.[58] AMPK is activated acutely at exercise intensities above ≈ 60% of maximal aerobic capacity.[61] Calorie restriction and exercise both activate mitochondrial biogenesis through activation of AMPK with an eNOS-dependent mechanism, as shown by experiments on eNOS knockout

mice.[62] Thus, the beneficial effects on longevity of calorie restriction, genetic makeup and exercise can be explained, at least in part, through eNOS-dependent activation of mitochondrial biogenesis.

During the aging process, oxidative stress increases in the arterial system either of humans and experimental models.[63] This phenomenon has been linked directly to the development of atherosclerotic vascular diseases (**Figure 1.4**).

We think that the state of the vascular system is the most important factor in determining health during aging. In fact, vascular system is responsible for the transport of oxygen and nutrients throughout the body and, therefore, is responsible of when and how the organs and systems could encounter suffering and ultimately fail. In the end, oxidative-stress-induced endothelial dysfunction is probably the key mechanism linking older age to increased risk of clinical cardiovascular disease and death.[64]

Free radicals play a physiological role in the vessel wall as well: they participate as second messengers in endothelium-dependent functions, in smooth muscle cell and endothelial cell growth and survival, and in remodeling of the vessel wall.[65] When these processes are out of control, they contribute to vascular alterations characterized by mitochondrial dysfunction and increased ROS production,[66] and lead, ultimately, to the development of cardiovascular pathologies, such as hypertension, stroke and coronary artery disease.[67, 68]

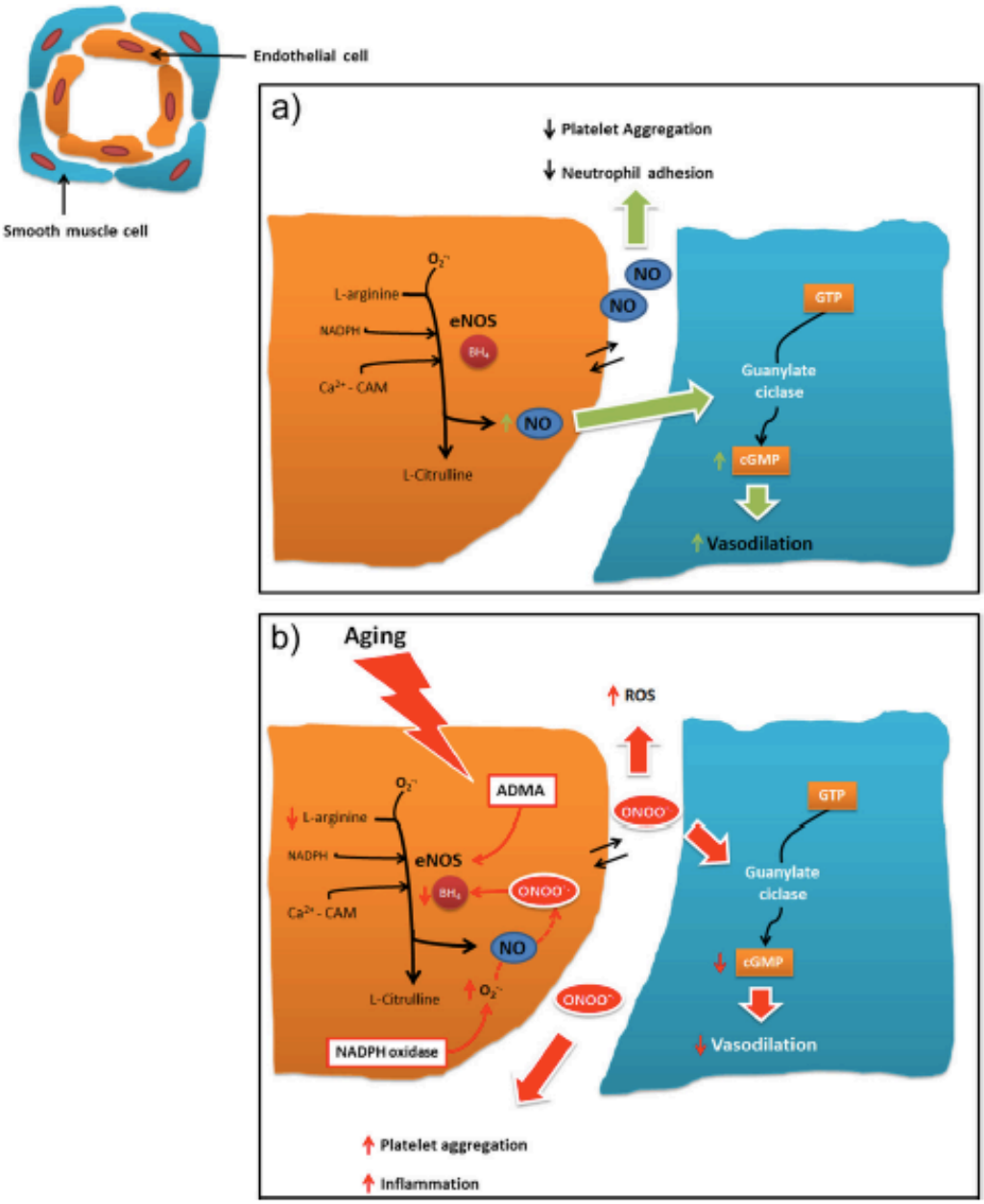

Figure 1.4 a) Representative nitric oxide pathway. b) Effects of aging on nitric oxide pathway.
BH4 = tetrahydrobiopterin; cGMP = cyclic guanosine monophosphate; GTP = guanosine triphosphate; NADPH = nicotinamide adenine dinucleotide phosphate; ONOO- = Peroxynitrite; ADMA = Dimethylarginine.

One of the most important mediators in the cardiovascular system is nitric oxide (NO). During aging, increased oxidative stress leads to a progressive decrease in NO production. In particular, this is caused by eNOS uncoupling − a phenomenon that promotes the formation of superoxide rather than NO − and decreased expression of the essential eNOS cofactor tetrahydrobiopterin (BH4).[69] In fact, superoxide produced mainly by NADPH oxidase may react with NO to produce peroxynitrite that, promoting eNOS uncoupling, contribute to the increase of superoxide and to the reduction of NO that may cause an acceleration of the atherosclerotic process.[70] Thus, abnormalities in eNOS signalling underlie endothelial dysfunction, a common finding in aging.

Several studies emphasize the importance of mitochondrial oxidative stress, which represents a typical characteristic of endothelial dysfunction that develops during aging and it is associated with the over-activation of an important enzyme, which is localized both in the cytoplasm that in membrane, namely NADPH oxidase.[71, 72]

Deshpande et al. demonstrated that Rac1 − a regulatory component of plasma membrane NAD(P)H oxidases − plays an important role in premature aging of the endothelium and in the development of associated vascular pathologies.[73, 74] In addition, other molecular mechanisms responsible for age-related mitochondrial oxidative stress in the vasculature involve dysregulation of antioxidant defences, such as peroxynitrite-mediated Nrf2/ARE (antioxidant response elements) dysfunction , nitration and inhibition of manganese superoxide dismutase (MnSOD), declines in glutathione (GSH) content and a dysfunctional electron transport chain.[63]

Nrf2 is a redox-sensitive transcription factor that upregulates the expression of numerous ARE genes that encode proteins that detoxify ROS and mediate the anti-aging effects of calorie restriction.[75] Recent findings demonstrate that Nrf2 dysfunction in the vasculature is associated with aging and contributes to the age-related dysregulation of GSH synthesis in various tissues.

Van der Loo et al. provided evidence for association between the formation of peroxynitrite and age-associated vascular dysfunction by demonstrating selective nitration of MnSOD − the major antioxidant enzyme in the mitochondria of all mammals − with increased age.[76] This finding was supported by a recent report showing that genetic inactivation of MnSOD in mutant mice resulted in premature death and that treatment with a SOD mimic dramatically prolonged survival .

Moreover, the activities of various electron transport chain oxido-reductases are deleteriously affected during aging. The mitochondria generate ATP from nutrients, and its synthesis via the mitochondrial respiratory chain is the result of a proton potential generated by the electron transport chain. Damage to this latter can cause breakdown of the proton potential, apoptosis and the generation of free radicals in a vicious cycle.[77]

According to the FRTA, ROS are the major candidates responsible for senescence and age-related diseases in which the redox balance is disturbed and generates oxidative stress. Indeed, senescence of endothelial cells has been proposed to be responsible for endothelial dysfunction and atherogenesis during aging. In fact, vascular cells

exhibiting the morphological features of cellular senescence have been found in atherosclerotic lesions.[78]

Relatively recent studies have demonstrated that inhibition of Sirt1 induces premature senescence and that Sirt1 overexpression reverts premature senescence induced by hydrogen peroxide . In macrophages in vitro and in rats in vivo, Sirt1 inhibits NF-kB and so hinders pro-inflammatory mediator release, protecting from the development of oxidative stress.[79]

Finally, there are several findings that relate telomere shortening to aging in vivo. Telomeres are regions of DNA, characterized by G-rich sequences located at the ends of linear chromosomes that can form four-stranded structures: they are considered a biological clock that measures mitotic time and determines the senescence of cell replication. There appears to be a correlation between telomere length, age and oxidative stress in human arteries at sites of elevated hemodynamic stress and, presumably, with a high cell turnover. Data suggest that G-rich strands are more vulnerable to oxidative damage and that faster telomere shortening rates are observed in cell strains that also have higher peroxide levels. Thus, telomere loss is clearly implicated in oxidative damage, accumulation of senescent cells in elderly individuals and reduction in lifespan[80] (**Figure 1.5**).

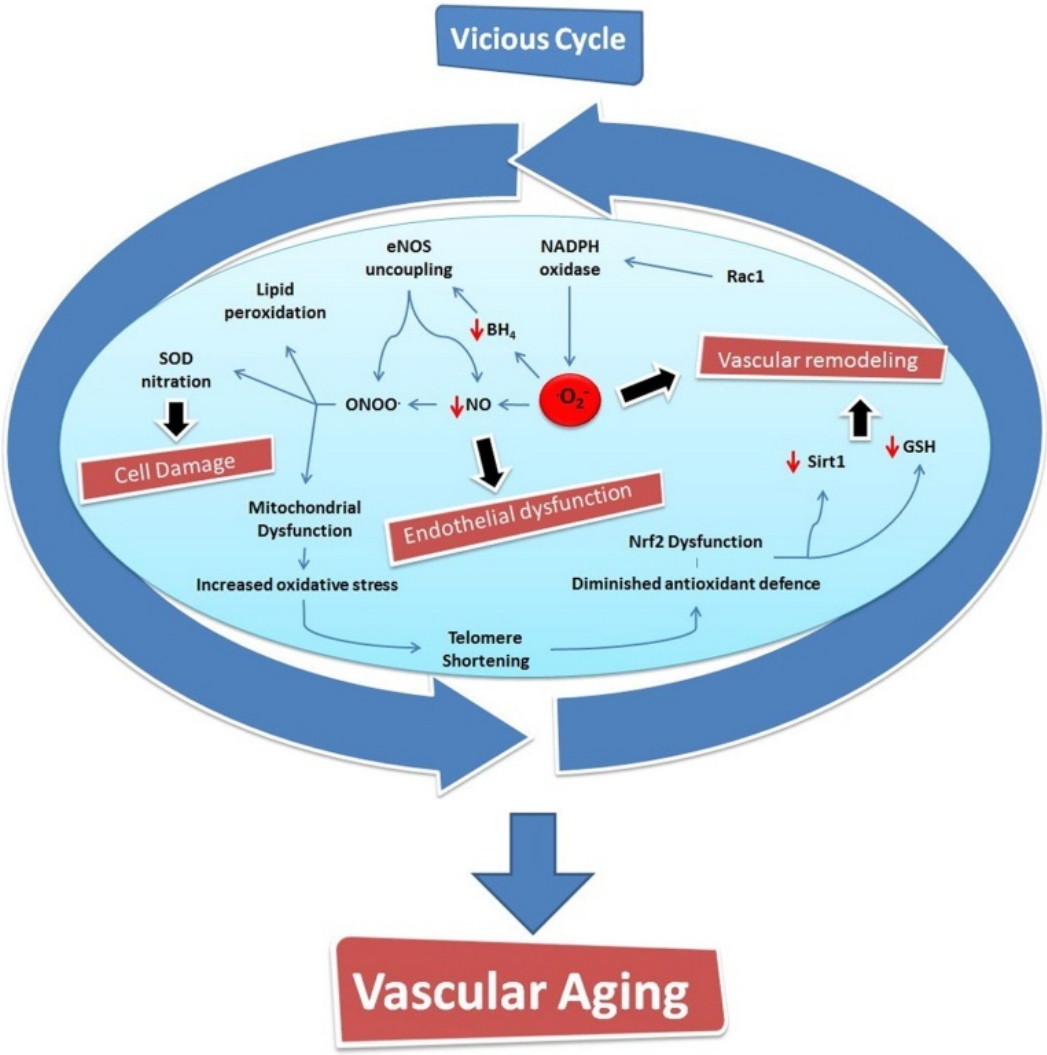

Figure 1.5 Schematic of the involvement of free radicals in vascular ageing.

1.6 Longevity populations

We recruited and genotyped 582 LLIs (age range 90-109 years) and 784 young control individuals (age range 18-45 years) as part of the Southern Italian Centenarian study (SICS). SICS LLIs were thoroughly investigated for demographic characteristics, medical history (past and present diseases), level of independence (Barthel Score),[81] and cognitive status (Cognitive Score) (**Table 1.2**).

Table 1.2 Characteristics of SICS screening-set (N=410) and SICS replication-set LLIs (N=116)

	SICS LLIs - Screening (N=410)						SICS LLIs - Replication (N=116)					
Variable/Disease	**N**	**%**	**Mean**	**SD**	**Min**	**Max**	**N**	**%**	**Mean**	**SD**	**Min**	**Max**
Demographics												
Gender (Males)	240	58.82					54	46.96				
Age			96.62	3.64	90	109			96.14	3.52	90	109
Patient's History												
Deceased, Age at Death	313	76.72	96.95	3.59	90	109	87	75.65	96.08	3.32	90	109
Smoking History	97	23.77					30	26.09				
Diabetes Mellitus	36	8.82	79.74	11.69	54	94	19	16.52	73.18	12.12	50	91
Overweight (BMI >25) [a]	74	25.00					23	24.73				
Osteoporosis	34	8.33	74.92	12.96	50	91	8	6.96	77.25	15.39	55	90
Heart Attack	32	7.84	83.07	11.39	50	97	11	9.57	81.73	10.55	60	93
Cardiac Arrythmia	81	19.85	86.09	9.51	50	102	21	18.26	80.35	16.8	20	96
Angina	7	1.72	76.4	12.03	60	92	1	0.87	80	NA	80	80
Congestive Heart	17	4.17	81.77	10.25	70	97	6	5.22	86	7.21	77	95
High Blood Pressure	124	30.39	79.47	11.27	38	104	57	49.57	74.31	14.58	20	96
Stroke	38	9.31	87.35	7.32	70	98	13	11.3	85.69	7.49	69	93
Kidney Disease	18	4.41	81.06	16.42	27	93	3	2.61	93.33	4.16	90	98
PVD Circulatory Problems	34	8.33	85.97	7.07	70	100	12	10.43	80.75	14.85	40	96
Cataracts	148	36.27	84.01	9.36	40	100	46	40	84.3	8.03	65	98
Glaucoma	13	3.19	86.11	8.33	66	93	6	5.22	94	NA	94	94
Macular Degeneration	10	2.45	85	7.78	77	93	9	7.83	78.33	3.51	75	82
Thyroid Condition	5	1.23	55.6	15.44	31	68	3	2.61	75.5	20.51	61	90

	SICS LLIs - Screening (N=410)						SICS LLIs - Replication (N=116)					
Variable/Disease	**N**	**%**	**Mean**	**SD**	**Min**	**Max**	**N**	**%**	**Mean**	**SD**	**Min**	**Max**
Emphysema/Bronchitis	89	21.81	74.92	15.81	35	102	26	22.61	76.21	14.81	50	94
Other Illnesses	34	8.33	75.5	25.54	10	103	10	8.7	67.29	29.49	15	90
Cancer	27	6.62	80.88	13.25	48	95	5	4.35	80.2	4.21	73	83
Parkinson's Disease	13	3.19	85.08	8.24	65	95	4	3.48	79.67	1.53	78	81
Dementia	15	3.68	86	5.66	78	94	2	1.74	90	NA	90	90
Depression	15	3.68	85.23	3.35	80	90	1	0.87	94	NA	94	94
Anxiety	13	3.19	85.82	11.92	60	98	3	2.61	81.33	14.01	70	97
Independence and Cognitive Score												
Barthel Score [c]			65.93	37.66	0	100			69.52	37.14	0	100
Cognitive Score [c]			28.85	10.33	0	34			27.65	11.79	0	34

Abbreviations: Variable/Disease, analyzed variable/disease; N = number of LLIs affected/carrying the disease/trait; %, percentage of LLIs carrying the disease/trait; Mean, SD, Min, Max: mean, standard deviation, minimum, maximum of the age at onset for each disease.
[a] Overweight condition: Body Mass Index (BMI) > 25. BMI has been calculated as Weight (kg) / (height (m) x height (m))
[b] Peripheral Vascular Disease Circulatory Problems
[c] Mean, standard deviation, minimum, maximum of the Barthel and Cognitive Scores distribution are reported instead of mean, standard deviation, minimum, maximum of the age at onset.

The control populations were constituted by a German and a US cohort. The German sample comprised 1,628 LLIs (age range, 95–110 years; mean age, 98.8 years) and 1,104 younger controls (age range, 60–75 years old; mean age, 66.8 years), and was first described by Nebel et al.[14] The study protocol was approved by the Ethics Committee of University Hospital Schleswig–Holstein (Campus Kiel), Germany, and local data protection authorities. The US-American study sample consisted of 1,461 LLIs with an age range of 91–119 years (mean age, 100.8 years) and 526 controls with an age range of 0–35 years (mean age, 28.2 years); these individuals were recruited by

Elixir Pharmaceuticals, either directly or through the New England Centenarian Study.[82, 83] The study protocol was approved by the Boston Medical Center's Institutional Review Board and by the Western Institutional Review Board.

1.7 Genotype determination and statistical data interpretation

Genotyping was carried out using the Illumina BeadChip 317K. All genotypes were evaluated using a quantitative quality score called GenCall, that assigns a score values from 0 to 1 and reflects the proximity within a cluster plot of the intensities of that genotype to the centroid of the nearest cluster. Samples and SNPs showing Call Rate lower than respectively 93% and 95 % as well as SNPs deviating from Hardy Weinberg Equilibrium (HWE) ($p < 1.72\text{x}10^{-7}$) or with Minor Allele Frequency (MAF) lower than 0.05 were removed. Principal Component Analysis (PCA) has been applied on a reduced set of autosomal markers showing r^2 estimates < 0.2, using the default outliers removal threshold (sigma=6) as implemented in Eigenstrat.[84] We looked for evidence of genetic population stratification on a subset of 454 LLIs and 591 young controls by applying PCA: a graphical inspection of the first two principal components revealed genetic homogeneity between LLIs and controls (**Figure 1.3**).

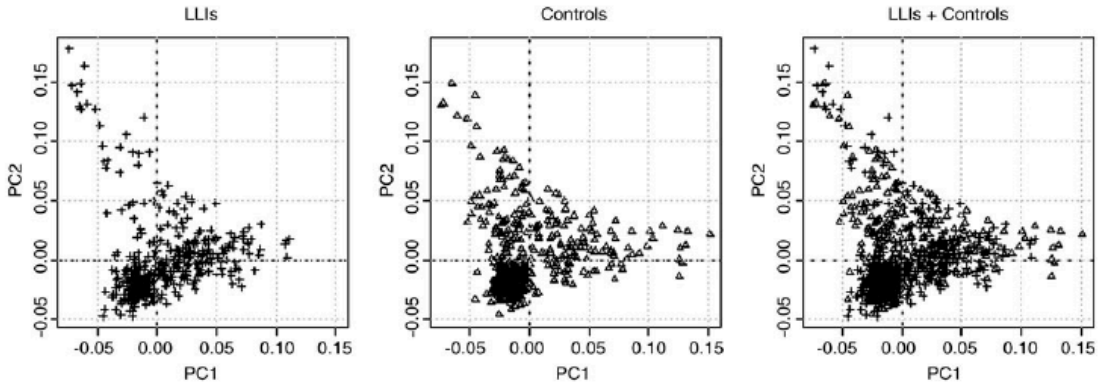

Figure 1.3 Population structure

Population structure of long-living individuals (LLIs) (+) and control subjects (Δ). Each scatter plot shows the first two principal components that were estimated using genotype data for Southern Italian Centenarian Study (SICS) LLIs and control subjects using the EigenSoft program. The two populations are ethnically identical, as shown in the right scatter plot.

1.8 Scope of the thesis

The scope of this work is the disclosure of molecular mechanisms that regulate aging process. In particular, the mechanisms involved in BPIFB4 pathway that we found mutated in three centenarians populations.

The introduction chapter speaks about the centenarian situation in the world and the evolution of this phenotype. It explains the players involved in the aging mechanisms, with a particular focus on the genetic background and its importance on the molecular pathways of free radicals and lipid metabolism. Finally, the chapter shows an overview on the study design adopted for this kind of research and the results obtained in this field.

The results chapter is constituted by the main publication of my doctoral project: "Genetic Analysis Reveals a Longevity-Associated Protein Modulating Endothelial Function and Angiogenesis" published on Circulation Research.

Finally, the discussion chapter shows the possibilities for antiaging treatments with the intent of delay or escape by the age associated diseases and achieve a healthier aging.

References

1. Perls TT. The different paths to 100. Am J Clin Nutr. 2006;83(2):484S-7S. doi:83/2/484S [pii].

2. Oeppen J, Vaupel JW. Demography. Broken limits to life expectancy. Science. 2002;296(5570):1029-31. doi:10.1126/science.1069675 296/5570/1029 [pii].

3. Trichopoulou A, Orfanos P, Norat T, Bueno-de-Mesquita B, Ocke MC, Peeters PH et al. Modified Mediterranean diet and survival: EPIC-elderly prospective cohort study. BMJ. 2005;330(7498):991. doi:bmj.38415.644155.8F [pii] 10.1136/bmj.38415.644155.8F.

4. Terry DF, Sebastiani P, Andersen SL, Perls TT. Disentangling the roles of disability and morbidity in survival to exceptional old age. Arch Intern Med. 2008;168(3):277-83. doi:168/3/277 [pii] 10.1001/archinternmed.2007.75.

5. Paolisso G, Gambardella A, Ammendola S, D'Amore A, Balbi V, Varricchio M et al. Glucose tolerance and insulin action in healty centenarians. Am J Physiol. 1996;270(5 Pt 1):E890-4.

6. Zulfiqar U, Jurivich DA, Gao W, Singer DH. Relation of high heart rate variability to healthy longevity. Am J Cardiol.105(8):1181-5. doi:S0002-9149(09)02852-5 [pii] 10.1016/j.amjcard.2009.12.022.

7. Perls T, Shea-Drinkwater M, Bowen-Flynn J, Ridge SB, Kang S, Joyce E et al. Exceptional familial clustering for extreme longevity in humans. J Am Geriatr Soc. 2000;48(11):1483-5.

8. Perls TT, Wilmoth J, Levenson R, Drinkwater M, Cohen M, Bogan H et al. Life-long sustained mortality advantage of siblings of centenarians. Proc Natl Acad Sci U S A. 2002;99(12):8442-7. doi:10.1073/pnas.122587599 99/12/8442 [pii].

9. Balch WE, Morimoto RI, Dillin A, Kelly JW. Adapting proteostasis for disease intervention. Science. 2008;319(5865):916-9. doi:10.1126/science.1141448.

10. Preissler S, Deuerling E. Ribosome-associated chaperones as key players in proteostasis. Trends Biochem Sci. 2012;37(7):274-83. doi:10.1016/j.tibs.2012.03.002.

11. Ioannidis JP, Thomas G, Daly MJ. Validating, augmenting and refining genome-wide association signals. Nat Rev Genet. 2009;10(5):318-29. doi:nrg2544 [pii] 10.1038/nrg2544.

12. Altshuler D, Daly MJ, Lander ES. Genetic mapping in human disease. Science. 2008;322(5903):881-8. doi:322/5903/881 [pii] 10.1126/science.1156409.

13. Deelen J, Beekman M, Uh HW, Helmer Q, Kuningas M, Christiansen L et al. Genome-wide association study identifies a single major locus contributing to survival into old age; the APOE locus revisited. Aging Cell.10(4):686-98. doi:10.1111/j.1474-9726.2011.00705.x.

14. Nebel A, Kleindorp R, Caliebe A, Nothnagel M, Blanche H, Junge O et al. A genome-wide association study confirms APOE as the major gene influencing survival in long-lived individuals. Mechanisms of ageing and development. 2011;132(6-7):324-30. doi:10.1016/j.mad.2011.06.008.

15. Schachter F, Faure-Delanef L, Guenot F, Rouger H, Froguel P, Lesueur-Ginot L et al. Genetic associations with human longevity at the APOE and ACE loci. Nat Genet. 1994;6(1):29-32. doi:10.1038/ng0194-29.

16. Willcox BJ, Donlon TA, He Q, Chen R, Grove JS, Yano K et al. FOXO3A genotype is strongly associated with human longevity. Proc Natl Acad Sci U S A. 2008;105(37):13987-92. doi:0801030105 [pii] 10.1073/pnas.0801030105.

17. Flachsbart F, Caliebe A, Kleindorp R, Blanche H, von Eller-Eberstein H, Nikolaus S et al. Association of FOXO3A variation with human longevity confirmed in German centenarians. Proc

Natl Acad Sci U S A. 2009;106(8):2700-5. doi:0809594106 [pii] 10.1073/pnas.0809594106.

18. Anselmi CV, Malovini A, Roncarati R, Novelli V, Villa F, Condorelli G et al. Association of the FOXO3A locus with extreme longevity in a southern Italian centenarian study. Rejuvenation Res. 2009;12(2):95-104. doi:10.1089/rej.2008.0827.

19. Li Y, Wang WJ, Cao H, Lu J, Wu C, Hu FY et al. Genetic association of FOXO1A and FOXO3A with longevity trait in Han Chinese populations. Hum Mol Genet. 2009;18(24):4897-904. doi:ddp459 [pii] 10.1093/hmg/ddp459.

20. Pawlikowska L, Hu D, Huntsman S, Sung A, Chu C, Chen J et al. Association of common genetic variation in the insulin/IGF1 signaling pathway with human longevity. Aging Cell. 2009;8(4):460-72. doi:ACE493 [pii] 10.1111/j.1474-9726.2009.00493.x.

21. Malovini A, Illario M, Iaccarino G, Villa F, Ferrario A, Roncarati R et al. Association study on long-living individuals from Southern Italy identifies rs10491334 in the CAMKIV gene that regulates survival proteins. Rejuvenation research. 2011;14(3):283-91. doi:10.1089/rej.2010.1114.

22. Christensen K, Johnson TE, Vaupel JW. The quest for genetic determinants of human longevity: challenges and insights. Nat Rev Genet. 2006;7(6):436-48. doi:nrg1871 [pii] 10.1038/nrg1871.

23. Kops GJ, Dansen TB, Polderman PE, Saarloos I, Wirtz KW, Coffer PJ et al. Forkhead transcription factor FOXO3a protects quiescent cells from oxidative stress. Nature. 2002;419(6904):316-21. doi:10.1038/nature01036 nature01036 [pii].

24. van der Horst A, Burgering BM. Stressing the role of FoxO proteins in lifespan and disease. Nat Rev Mol Cell Biol. 2007;8(6):440-50. doi:nrm2190 [pii] 10.1038/nrm2190.

25. Samuel SM, Thirunavukkarasu M, Penumathsa SV, Paul D, Maulik N. Akt/FOXO3a/SIRT1-mediated cardioprotection by n-

tyrosol against ischemic stress in rat in vivo model of myocardial infarction: switching gears toward survival and longevity. J Agric Food Chem. 2008;56(20):9692-8. doi:10.1021/jf802050h.

26. Suh Y, Atzmon G, Cho MO, Hwang D, Liu B, Leahy DJ et al. Functionally significant insulin-like growth factor I receptor mutations in centenarians. Proc Natl Acad Sci U S A. 2008;105(9):3438-42. doi:0705467105 [pii] 10.1073/pnas.0705467105.

27. Larson MG, Atwood LD, Benjamin EJ, Cupples LA, D'Agostino RB, Sr., Fox CS et al. Framingham Heart Study 100K project: genome-wide associations for cardiovascular disease outcomes. BMC Med Genet. 2007;8 Suppl 1:S5. doi:1471-2350-8-S1-S5 [pii] 10.1186/1471-2350-8-S1-S5.

28. Benigni A, Corna D, Zoja C, Sonzogni A, Latini R, Salio M et al. Disruption of the Ang II type 1 receptor promotes longevity in mice. J Clin Invest. 2009;119(3):524-30. doi:36703 [pii] 10.1172/JCI36703.

29. Landers JE, Melki J, Meininger V, Glass JD, van den Berg LH, van Es MA et al. Reduced expression of the Kinesin-Associated Protein 3 (KIFAP3) gene increases survival in sporadic amyotrophic lateral sclerosis. Proc Natl Acad Sci U S A. 2009;106(22):9004-9. doi:0812937106 [pii] 10.1073/pnas.0812937106.

30. Bolger TA, Zhao X, Cohen TJ, Tsai CC, Yao TP. The neurodegenerative disease protein ataxin-1 antagonizes the neuronal survival function of myocyte enhancer factor-2. J Biol Chem. 2007;282(40):29186-92. doi:M704182200 [pii] 10.1074/jbc.M704182200.

31. Blaeser F, Ho N, Prywes R, Chatila TA. Ca(2+)-dependent gene expression mediated by MEF2 transcription factors. J Biol Chem. 2000;275(1):197-209.

32. Racioppi L, Means AR. Calcium/calmodulin-dependent kinase IV in immune and inflammatory responses: novel routes for an ancient traveller. Trends Immunol. 2008;29(12):600-7. doi:S1471-4906(08)00226-3 [pii] 10.1016/j.it.2008.08.005.

33. Ohmae S, Takemoto-Kimura S, Okamura M, Adachi-Morishima A, Nonaka M, Fuse T et al. Molecular identification and characterization of a family of kinases with homology to Ca2+/calmodulin-dependent protein kinases I/IV. J Biol Chem. 2006;281(29):20427-39. doi:M513212200 [pii] 10.1074/jbc.M513212200.

34. Newton-Cheh C, Guo CY, Wang TJ, O'Donnell C J, Levy D, Larson MG. Genome-wide association study of electrocardiographic and heart rate variability traits: the Framingham Heart Study. BMC Med Genet. 2007;8 Suppl 1:S7. doi:1471-2350-8-S1-S7 [pii] 10.1186/1471-2350-8-S1-S7.

35. Thayer JF, Yamamoto SS, Brosschot JF. The relationship of autonomic imbalance, heart rate variability and cardiovascular disease risk factors. Int J Cardiol.141(2):122-31. doi:S0167-5273(09)01487-9 [pii] 10.1016/j.ijcard.2009.09.543.

36. Sebastiani P, Solovieff N, Dewan AT, Walsh KM, Puca A, Hartley SW et al. Genetic signatures of exceptional longevity in humans. PLoS One.7(1):e29848. doi:10.1371/journal.pone.0029848 PONE-D-11-23542 [pii].

37. Fontana L, Partridge L, Longo VD. Extending healthy life span--from yeast to humans. Science.328(5976):321-6. doi:328/5976/321 [pii] 10.1126/science.1172539.

38. Bokov A, Chaudhuri A, Richardson A. The role of oxidative damage and stress in aging. Mechanisms of ageing and development. 2004;125(10-11):811-26. doi:10.1016/j.mad.2004.07.009.

39. Harman D. Aging: a theory based on free radical and radiation chemistry. J Gerontol. 1956;11(3):298-300.

40. Harman D. The aging process. Proc Natl Acad Sci U S A. 1981;78(11):7124-8.

41. Pearl R. The Rate of Living, Being an Account of Some Experimental Studies on the Biology of Life Duration. New York: Alfred A. Knopf; 1928.

42. Dai DF, Rabinovitch PS, Ungvari Z. Mitochondria and cardiovascular aging. Circ Res.110(8):1109-24. doi:110/8/1109 [pii] 10.1161/CIRCRESAHA.111.246140.

43. Ungvari Z, Orosz Z, Labinskyy N, Rivera A, Xiangmin Z, Smith K et al. Increased mitochondrial H2O2 production promotes endothelial NF-kappaB activation in aged rat arteries. Am J Physiol Heart Circ Physiol. 2007;293(1):H37-47. doi:01346.2006 [pii] 10.1152/ajpheart.01346.2006.

44. Erusalimsky JD. Vascular endothelial senescence: from mechanisms to pathophysiology. J Appl Physiol (1985). 2009;106(1):326-32. doi:91353.2008 [pii] 10.1152/japplphysiol.91353.2008.

45. Judge S, Jang YM, Smith A, Selman C, Phillips T, Speakman JR et al. Exercise by lifelong voluntary wheel running reduces subsarcolemmal and interfibrillar mitochondrial hydrogen peroxide production in the heart. Am J Physiol Regul Integr Comp Physiol. 2005;289(6):R1564-72. doi:00396.2005 [pii] 10.1152/ajpregu.00396.2005.

46. Puca AA, Andrew P, Novelli V, Anselmi CV, Somalvico F, Cirillo NA et al. Fatty acid profile of erythrocyte membranes as possible biomarker of longevity. Rejuvenation Res. 2008;11(1):63-72. doi:10.1089/rej.2007.0566.

47. Shmookler Reis RJ, Xu L, Lee H, Chae M, Thaden JJ, Bharill P et al. Modulation of lipid biosynthesis contributes to stress resistance and longevity of C. elegans mutants. Aging (Albany NY).3(2):125-47. doi:100275 [pii].

48. Kato T, Shimano H, Yamamoto T, Ishikawa M, Kumadaki S, Matsuzaka T et al. Palmitate impairs and eicosapentaenoate restores insulin secretion through regulation of SREBP-1c in pancreatic islets. Diabetes. 2008;57(9):2382-92. doi:db06-1806 [pii] 10.2337/db06-1806.

49. Chatterjee MT, Khalawan SA, Curran BP. Cellular lipid composition influences stress activation of the yeast general stress response element (STRE). Microbiology. 2000;146 (Pt 4):877-84. doi:10.1099/00221287-146-4-877.

50. Terry DF, McCormick M, Andersen S, Pennington J, Schoenhofen E, Palaima E et al. Cardiovascular disease delay in centenarian offspring: role of heat shock proteins. Ann N Y Acad Sci. 2004;1019:502-5. doi:10.1196/annals.1297.092 1019/1/502 [pii].

51. Kermorvant-Duchemin E, Sennlaub F, Sirinyan M, Brault S, Andelfinger G, Kooli A et al. Trans-arachidonic acids generated during nitrative stress induce a thrombospondin-1-dependent microvascular degeneration. Nat Med. 2005;11(12):1339-45. doi:nm1336 [pii] 10.1038/nm1336.

52. Mattson MP. Hormesis defined. Ageing Res Rev. 2008;7(1):1-7. doi:S1568-1637(07)00071-2 [pii] 10.1016/j.arr.2007.08.007.

53. Yang W, Hekimi S. A mitochondrial superoxide signal triggers increased longevity in Caenorhabditis elegans. PLoS Biol. 2010;8(12):e1000556. doi:10.1371/journal.pbio.1000556.

54. Weindruch R, Walford RL, Fligiel S, Guthrie D. The retardation of aging in mice by dietary restriction: longevity, cancer, immunity and lifetime energy intake. J Nutr. 1986;116(4):641-54.

55. Guevara-Aguirre J, Balasubramanian P, Guevara-Aguirre M, Wei M, Madia F, Cheng CW et al. Growth hormone receptor deficiency is associated with a major reduction in pro-aging signaling, cancer, and diabetes in humans. Sci Transl Med.3(70):70ra13. doi:3/70/70ra13 [pii] 10.1126/scitranslmed.3001845.

56. Bluher M, Kahn BB, Kahn CR. Extended longevity in mice lacking the insulin receptor in adipose tissue. Science. 2003;299(5606):572-4. doi:10.1126/science.1078223 299/5606/572 [pii].

57. Ogg S, Paradis S, Gottlieb S, Patterson GI, Lee L, Tissenbaum HA et al. The Fork head transcription factor DAF-16 transduces insulin-like metabolic and longevity signals in C. elegans. Nature. 1997;389(6654):994-9. doi:10.1038/40194.

58. Cau SB, Carneiro FS, Tostes RC. Differential modulation of nitric oxide synthases in aging: therapeutic opportunities. Front Physiol.3:218. doi:10.3389/fphys.2012.00218.

59. Wojtaszewski JF, Nielsen P, Hansen BF, Richter EA, Kiens B. Isoform-specific and exercise intensity-dependent activation of 5'-AMP-activated protein kinase in human skeletal muscle. J Physiol. 2000;528 Pt 1:221-6. doi:PHY_1384 [pii].

60. Lewis GD, Farrell L, Wood MJ, Martinovic M, Arany Z, Rowe GC et al. Metabolic signatures of exercise in human plasma. Sci Transl Med.2(33):33ra7. doi:2/33/33ra37 [pii] 10.1126/scitranslmed.3001006.

61. Palacios OM, Carmona JJ, Michan S, Chen KY, Manabe Y, Ward JL, 3rd et al. Diet and exercise signals regulate SIRT3 and activate AMPK and PGC-1alpha in skeletal muscle. Aging (Albany NY). 2009;1(9):771-83.

62. Nisoli E, Clementi E, Paolucci C, Cozzi V, Tonello C, Sciorati C et al. Mitochondrial biogenesis in mammals: the role of endogenous nitric oxide. Science. 2003;299(5608):896-9. doi:10.1126/science.1079368 299/5608/896 [pii].

63. Ungvari Z, Sonntag WE, Csiszar A. Mitochondria and aging in the vascular system. J Mol Med (Berl). 2010;88(10):1021-7. doi:10.1007/s00109-010-0667-5.

64. Brandes RP, Fleming I, Busse R. Endothelial aging. Cardiovascular research. 2005;66(2):286-94. doi:10.1016/j.cardiores.2004.12.027.

65. Fortuno A, San Jose G, Moreno MU, Diez J, Zalba G. Oxidative stress and vascular remodelling. Experimental physiology. 2005;90(4):457-62. doi:10.1113/expphysiol.2005.030098.

66. Griendling KK, Harrison DG. Dual role of reactive oxygen species in vascular growth. Circulation research. 1999;85(6):562-3.

67. El Assar M, Angulo J, Vallejo S, Peiro C, Sanchez-Ferrer CF, Rodriguez-Manas L. Mechanisms involved in the aging-induced

vascular dysfunction. Frontiers in physiology. 2012;3:132. doi:10.3389/fphys.2012.00132.

68. Vecchione C, Carnevale D, Di Pardo A, Gentile MT, Damato A, Cocozza G et al. Pressure-induced vascular oxidative stress is mediated through activation of integrin-linked kinase 1/betaPIX/Rac-1 pathway. Hypertension. 2009;54(5):1028-34. doi:10.1161/HYPERTENSIONAHA.109.136572.

69. Puca AA, Carrizzo A, Ferrario A, Villa F, Vecchione C. Endothelial nitric oxide synthase, vascular integrity and human exceptional longevity. Immunity & ageing : I & A. 2012;9(1):26. doi:10.1186/1742-4933-9-26.

70. Schulz E, Jansen T, Wenzel P, Daiber A, Munzel T. Nitric oxide, tetrahydrobiopterin, oxidative stress, and endothelial dysfunction in hypertension. Antioxidants & redox signaling. 2008;10(6):1115-26. doi:10.1089/ars.2007.1989.

71. Finkel T. Oxidant signals and oxidative stress. Current opinion in cell biology. 2003;15(2):247-54.

72. Vecchione C, Brandes RP. Withdrawal of 3-hydroxy-3-methylglutaryl coenzyme A reductase inhibitors elicits oxidative stress and induces endothelial dysfunction in mice. Circulation research. 2002;91(2):173-9.

73. Deshpande SS, Qi B, Park YC, Irani K. Constitutive activation of rac1 results in mitochondrial oxidative stress and induces premature endothelial cell senescence. Arteriosclerosis, thrombosis, and vascular biology. 2003;23(1):e1-6.

74. Vecchione C, Aretini A, Marino G, Bettarini U, Poulet R, Maffei A et al. Selective Rac-1 inhibition protects from diabetes-induced vascular injury. Circulation research. 2006;98(2):218-25. doi:10.1161/01.RES.0000200440.18768.30.

75. Ungvari Z, Bailey-Downs L, Sosnowska D, Gautam T, Koncz P, Losonczy G et al. Vascular oxidative stress in aging: a homeostatic failure due to dysregulation of NRF2-mediated antioxidant response. American journal of physiology Heart and circulatory

physiology. 2011;301(2):H363-72.
doi:10.1152/ajpheart.01134.2010.

76. van der Loo B, Labugger R, Skepper JN, Bachschmid M, Kilo J, Powell JM et al. Enhanced peroxynitrite formation is associated with vascular aging. The Journal of experimental medicine. 2000;192(12):1731-44.

77. Lee HC, Wei YH. Mitochondria and aging. Advances in experimental medicine and biology. 2012;942:311-27. doi:10.1007/978-94-007-2869-1_14.

78. Minamino T, Miyauchi H, Yoshida T, Ishida Y, Yoshida H, Komuro I. Endothelial cell senescence in human atherosclerosis: role of telomere in endothelial dysfunction. Circulation. 2002;105(13):1541-4.

79. Alcendor RR, Gao S, Zhai P, Zablocki D, Holle E, Yu X et al. Sirt1 regulates aging and resistance to oxidative stress in the heart. Circulation research. 2007;100(10):1512-21. doi:10.1161/01.RES.0000267723.65696.4a.

80. Saretzki G, Von Zglinicki T. Replicative aging, telomeres, and oxidative stress. Annals of the New York Academy of Sciences. 2002;959:24-9.

81. Silver MH, Jilinskaia E, Perls TT. Cognitive functional status of age-confirmed centenarians in a population-based study. J Gerontol B Psychol Sci Soc Sci. 2001;56(3):P134-40.

82. Geesaman BJ, Benson E, Brewster SJ, Kunkel LM, Blanche H, Thomas G et al. Haplotype-based identification of a microsomal transfer protein marker associated with the human lifespan. Proceedings of the National Academy of Sciences of the United States of America. 2003;100(24):14115-20. doi:10.1073/pnas.1936249100 1936249100 [pii].

83. Novelli V, Viviani Anselmi C, Roncarati R, Guffanti G, Malovini A, Piluso G et al. Lack of replication of genetic associations with human longevity. Biogerontology. 2008;9(2):85-92. doi:10.1007/s10522-007-9116-4.

84. Price AL, Patterson NJ, Plenge RM, Weinblatt ME, Shadick NA, Reich D. Principal components analysis corrects for stratification in genome-wide association studies. Nat Genet. 2006;38(8):904-9. doi:ng1847 [pii] 10.1038/ng1847.

Chapter 2.

Genetic Analysis Reveals a Longevity-Associated Protein Modulating Endothelial Function and Angiogenesis

Genetic Analysis Reveals a Longevity-Associated Protein Modulating Endothelial Function and Angiogenesis

Francesco Villa,* Albino Carrizzo,* Chiara C. Spinelli,* Anna Ferrario,* Alberto Malovini, Anna Maciąg, Antonio Damato, Alberto Auricchio, Gaia Spinetti, Elena Sangalli, Zexu Dang, Michele Madonna, Mariateresa Ambrosio, Leopoldo Sitia, Paolo Bigini, Gaetano Calì, Stefan Schreiber, Thomas Perls, Sergio Fucile, Francesca Mulas, Almut Nebel, Riccardo Bellazzi, Paolo Madeddu, Carmine Vecchione, Annibale A. Puca

Rationale: **Long living individuals show delay of aging, which is characterized by the progressive loss of cardiovascular homeostasis, along with reduced endothelial nitric oxide synthase activity, endothelial dysfunction, and impairment of tissue repair after ischemic injury.**

Objective: **Exploit genetic analysis of long living individuals to reveal master molecular regulators of physiological aging and new targets for treatment of cardiovascular disease.**

Methods and Results: **We show that the polymorphic variant rs2070325 (Ile229Val) in bactericidal/permeability-increasing fold-containing-family-B-member-4 (BPIFB4) associates with exceptional longevity, under a recessive genetic model, in 3 independent populations. Moreover, the expression of BPIFB4 is instrumental to maintenance of cellular and vascular homeostasis through regulation of protein synthesis. BPIFB4 phosphorylation/activation by protein-kinase-R–like endoplasmic reticulum kinase induces its complexing with 14-3-3 and heat shock protein 90, which is facilitated by the longevity-associated variant. In isolated vessels, BPIFB4 is upregulated by mechanical stress, and its knock-down inhibits endothelium-dependent vasorelaxation. In hypertensive rats and old mice, gene transfer of longevity-associated variant-BPIFB4 restores endothelial nitric oxide synthase signaling, rescues endothelial dysfunction, and reduces blood pressure levels. Furthermore, BPIFB4 is implicated in vascular repair. BPIFB4 is abundantly expressed in circulating $CD34^+$ cells of long living individuals, and its knock-down in endothelial progenitor cells precludes their capacity to migrate toward the chemoattractant SDF-1. In a murine model of peripheral ischemia, systemic gene therapy with longevity-associated variant-BPIFB4 promotes the recruitment of hematopoietic stem cells, reparative vascularization, and reperfusion of the ischemic muscle.**

Conclusions: **Longevity-associated variant-BPIFB4 may represent a novel therapeutic tool to fight endothelial dysfunction and promote vascular reparative processes. (*Circ Res*. 2015;117:333-345. DOI: 10.1161/CIRCRESAHA.117.305875.)**

Key Words: aging ■ endothelial progenitor cell ■ endothelial function ■ endothelial nitric oxide synthase ■ longevity ■ vascular reactivity

Aging is an independent risk factor associated with endothelial dysfunction, impaired angiogenesis, and loss of protein homeostasis, or proteostasis, the decline of which is contrasted by adaptive cellular responses.[1] The mechanisms that help cells adapt and survive under stressful conditions include the activation of heat shock factor protein 1–controlled heat shock proteins (HSPs), ribosomal biogenesis, and protein

Editorial, see p 309
In This Issue, see p 301

Original received December 17, 2014; revision received May 28, 2015; accepted June 1, 2015. In April 2015, the average time from submission to first decision for all original research papers submitted to *Circulation Research* was 13.84 days.

From the National Research Council, Institute for Biomedical Technologies, Segrate (MI), Italy (F.V., C.C.S., A.F.); IRCCS Neuromed, Department of Vascular Physiopathology, Pozzilli (IS), Italy (A.C., A.D., M.M., M.A., S.F., C.V.); Department of Industrial and Information Engineering, University of Pavia, Pavia, Italy (A. Malovini, F.M., R.B.); IRCCS Multimedica, Cardiovascular Department, Milan, Italy (A. Maciąg, G.S., E.S., A.A.P.); Department of Translational Medicine, "Federico II" University, Naples, Italy (A.A.); TIGEM (Telethon Institute of Genetics and Medicine), Naples, Italy (A.A.); Department of Experimental Cardiovascular Medicine, Bristol Heart Institute, University of Bristol, Bristol, United Kingdom (Z.D., P.M.); Department of Biochemistry and Molecular Pharmacology IRCCS Istituto di Ricerche Farmacologiche "Mario Negri", Milan, Italy (L.S., P.B.); National Research Council, Institute of Experimental Endocrinology and Oncology (IEOS), Naples, Italy (G.C.); Institute of Clinical Molecular Biology, Christian-Albrechts University and the Schleswig-Holstein University Hospital, Kiel, Germany (S.S., A.N.); Geriatrics Section, Department of Medicine, Boston Medical Center, Boston University School of Medicine, Boston, MA (T.P.); Dipartimento di Fisiologia e Farmacologia, Sapienza Università di Roma, Rome, Italy (S.F.); and Dipartimento di Medicina e Chirurgia, Università degli Studi di Salerno, 84081 Baronissi (SA), Italy (C.V., A.A.P.).

*These authors contributed equally to this article.

The online-only Data Supplement is available with this article at http://circres.ahajournals.org/lookup/suppl/doi:10.1161/CIRCRESAHA.117.305875/-/DC1.

Correspondence to Annibale A. Puca, Università degli Studi di Salerno, Via S. Allende–84081, Baronissi (SA), Italy. E-mail apuca@unisa.it or Carmine Vecchione, Università degli Studi di Salerno, Via S. Allende–84081, Baronissi (SA), Italy. E-mail cvecchione@unisa.it

Nonstandard Abbreviations and Acronyms	
BPIFB4	bactericidal/permeability-increasing fold-containing-family-B-member-4
EPC	endothelial progenitor cells
HSP90	heat shock protein 90
LAV	longevity-associated variant
LLIs	long living individuals
MNC	mononuclear cells
PERK	protein kinase R–like endoplasmic reticulum kinase
SHR	spontaneously hypertensive rats

synthesis and are at least in part orchestrated by growth factors, as observed in *Caenorhabditis elegans*, in which heat shock factor protein 1 is under the control of insulin/IGF-1-like signaling.[2] Importantly, IGF-1-like signaling modulation of heat shock factor protein 1 is necessary for controlling longevity[3] and through modulation of FOXO (forkhead box O) transcription factors, also for stem cell maintenance.[4,5] Therefore, a spectrum of shared mechanisms modulate development, response to stress, and aging.[6] Furthermore, IGF-1-like signaling regulates activation of endothelial nitric oxide synthase (eNOS), a fundamental step for the beneficial effects of calorie restriction and exercise—environmental components that influence health and life-span—as underlined by the abolishment of the positive effects of caloric restriction in eNOS-knockout mice.[7–9] eNOS has a key role in maintaining vascular function and integrity by generating nitric oxide (NO), a potent vasorelaxant and an inducer of angiogenesis and vasculogenesis.[10–12] Dysfunction of eNOS signaling is observed in several pathological conditions, such as cardiovascular, immunologic, metabolic, and neural diseases.[13]

Exceptional longevity is an inheritable trait; long-lived individuals (LLIs), when compared with younger populations, have a reduced incidence of cardiovascular disease[14,15] and a delayed ageing, a phenomenon that is in part genetically driven.[16] Thus, nonhypothesis-based genetic approaches could uncover novel proteins that control aging and disease resistance.

Here, we report genetic findings that have allowed us to unequivocally identify BPI fold–containing family B member 4/palate lung and nasal epithelium clone 4 (BPIFB4/LPLUNC4)—a member of a family of proteins involved in innate immunity, but whose function remains elusive[17]—as a gene associated with exceptional longevity. Translating these findings into therapeutic outcomes, we found that BPIFB4 is downregulated in old mice and that forced expression of the longevity-associated variant (LAV) of BPIFB4 rescues age-related endothelial dysfunction. Additionally, LAV-BPIFB4 restores endothelial function and blood pressure levels in a hypertensive model and old mice and promotes reparative angiogenesis and recruitment of stem cells to the ischemic limb muscle of mice subjected to unilateral femoral artery ligation. Thus, LAV-BPIFB4 may constitute a novel treatment for vascular diseases, hypertension, and ischemia.

Methods

A supplemental section for more detailed methods is available online at http://circres.ahajournals.org.

LLI Populations

The LLI populations are described extensively elsewhere.[18–21]

Transcriptome Analysis

Transcriptome analysis was performed on total RNA of transfected HEK293T (human embryonic kidney 293T) cells using BeadChip Illumina. Complete data sets are available in Gene Expression Omnibus database (www.ncbi.nlm.nih.gov/geo) in GSE63912.

Endothelial Progenitor Cell Migration Assay

To perform migration assay, mononuclear cells (MNCs) were isolated and endothelial progenitor cells (EPC) enriched as described previously.[22,23] Antigenic profile was assessed using a FACS Canto flow cytometer and FACS Diva software (Becton, Dickinson and Company). Migration was performed as described elsewhere.[22,24,25]

Evaluation of Vascular Reactivity

To evaluate the vascular reactivity in ex vivo transfected mouse vessels, second-order branches of the mesenteric arterial tree were removed from C57BL6 mice and transfected as described previously.[26]

Vasoconstriction was assessed with KCl or phenylephrine in control conditions and after N^G-nitro-L-arginine methyl ester (L-NAME) exposure. Responses were tested before and after transfection. Endothelium-dependent and -independent relaxations were assessed by measuring the dilatory responses of mesenteric arteries to cumulative concentrations of acetylcholine or nitroglycerine, respectively, in vessels precontracted with U46619.[27] Caution was taken to avoid endothelial damage; functional integrity was reflected by the response to acetylcholine (10^{-6} mol/L).[28]

Infection of Hypertensive Rats

Femoral arteries of AAV-infected spontaneously hypertensive rats (SHR) were analyzed in this study. The experimental protocol for this project was approved by the Istituto Neurologico Mediterraneo Neuromed, Italy, and complies with National Institute Health guidelines for care and use of laboratory animals. Femoral arteries were excised and placed on a wire system[28] to perform vascular reactivity studies. Blood pressure was evaluated in another experimental series of SHRs (11-week-old) by tail-cuff plethysmography for 1 week as previously described.[28]

Infection of Hindlimb Ischemia Mice Models

Infection with AAV and measurement of superficial blood flow and neovascularization were performed in accordance with the Guide for the Care and Use of Laboratory Animals (The Institute of Laboratory Animal Resources, 1996) and with approval of the British Home Office and the University of Bristol.

Foot blood flow was measured immediately after ischemia and then at 7, 14, and 21 days (n=10 mice/group). Muscle cryosections with thickness of 5 μm were used for immunohistochemical analyses.

Evaluation of the modulation in recruitment of total and short-term and long-term reconstituting Lin^- $Sca\text{-}1^+cKit^+$ cells in the ischemic muscles of AAV-injected mice was assessed using a multicolor flow cytometry.

Analysis of gene expression was performed on ischemic muscles and femoral arteries collected 1 week from induction of ischemia and gene therapy.

Statistical Analyses

The reader may refer to Malovini et al[21] for details about the statistical methods and procedures applied to the analysis of data deriving from the genome-wide scan. For all statistical detailed information, refer the statistical method sections in the Online Data Supplement.

Results

rs2070325 in BPIFB4 Associates With Exceptional Longevity in Three Independent Populations

To follow up our previous hypothesis-generating genome-wide association study (Online Text I),[21] we designed a 2-stage replication effort on 4 variations reported among the top findings ($P<1\times10^{-4}$) of that study. To this end, 2 nonsynonymous SNPs—that is, rs2070325 and rs571391—and 2 intronic markers—that is, rs7583529 and rs285097, which tagged the functional variants rs7917 and rs16955011 ($r^2>0.8$

in the HapMap CEU panel), respectively—were tested for association in 2 independent cohorts, the first of which was recruited for the German Longevity Study[20] and the second for a US-based effort[18,19] (Online Text II).

Of the 4 variations tested with TaqMan assays, only rs2070325—which induces the amino acid change Ile229Val in BPIFB4 (identifier: P59827-2)—replicated the association observed in the screening cohort under the recessive genetic model (OR=2.42; 95% CI=1.56–3.77; $P=5.8\times10^{-5}$; power >0.85) in the German Longevity Study (OR=1.43; 95% CI=1.12–1.80; $P=0.0036$). This variant was found associated with the longevity phenotype also in the US replication set (OR=1.60; 95% CI=1.14–2.24; $P=0.0063$; Online Table I). Meta-analysis of the 2 populations confirmed this finding (3060 LLIs and 1609 controls: OR=1.49; 95% CI=1.22–1.81; $P=7.59\times10^{-5}$; power>0.90) and that of the screening and replication sets combined (3464 LLIs and 2160 controls; Bonferroni-adjusted significance threshold: $P<3.22\times10^{-7}$; OR=1.61; 95% CI=1.34–1.92; $P=2.4\times10^{-7}$; power >0.80; Online Figure I and Online Text III).

rs2070325 Is Associated With a Quadruple-SNP Haplotype

Haplotype analysis revealed patterns of strong linkage disequilibrium (LD: $r^2>0.8$, $D'>0.9$) within the *BPIFB4* genomic locus, delimiting a region highly enriched in nonsynonymous SNPs: the rs2070325 variation of *BPIFB4* tagged rs2889732 (Asn281Thr), rs11699009 (Leu488Phe), and rs11696307 (Ile494Thr), codifying, respectively, for wild-type (WT; allele frequency, 66%) and LAV (allele frequency, 29.5%) isoforms (Online Text IV).

CD34$^+$ Cells From LLIs Donors Abundantly Express BPIFB4

BPIFB4 has been found expressed in olfactory epithelium, MNCs, and Bowman's gland.[29] We found BPIFB4 also expressed in germline, stem, progenitor, and fetal cells (Online Figures II and IIIA and Online Text V). Moreover, circulating CD34$^+$ cells, which are enriched with proangiogenic progenitors, had higher BPIFB4 RNA levels in LLIs as compared with ethnically matched young controls, suggesting a possible implication of BPIFB4 in cellular mechanisms of vascular repair (Online Figure IIIB). To further evaluate the involvement of BPIFB4 in proangiogenic cell function, we studied the impact of BPIFB4 knock-out on in vitro migration activity of culture-selected EPCs from healthy human donors. We observed a lack of migration toward the classical chemoattractant SDF-1a in EPCs lacking BPIFB4 (Online Figure IV).

BPIFB4 Overexpression Induces an Adaptive Stress Response and Proteostasis

To gain information on the role of BPIFB4 and its LAV in gene expression regulation, we performed genome-wide transcriptional profiling of HEK293T cells transfected with an empty-, WT- or LAV-BPIFB4-encoding vector. BPIFB4 isoforms activated adaptive stress responses and proteostasis, 2 key aspects for improved organism survival[9] and stem cell maintenance,[30] and potentiated small noncoding RNAs supportive of the spliceosome, genomic integrity machinery, and telomere maintenance (Online Figures V and VIA, Online Text VI and Online Tables III–VII). Altogether these data are indicative of a role of BPIFB4 in organism homeostasis.

PERK Modulates the Complexing of LAV-BPIFB4 With 14-3-3

To further dissect the molecular determinants underlying the mechanism of action of BPIFB4, we analyzed the structure of the protein motifs in its sequence. We identified a protein kinase R–like endoplasmic reticulum kinase (PERK) substrate motif (amino acids 73–80: EXSXRXXR/EGSIRDLR).[31,32] PERK is a known transducer of the unfolded protein response, reducing endoplasmic reticulum protein loading through the inhibition of protein synthesis mediated by phosphorylation of eukaryotic translation initiation factor 2-alpha.[33] Thus, a PERK substrate motif on BPIFB4 would indicate a role of BPIFB4 as a downstream effector. Specifically, we observed a reduction of eukaryotic translation initiation factor 2-alpha phosphorylation on transfection with BPIFB4 (Online Figure VIB). These findings suggest that BPIFB4 is part of a cascade of events orchestrated by PERK aimed at reducing endoplasmic reticulum stress. Further sequence analysis revealed the presence of an atypical 14-3-3 binding motif (amino acids 80–86: RXSXXXS/RNSGYRS).[17] 14-3-3 modulates cell signaling by binding and retaining proteins within the cytoplasm depending on their phosphorylation status.[34]

We next compared LAV-BPIFB4 and WT-BPIFB4 for potential interaction with 14-3-3 in vitro. Immunoprecipitation and confocal analyses revealed that LAV-BPIFB4 was mainly localized in the cytoplasm and efficiently formed a complex with 14-3-3, whereas WT-BPIFB4 was mostly nuclear (Online Figures VII–IX and Online Text VII). Cells transfected with LAV-BPIFB4 mutated either at serine 75 (LAV-BPIFB4^{mutPERK}) or at serine 82 (LAV-BPIFB4$^{mut14\text{-}3\text{-}3}$), which is part of the 14-3-3 binding motif, failed to immunoprecipitate 14-3-3, thus indicating a role of these sites in 14-3-3 recruitment (Online Figure VII).

Further characterization of LAV-BPIFB4 interactions revealed that it forms a complex with heat shock protein 90 (HSP90), a phenomenon that does not take place in cells transfected with LAV-BPIFB4^{mutPERK} or LAV-BPIFB4$^{mut14\text{-}3\text{-}3}$ (Online Figure VII). Pharmacological inhibition of PERK with GSK2606414 after transfection with LAV-BPIFB4 impeded the immunoprecipitation of 14-3-3 and HSP90 (Online Figure VII). These findings link PERK-mediated phosphorylation of LAV-BPIFB4 to its 14-3-3 binding activity, which is central for the recruitment of HSP90, a known eNOS activator.[35] Of note, WT-BPIFB4 coimmunoprecipitated with HSP90, but not with 14-3-3, as detected by Western blotting. However, WT-BPIFB4$^{mut14\text{-}3\text{-}3}$ failed to immunoprecipitate with HSP90 (Online Figure VII). This indicates that WT-BPIFB4 has a reduced, rather than no ability to recruit 14-3-3, which is a step needed for forming a complex with HSP90.

eNOS Is Phosphorylated in Homozygotic rs2070325 MNCs

Aging is generally associated with a significant reduction in NO bioavailability, which leads to endothelial dysfunction.[36] Based on the above observations of HSP90 recruitment by BPIFB4 and the latter being expressed in MNCs, we assessed the effect of the A/A (homozygotic major allele), A/a (heterozygotic allele), and a/a (homozygotic minor allele) genotypes of rs2070325 on the activity status of eNOS in MNCs from healthy blood donors. We found increased

eNOS phosphorylation at serine 1177—an activation site of the enzyme—in a/a carriers (Figure 1).

BPIFB4 Is Present in the Vessel Wall and Modulates Vascular Tone

Based on the evidence of enhanced eNOS phosphorylation in MNCs with an rs2070325 genotype, we explored the role of BPIFB4 in the modulation of vascular tone, a process in which NO plays a prominent role.[36] In mouse mesenteric arteries—a typical resistance vessel involved in blood pressure homeostasis—expression of the protein was upregulated on application of a biomechanical stress (ie, increased intraluminal pressure for 1 hour; Figure 2A). Inhibition of BPIFB4 expression had a detrimental effect on vascular function: in fact, siRNA-mediated knockdown of BPIFB4 induced marked reductions in phenylephrine- and potassium-evoked vasoconstrictions and acetylcholine-evoked endothelial vasorelaxation (Figure 2B). These effects were associated with the inhibition of eNOS

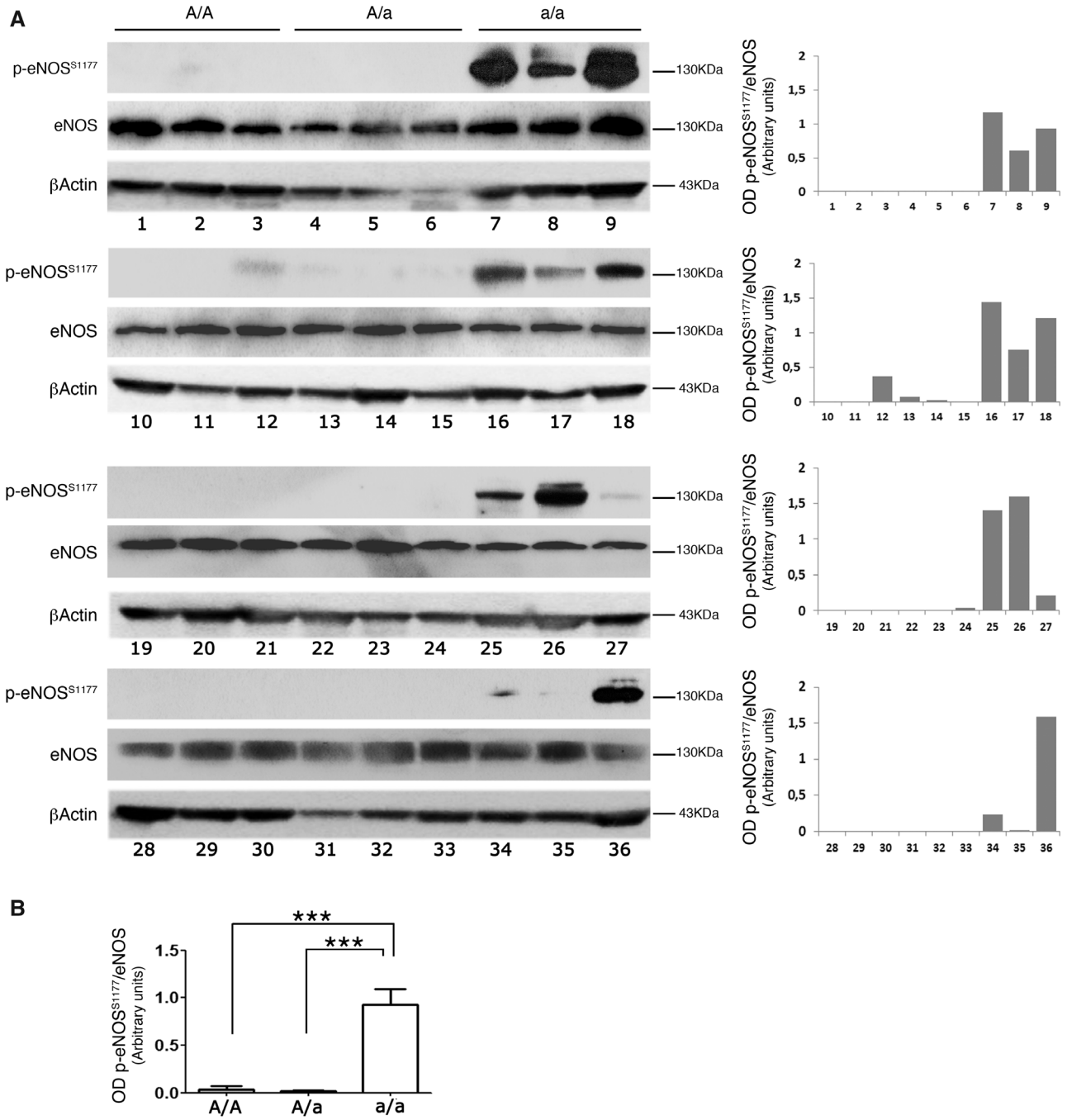

Figure 1 . Evaluation of endothelial nitric oxide synthase (eNOS) phosphorylation in subjects carrying variations on *BPIFB4*. A, Phosphorylation status of eNOS on serine 1177 in ex vivo mononuclear cells (MNCs) of subjects A/A (N=12), A/a (N=12), or a/a (N=12) for rs2070325. Right plots give the optical density ratio between the phosphorylated and total forms of eNOS. **B**, Plot of average values. Values are means±SEM. Statistical analysis was performed with Student's *t* test; ***P<0.001. BPIFB4 indicates bactericidal/permeability-increasing fold-containing-family-B-member-4.

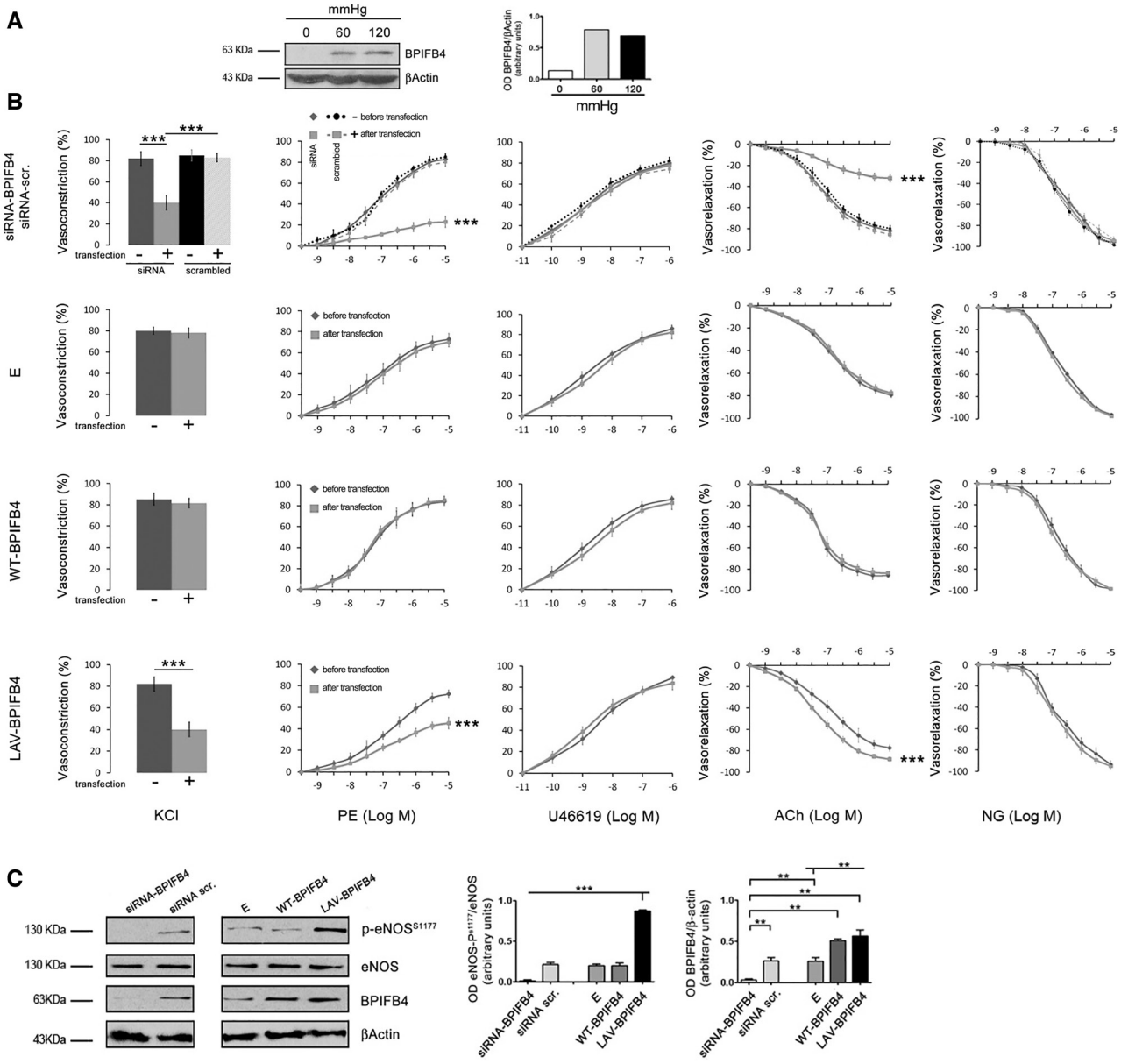

Figure 2 . Expression of BPIFB4 in perfused vessels and effects of its variants on vascular reactivity and on phosphorylation of endothelial nitric oxide synthase (eNOS) in mesenteric arteries. A, BPIFB4 protein expression in ex vivo mouse mesenteric arteries perfused with increasing pressure levels. The right graph gives quantification of BPIFB4 protein. **B**, Graphs show, from left to right, the ex vivo response of mouse mesenteric arteries to potassium (80 mmol/L KCl) and the dose responses to phenylephrine (PE), the thromboxane agonist U46619, endothelium-dependent vasorelaxant acetylcholine (ACh), and endothelium-independent vasorelaxant nitroglycerin (NG). In the first row, vascular responses are measured before (-◆–) and after (-■-+) transfection with short interfering (si) RNA for BPIFB4, and before (•●•–) and after (-■-+) transfection with scrambled siRNA. In the consecutive rows, before (-◆–) and after (-■-+) transfection with an empty (E) plasmid or with wild-type (WT) or the longevity-associated variant (LAV) BPIFB4-encoding plasmids. Values are means±SEM. N=7. **C**, Western blot of 7 pooled experiments on ex vivo mouse mesenteric arteries. Graphs show quantification of eNOS phosphorylation and BPIFB4. Values are means±SEM, N=3 pools of experiments. Statistics was performed using ANOVA; ***P*<0.01; ****P*<0.001. BPIFB4 indicates bactericidal/permeability-increasing fold-containing-family-B-member-4.

phosphorylation at serine 1177 (Figure 2C). In contrast, silencing of BPIFB4 expression did not affect the endothelium-independent vasorelaxation response evoked by nitroglycerin (NG).

Transfection of Arteries With LAV-BPIFB4 Enhances eNOS Phosphorylation and eNOS-Dependent Vasomotion Through PERK and 14-3-3 Binding

We transfected mesenteric arteries ex vivo with plasmids encoding a variant tagged with green fluorescent protein. Overexpression of WT-BPIFB4 did not interfere with vascular reactivity (Figure 2B), whereas the expression of LAV-BPIFB4 significantly enhanced acetylcholine-evoked vasorelaxation (Figure 2B) and promoted phosphorylation of eNOS at serine 1177 (Figure 2C). Of note, acetylcholine-evoked vasorelaxation was more efficiently inhibited with N^G-nitro-L-arginine methyl ester (L-NAME) in LAV-BPIFB4–expressing resistance vessels than in vessels exposed to an empty vector, indicating a higher dependency on eNOS in the former. In contrast, forced BPIFB4 expression did not affect

the endothelium-independent vasorelaxation response evoked by NO (Online Figure X and Online Text VIII).

We then assessed the role of PERK and 14-3-3 binding in the activation of eNOS-dependent vascular responses by LAV-BPIFB4. To this aim, we transfected mouse mesenteric arteries ex vivo with LAV-BPIFB4^{mutPERK} or LAV-BPIFB4$^{mut14-3-3}$ and observed these mutants are devoid of the features manifested by LAV-BPIFB4 (Figure 3A and 3B). Likewise, pharmacological inhibition of PERK with GSK2606414 negated the effect of LAV-BPIFB4 on eNOS phosphorylation and vascular reactivity (Figure 3A–3C).

Phosphorylation of BPIFB4 at serine 75 was higher in mesenteric vessels transfected with LAV-BPIFB4 than in those transfected with WT-BPIFB4 (Figure 3D). Treatment with GSK2606414 reduced the level of phosphorylation at serine 75 on LAV-BPIFB4, as well as at serine 1177 on eNOS, supporting the role of PERK in potentiating the phosphorylation status of LAV-BPIFB4 and eNOS (Figure 3C). Because mesenteric vessels transfected with WT-BPIFB4$^{mut14-3-3}$ also displayed endothelial dysfunction, it is plausible that WT-BPIFB4, similarly to LAV-BPIFB4, requires binding to 14-3-3 for activation of eNOS (Online Figure XI). Additionally, HSP90 seems to be implicated in LAV-BPIFB4–induced potentiation of eNOS, as documented by results showing LAV-BPIFB4's failure to modulate eNOS/vascular responses on inhibition of HSP90 with SNX5422 (Online Figure XII). As a result, we hypothesize a model in which BPIFB4 needs to be phosphorylated by PERK to recruit 14-3-3, thus allowing the formation of a complex with HSP90 for final activation of eNOS. This cascade of events is potentiated in the presence of LAV-BPIFB4 (Online Figure XIII).

We also observed apparently paradoxical reductions in potassium- and phenylephrine-evoked vasoconstrictions by LAV-BPIFB4 compared with WT-BPIFB4 (Figure 2B). This effect was partially rescued by the eNOS inhibitor L-NAME, suggesting that LAV-BPIFB4–mediated enhancement of NO production modulated adrenergic and potassium vascular responses (Figure 3B). Additionally, as shown in Online Figure XIV, L-NAME enhanced phenylephrine and KCl vascular responses without affecting U46619 vasoconstriction. These results indicate that the NO signaling is not involved in the vascular response evoked by U46619.

Forced Expression of LAV-BPIFB4 In Vivo Enhances eNOS Function and Reduces Blood Pressure

To evaluate the in vivo relevance of the findings obtained through plasmid transfection, we generated WT-BPIFB4-, LAV-BPIFB4-, and green fluorescent protein–encoding adeno-associated viral vectors (AAV serotype 9 with a TBG promoter) and used them to transduce normotensive mice through the femoral artery.[37] We found that AAV-LAV-BPIFB4 enhances NO-mediated vasorelaxation in femoral arteries and also in mesenteric arteries, a vascular district different from the one used for gene delivery (Online Figure XVA). Both vessels represent the prototype of resistance vessels involved in blood pressure homeostasis.[28,38–41] As expected, enhanced vasorelaxation by AAV-LAV-BPIFB4 was associated with potentiation of eNOS phosphorylation (Online Figure XVB) and interestingly with a reduction of both systolic and diastolic blood pressure (Online Figure XVI). In contrast, transduction with AAV-WT-BPIFB4 did not exert molecular and vasorelaxant effects in this model (Online Figure XV). It should again acknowledge that the observed effects were endothelium-dependent as no potentiation of NG-induced vasorelaxation was observed.

Investigation of the association between duration of transgene expression and functional/molecular outcomes indicates persistence of LAV-BPIFB4 expression ≤3 weeks after systemic delivery of the AVV vector, along with enhancement of endothelial vasorelaxation (Online Figure XVIIA) and eNOS phosphorylation (Online Figure XVIIB). On the other hand, the effect of LAV-BPIFB4 infection on blood pressure reduction was counteracted by compensatory mechanisms after 1 week (Online Figure XVIIC).

Analyses of different tissues from AAV-LAV-BPIFB4–infected mice showed overexpression of BPIFB4 in femoral bone marrow, brain, adipose tissue, and endothelium, but not in liver, blood serum, and MNCs (see details in Online Figures XVIII and XIX and Online Text IX). In addition, we quantified the abundance of CD31$^+$ endothelial cells expressing BPIFB4 and found a significant increase of CD31$^+$/BPIFB4$^+$ endothelial cells AAV-LAV-BPIFB4–infected mice in comparison with AAV-green fluorescent protein–infected mice (Online Text IX).

Next, to strengthen the involvement of eNOS/NO signaling in the in vivo vascular effects of AAV-LAV-BPIFB4, we injected the vector in eNOS-knock-out and control mice. Results show that AAV-LAV-BPIFB4 fails to exert hemodynamic effects in conditions of eNOS deficiency (Online Figure XXA), despite an efficient LAV-BPIFB4 overexpression was confirmed in these animals by Western blot analysis (Online Figure XXB).

In Vivo Gene Therapy With LAV-BPIFB4 Rescues a Genetic Hypertensive Trait

We next studied the antihypertensive effect of LAV-BPIFB4 gene therapy in SHR, a model of essential hypertension characterized by endothelial dysfunction.[42] Systemic delivery of LAV-BPIFB4 improved endothelial vasorelaxation and enhanced eNOS phosphorylation in vessels, along with normalized blood pressure (Figure 4).

We next explored if forced LAV-BPIFB4 expression has an impact on hypertensive vascular remodeling. As expected, and in agreement with previous reports, SHRs show an increase in media:lumen ratio and media thickness as compared with normotensive WKY rats,[43,44] indicating hypertrophic remodeling. Intriguingly, although capable of normalizing blood pressure levels in SHRs, LAV-BPIFB4 failed to rescue vascular remodeling. These data indicate that the hypertrophically remodeled vasculature of chronically hypertensive rats remains functionally sensitive to the vasodilatory action of LAV-BPIFB4 (Online Figure XXI).

In Vivo Gene Therapy With LAV-BPIFB4 Reverts Vascular Ageing

Aging is an independent cardiovascular risk factor associated with an impairment of endothelial function because of

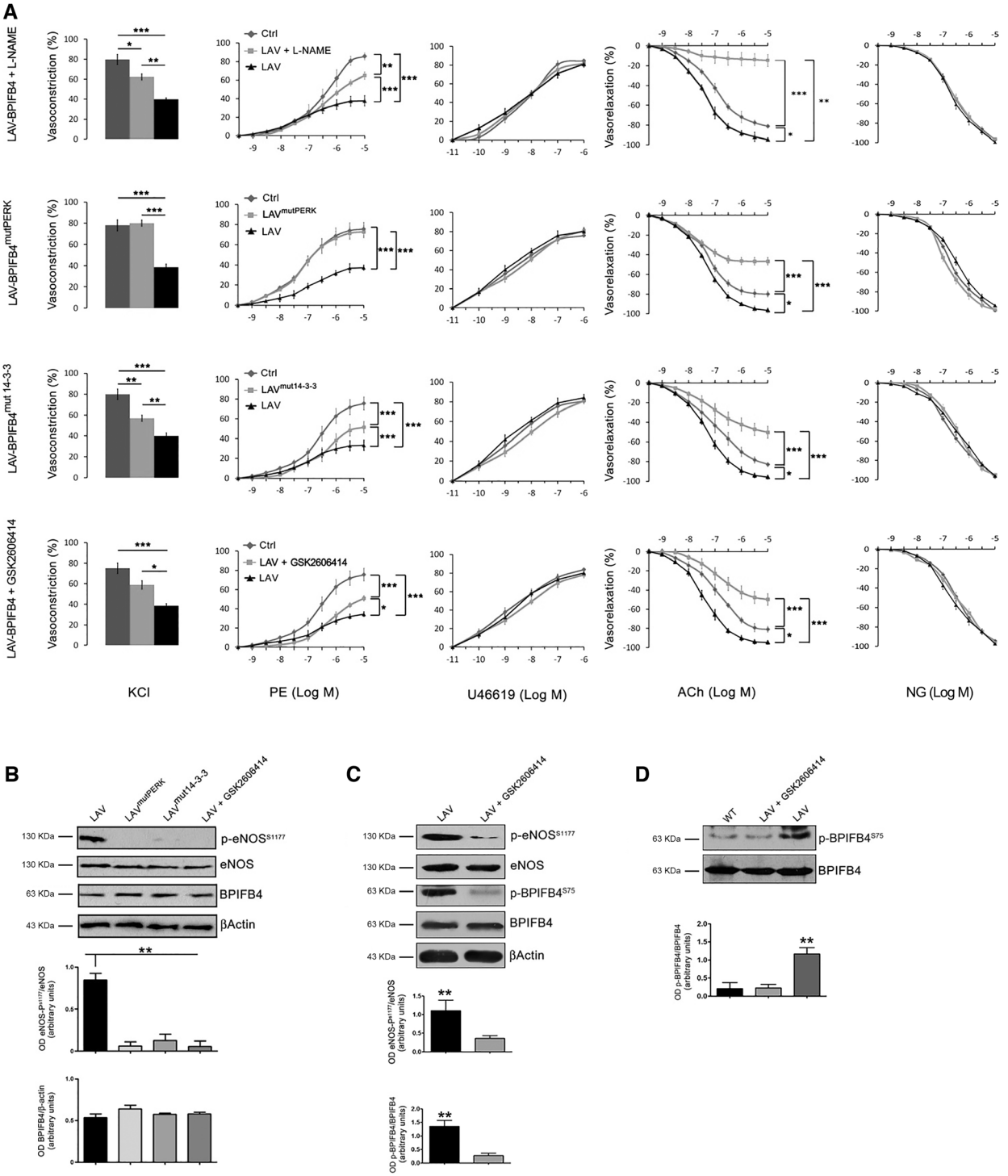

Figure 3 . Effect of the nitric oxide (NO) inhibitor L-NAME, LAV-BPIFB4^{mutPERK}, LAV-BPIFB4$^{mut14-3-3}$, and the PERK inhibitor GSK2606414 on LAV-BPIFB4-mediated vascular reactivity and on phosphorylation of eNOS in mesenteric arteries. A, Graphs show, from left to right, the vascular response of ex vivo mouse mesenteric arteries to potassium (80 mmol/L KCl) and the dose responses to phenylephrine (PE), the thromboxane agonist U46619, acetylcholine (ACh), to nitroglycerin (NG) before (-◆-) and after transfection with LAV-BPIFB4 (-▲-), or after transfection with LAV-BPIFB4 plus L-NAME (300 μM) in the first row, LAV-BPIFB4^{mutPERK} in the second row, LAV-BPIFB4$^{mut14-3-3}$ in the third row, and LAV-BPIFB4 plus GSK2606414 (0.5 μM; -■-) in the last row. Values are means±SEM. N=7 experiments per group. Statistics was performed using ANOVA; *P<0.05; **P<0.01; ***P<0.001 before vs after transfection or treatment. **B,** Western blot of 7 pooled experiments on ex vivo mouse mesenteric arteries transfected with LAV-BPIFB4, LAV-BPIFB4 ^{mutPERK}, LAV-BPIFB4$^{mut14-3-3}$, or LAV-BPIFB4 plus GSK2606414. Graphs show quantification of eNOS phosphorylation and BPIFB4. Values are means±SEM, N=2 pools of experiments. **C**, Western blot of 4 pooled experiments on ex vivo mouse mesenteric arteries with LAV-BPIFB4 or LAV-BPIFB4 plus GSK2606414. Graphs show quantification of eNOS and BPIFB4 phosphorylation. N=3 pool of experiments. **D**, Western blot of 4 pooled experiments on ex vivo mouse mesenteric arteries with WT-BPIFB4, LAV-BPIFB4 alone LAV-BPIFB4 plus GSK2606414. Graphs show quantification of eNOS and BPIFB4 phosphorylation. N=3 pool of experiments. For B, C, and D, statistics was performed using ANOVA; **P<0.01. BPIFB4 indicates bactericidal/permeability-increasing fold-containing-family-B-member-4; and LAV, longevity-associated variant.

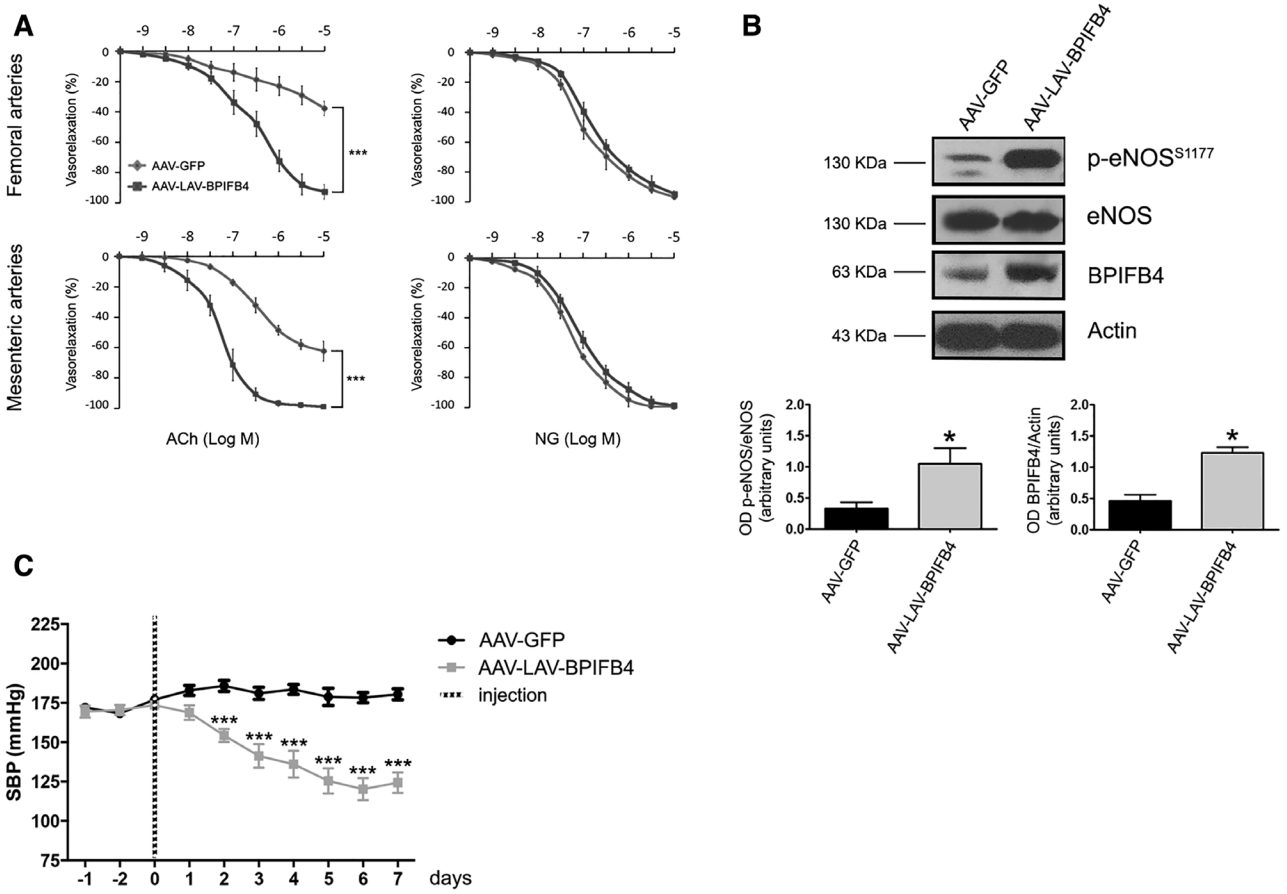

Figure 4 . Treatment of hypertensive rats with AAV-LAV-BPIFB4 results in pressure normalization. A, Graph of the vascular response to acetylcholine (ACh) and nitroglycerin (NG) of ex vivo femoral and mesenteric arteries from spontaneously hypertensive rats (SHRs) injected with AAV-GFP (-◆-; n=5) or AAV-LAV-BPIFB4 (-■-; n=5). Values are means±SEM. **B**, Representative Western blot for endothelial nitric oxide synthase (eNOS) phosphorylation and BPIFB4 in femoral arteries from SHRs injected with AAV-GFP or AAV-LAV-BPIFB4. The right graph gives the quantification of eNOS phosphorylation and BPIFB4 of 3 pooled experiments. **C**, Systolic blood pressure (SBP) of SHR treated with AAV-GFP (-●-; n=5) or AAV-LAV-BPIFB4 (-■-; n=5). Values are means±SEM. Statistics was performed using ANOVA; **P*<0.05; ****P*<0.001. BPIFB4 indicates bactericidal/permeability-increasing fold-containing-family-B-member-4; GFP, green fluorescent protein; and LAV, longevity-associated variant.

an imbalance between vasodilator and vasoconstriction substances and a progressive reduction in NO bioavailability.[36,45,46] We confirm these typical features in old mice and provide new evidence of their association with downregulation of BPIFB4 (Figure 5B), thus strengthening the rationale for LAV-BPIFB4 gene therapy. Importantly, systemic delivery of AAV-LAV-BPIFB4 upregulates BPIFB4 and restores endothelial vasorelaxation and eNOS phosphorylation to the levels found in young animals (Figure 5A and 5B). The vasoactive effect was endothelium-dependent as denoted in experiments using NG (Figure 5A). Additionally, administration of AAV-LAV-BPIFB4 reduces blood pressure levels in both young and old mice (Figure 5C).

In Vivo Gene Therapy With LAV-BPIFB4 Enhances Postischemic Reparative Neovascularization and Reperfusion

We then evaluated the therapeutic effect of AAV-LAV-BPIFB4 on revascularization, a process reduced during aging and 1 dependent on efficient homing of circulating proangiogenic cells.[47] We investigated whether circulating progenitor cell homing to the ischemic muscles was enhanced by AAV-LAV-BPIFB4. To this end, lineage negative cKit$^+$Sca-1$^+$ cells and subpopulations of CD34$^-$ and CD34$^+$ Lin$^-$ Sca-1$^+$cKit$^+$ cells—which in the mouse represent long-term and short-term reconstituting hematopoietic stem cells, respectively—were counted in enzymatically digested ischemic muscles 3 days after induction of ischemia (Online Figure XXIIA). The gating strategy for identification of these progenitor cell populations is shown in Online Figures XXIIA and XXIII. AAV-LAV-BPIFB4 increased the recruitment of total and both short- and long-term reconstituting Lin$^-$ Sca-1$^+$cKit$^+$ cells to ischemic muscle (Online Figure XXIIB). This finding suggests a therapeutic effect of LAV-BPIFB4 in ischemic vascular disease. Accordingly, in the mouse hindlimb ischemia model, AAV-LAV-BPIFB4 induced a significant recovery of superficial blood flow, as assessed by laser Doppler scanning at the level of the foot and whole limb 3 weeks after unilateral ligature of the femoral artery (Figure 6A; Online Figure XXIV). A tendency of blood flow to improve was also observed in mice given AAV-WT-BPIFB4, but the effect did not reach statistical significance. The hemodynamic benefit exerted by AAV-LAV-BPIFB4 corresponded with an increase in capillary and arteriole density (Online Figure XXV and

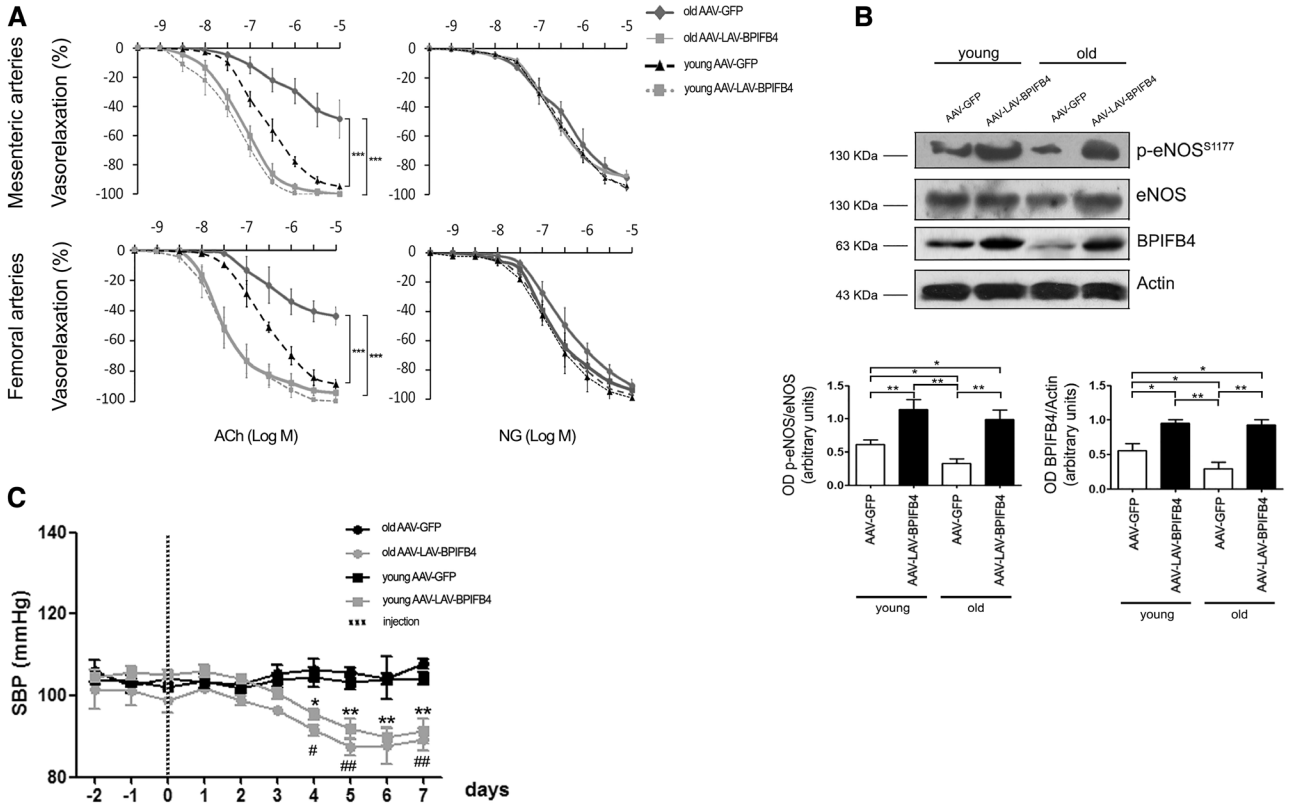

Figure 5 . Effect of AAV-LAV-BPIFB4 on blood pressure, vascular reactivity, and endothelial nitric oxide synthase (eNOS) phosphorylation in old and young mice. A, Graphs show vascular responses to acetylcholine (ACh) and nitroglycerin (NG) of mesenteric and femoral arteries from old and young mice injected with AAV-GFP (-▲-n=5; -◆-n=5) or AAV-LAV-BPIFB4 (-■-n=5; -■-n=5). Values are means±SEM. **B**, Western blot of 5 pooled experiments on mesenteric arteries injected from mice given AAV-GFP or AAV-LAV-BPIFB4. Graphs show quantification of eNOS phosphorylation and BPIFB4. Values are means±SEM, N=3 pools of experiments. **C**, Systolic blood pressure (SBP) in old and young mice treated with AAV-GFP (-●-n=5; -■-n=5) or AAV-LAV-BPIFB4 (-●-n=5; -■-n=5). Values are means±SEM. Statistics was performed using ANOVA; **P*<0.05; ***P*<0.01. BPIFB4 indicates bactericidal/permeability-increasing fold-containing-family-B-member-4; GFP, green fluorescent protein; and LAV, longevity-associated variant.

Online Tables VIII and IX). In this model, AAV-LAV-BPIFB4 was injected systemically through the tail vein. To confirm transgene expression, we performed additional immunohistochemistry studies that confirm the transgene expression in limb muscles, at the level of capillaries and arterioles (Online Figure XXVI and Online Text IX). Additionally, we investigated the impact of AAV-LAV-BPIFB4 on the expression of proangiogenic and oxidative stress scavenging factors. Results show the upregulation of vascular endothelial growth factor (VEGF) and SOD-3 in ischemic muscles of AAV-LAV-BPIFB4-injected mice. Furthermore, similar inductive phenomena were observed in femoral arteries (Figure 6B).

To be noted, we observed a transient reduction in blood pressure after the intravenous administration of AAV-LAV-BPIFB4 similarly to what observed with intra-arterial procedure, as shown in Online Figure XXVII. This is in keeping with improved native angiogenic response induced by vasodilator peptides, proteins, and drugs impacting on NO formation, like kinins, kallikrein, and converting enzyme inhibitors, which also favor blood pressure reduction.[48–50]

Discussion

Recent landmark studies have significantly improved our understanding of the genetic determinants of slow aging.[51–53] Unfortunately, only apolipoprotein E (APOE) ε4 has reached the penalizing genome-wide threshold of significance to date.[20] Therefore, to identify genes and genetic variants that influence human health through interaction with environmental factors, alternative approaches are needed, such as multistage study designs aimed at reducing the statistical penalty.[18,20,54,55] In line with this, the present study adopted a combination of a multistage genetic and functional approach to investigate whether a candidate gene, that is, BPIFB4, is associated with exceptional longevity. Our findings strongly indicate the pivotal role of BPIFB4 in preserving the ability to activate an adaptive stress response and proteostasis, 2 physiological processes negatively affected by aging.[6]

BPIFB4 belongs to the superfamily of bactericidal BPI/PLUNC proteins, which are central to the host innate immune response against bacteria in regions of significant bacterial exposure, like the mouth, nose, and lungs. The expression of the activity-enhanced polymorphic variant LAV-BPIFB4 might initially produce privileged survival through better resistance to infectious diseases. The variant may offer additional advantages because of its ability to activate the NO-releasing enzyme eNOS. NO and peroxynitrite, which is generated by the interaction of NO with $O2^-$ during the respiratory burst, are mediators of the bactericidal effects of macrophages through inactivation of heme-containing enzymes, including cytochrome oxidases and cytochrome P450. Interestingly,

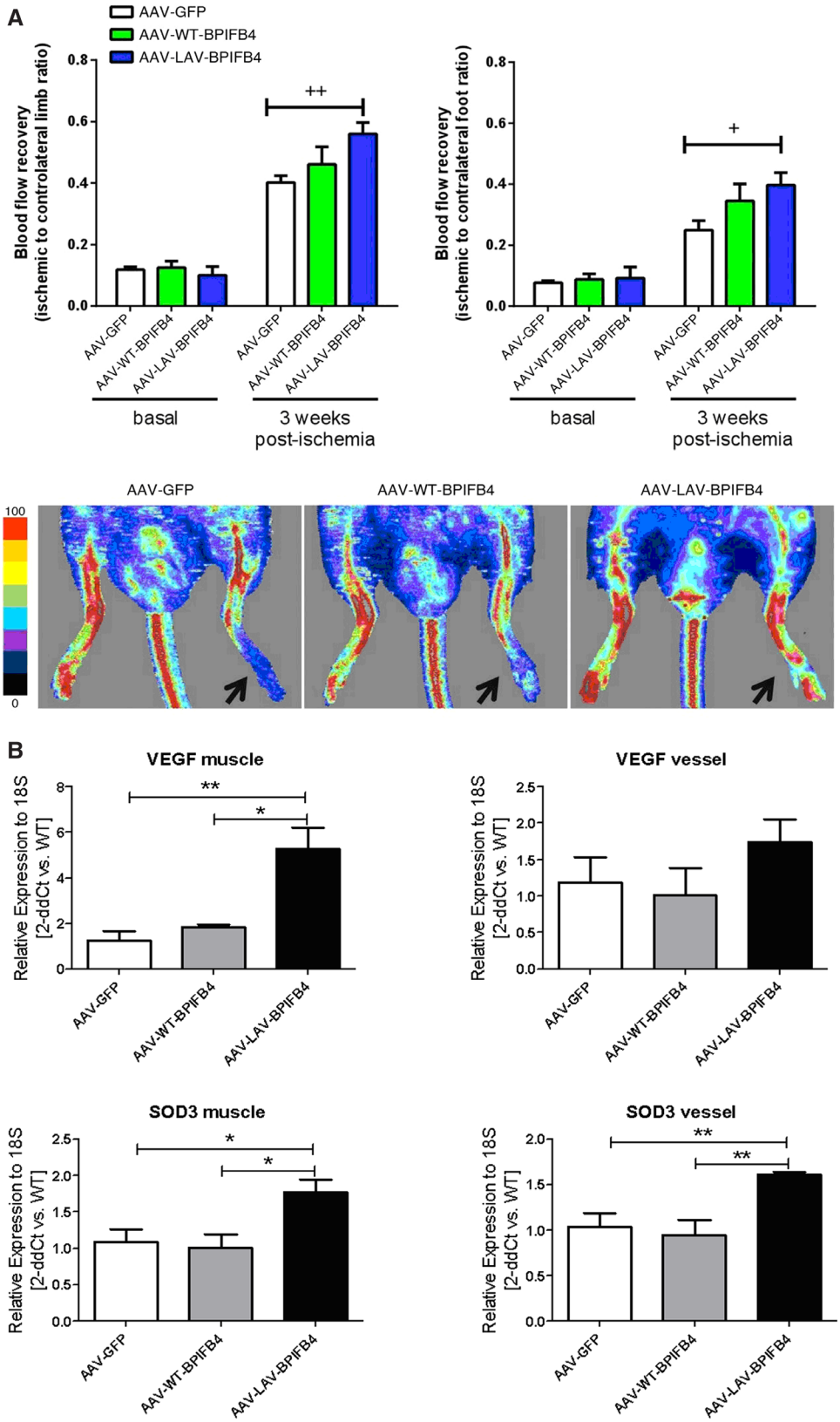

Figure 6 . Effect of longevity-associated variant (LAV)-BPFIB4 on postischemic recovery of superficial blood flow in mice. A, Bar graph and representative images of blood flow recovery at the level of limb and foot, as assessed by laser Doppler flowmetry; arrows indicate the ischemic side 3 weeks postprocedure. Values are mean±SE of N=10 per group. **B**, Bar graphs show expression of vascular endothelial growth factor (VEGF) and SOD-3 in muscles and femoral arteries 1 week postischemia (N=4 per group). BPIFB4 indicates bactericidal/permeability-increasing fold-containing-family-B-member-4.

development and refining of this prosurvival mechanism has facilitated exceptional longevity by ensuring better adaptation to stress conditions through improved function of ribosomal biogenesis, protein synthesis, and cardiovascular homeostasis.

Data from gene arrays of HEK293T cells indicate that BPIFB4 activates adaptive stress responses and proteostasis, 2 key aspects for improved organism survival,[9] as well as stem cell maintenance.[30] Analysis of BPIFB4's sequence revealed a phosphorylation site for PERK, which is a further link between BPIFB4 and the stress response. A key element that makes LAV-BPIFB4 uniquely suited to confer physiological advantages is its peculiar ability to be superiorly phosphorylated by PERK and, thereby recruit the eNOS-activating factor HSP90. Although both LAV-BPIFB4 and WT-BPIFB4 can form an activated complex with HSP90, only LAV-BPIFB4 is capable of making this complex more productive for eNOS activation through post-transcriptional modulation by 14-3-3. In this regard, BPIFB4 sequence analysis revealed an atypical 14-3-3 binding site. Thus, 14-3-3 may modulate BPIFB4-mediated cell signaling by binding and retaining the latter within the cytoplasm on the basis of its phosphorylation status at serine 75. In fact, immunoprecipitation and confocal microscopy studies showed the LAV-BPIFB4 complexes efficiently with 14-3-3, a phenomenon that apparently did not occur with WT-BPIFB4. In support of the importance of PERK-mediated phosphorylation at serine 75 and of serine 82 for LAV-BPIFB4's binding to 14-3-3, LAV-BPIFB4$^{mut14\text{-}3\text{-}3}$, LAV-BPIFB4^{mutPERK}, or LAV-BPIFB4 with GSK2606414 (PERK inhibitor) failed to immunoprecipitate 14-3-3.

A landmark finding of this study is the recognition that BPIFB4 plays a crucial role in maintenance of vascular homeostasis and that LAV-BPIFB4 exerts extraprotection. We show that biomechanical stress caused by increased arterial pressure upregulates BPIFB4 expression and that BPIFB4 silencing induces eNOS/endothelial dysfunction. Moreover, we found that LAV-BPIFB4 potentiated eNOS signaling in mouse vessels. In line with cellular data, studies in isolated vessels showed that the LAV-BPIFB4/HSP90 complex was dependent on PERK phosphorylation and 14-3-3 binding, with endothelial dysfunction ensuing on transfection of vessels with LAV-BPIFB4$^{mut14\text{-}3\text{-}3}$, LAV-BPIFB4^{mutPERK}, or LAV-BPIFB4 with GSK2606414. Similarly, WT-BPIFB4 binds to HSP90 and modulates endothelial function through a 14-3-3-mediated mechanism, as shown by mutagenesis of serine 82 (WT-BPIFB4$^{mut14\text{-}3\text{-}3}$). However, LAV-BPIFB4 may have a more potent vasculoprotective effect because of its increased ability to bind 14-3-3.

Endothelial dysfunction is a systemic pathological state characterized by a reduction in the bioavailability of and responsiveness to vasodilators, and altered vascular wall metabolism. Because of its major causal role in cardiovascular diseases, such as hypertension and ischemia, therapeutic agents that restore endothelial function are of clinical interest. In this context, a body of evidence pinpoints eNOS as a major player in blood pressure homeostasis and eNOS downregulation as a hallmark of cardiovascular disease.[56] Hence, we evaluated the effect of LAV-BPIFB4 in a rat model of essential hypertension characterized by impaired endothelial function. The in vivo administration of LAV-BPIFB4 normalized blood pressure levels and endothelial function in genetically hypertensive rats, without influencing vascular remodeling.

It is well known that cardiovascular risk is markedly increased in aged individuals. Our results show the association of dysfunctional endothelial-dependent vasorelaxation, reduced eNOS phosphorylation, and BPIFB4 downregulation in old mice. Importantly, we also newly demonstrate that forced BPIFB4 expression by AAV-LAV-BPIFB4 restores endothelium-dependent vasorelaxation, eNOS phosphorylation, and reduces blood pressure levels in old mice.

These results strongly candidate LAV-BPIFB4 as new therapeutic agent able to enhance endothelial NO release and reduce high blood pressure levels. We also recorded the higher expression of *BPIFB4* in the CD34^{+} cells of LLIs and the absence of migration ability in EPCs after SDF-1 stimulation in the absence of BPIFB4. Thus, high levels of BPIFB4 could protect LLIs by improving revascularization, a process dependent on the migration ability of EPCs.[47] In line, in a mouse model of hindlimb ischemia, LAV-BPIFB4 exerted a beneficial effect, significantly increasing homing of progenitor cells, enhancing blood flow, and spontaneous revascularization in the affected limb. Of note, only the LAV isoform confers substantial protection from acute ischemia through potentiation of vascular repair, which is associated with activation of VEGF and SOD3 in ischemic skeletal muscles, suggesting a role of proangiogenic and ROS scavenging mechanisms. More studies are needed to clarify the role of the effect of blood pressure lowering on this vascular phenotype. In conclusion, BPIFB4 is a multitasking protein involved in processes that are important for cellular and organism homeostasis and whose role in modulating eNOS is potentiated by the variations harbored by the LAV isoform. We have unraveled the molecular determinants linking functional vasculature responses, endothelial function, and a specific genetic trait and have identified BPIFB4 as a potential tool for innovative therapeutic strategies for aging, vascular repair, and endothelial dysfunction. Finally, we have found that genetic traits enriched in centenarians might be exploited to combat and attenuate cardiovascular disease at earlier stages of life. Thus, investigating exceptional longevity could bestow us with new knowledge instrumental to extending a clinical benefit to the population at large.

Acknowledgments

We thank the Doctorate School of Translational and Molecular Medicine (DIMET), Università degli Studi di Milano–Bicocca, Italy (F. Villa), and the Doctorate School of Molecular Medicine, Università degli Studi di Milano, Italy (A. Ferrario and C.C. Spinelli).

Sources of Funding

This work was supported by FIRB grants from the Italian Ministry of University and Research (AUTOMED–RBAP11Z3YA to A.A. Puca); Italian Ministry of Health (Giovani Ricercatori 2010 2302354); ITALBIONET (Italian Bioinformatics Network to R. Bellazzi); by Fondazione Umberto Veronesi fellowship (to A. Ferrario), and British Heart Foundation and Medical Research Council (to P. Madeddu).

Disclosures

A.A. Puca and C. Vecchione have filed a patent. The other authors report no conflicts.

References

1. Balch WE, Morimoto RI, Dillin A, Kelly JW. Adapting proteostasis for disease intervention. *Science*. 2008;319:916–919. doi: 10.1126/science.1141448.
2. Preissler S, Deuerling E. Ribosome-associated chaperones as key players in proteostasis. *Trends Biochem Sci*. 2012;37:274–283. doi: 10.1016/j.tibs.2012.03.002.
3. Hsu AL, Murphy CT, Kenyon C. Regulation of aging and age-related disease by DAF-16 and heat-shock factor. *Science*. 2003;300:1142–1145. doi: 10.1126/science.1083701.
4. Tothova Z, Kollipara R, Huntly BJ, Lee BH, Castrillon DH, Cullen DE, McDowell EP, Lazo-Kallanian S, Williams IR, Sears C, Armstrong SA, Passegué E, DePinho RA, Gilliland DG. FoxOs are critical mediators of hematopoietic stem cell resistance to physiologic oxidative stress. *Cell*. 2007;128:325–339. doi: 10.1016/j.cell.2007.01.003.
5. Paik JH, Ding Z, Narurkar R, et al. FoxOs cooperatively regulate diverse pathways governing neural stem cell homeostasis. *Cell Stem Cell*. 2009;5:540–553. doi: 10.1016/j.stem.2009.09.013.
6. Rando TA. Stem cells, ageing and the quest for immortality. *Nature*. 2006;441:1080–1086. doi: 10.1038/nature04958.
7. Mercken EM, Carboneau BA, Krzysik-Walker SM, de Cabo R. Of mice and men: the benefits of caloric restriction, exercise, and mimetics. *Ageing Res Rev*. 2012;11:390–398. doi: 10.1016/j.arr.2011.11.005.
8. Zhang QJ, McMillin SL, Tanner JM, Palionyte M, Abel ED, Symons JD. Endothelial nitric oxide synthase phosphorylation in treadmill-running mice: role of vascular signalling kinases. *J Physiol*. 2009;587:3911–3920. doi: 10.1113/jphysiol.2009.172916.
9. Nisoli E, Tonello C, Cardile A, Cozzi V, Bracale R, Tedesco L, Falcone S, Valerio A, Cantoni O, Clementi E, Moncada S, Carruba MO. Calorie restriction promotes mitochondrial biogenesis by inducing the expression of eNOS. *Science*. 2005;310:314–317. doi: 10.1126/science.1117728.
10. Kolluru GK, Bir SC, Kevil CG. Endothelial dysfunction and diabetes: effects on angiogenesis, vascular remodeling, and wound healing. *Int J Vasc Med*. 2012;2012:918267. doi: 10.1155/2012/918267.
11. Bir SC, Xiong Y, Kevil CG, Luo J. Emerging role of PKA/eNOS pathway in therapeutic angiogenesis for ischaemic tissue diseases. *Cardiovasc Res*. 2012;95:7–18. doi: 10.1093/cvr/cvs143.
12. Walsh T, Donnelly T, Lyons D. Impaired endothelial nitric oxide bioavailability: a common link between aging, hypertension, and atherogenesis? *J Am Geriatr Soc*. 2009;57:140–145. doi: 10.1111/j.1532-5415.2008.02051.x.
13. Moncada S, Higgs EA. Molecular mechanisms and therapeutic strategies related to nitric oxide. *FASEB J*. 1995;9:1319–1330.
14. Terry DF, Sebastiani P, Andersen SL, Perls TT. Disentangling the roles of disability and morbidity in survival to exceptional old age. *Arch Intern Med*. 2008;168:277–283. doi: 10.1001/archinternmed.2007.75.
15. Perls TT, Wilmoth J, Levenson R, Drinkwater M, Cohen M, Bogan H, Joyce E, Brewster S, Kunkel L, Puca A. Life-long sustained mortality advantage of siblings of centenarians. *Proc Natl Acad Sci U S A*. 2002;99:8442–8447. doi: 10.1073/pnas.122587599.
16. Heyn H, Li N, Ferreira HJ, et al. Distinct DNA methylomes of newborns and centenarians. *Proc Natl Acad Sci U S A*. 2012;109:10522–10527. doi: 10.1073/pnas.1120658109.
17. Bingle CD, Seal RL, Craven CJ. Systematic nomenclature for the PLUNC/PSP/BSP30/SMGB proteins as a subfamily of the BPI fold-containing superfamily. *Biochem Soc Trans*. 2011;39:977–983. doi: 10.1042/BST0390977.
18. Novelli V, Viviani Anselmi C, Roncarati R, Guffanti G, Malovini A, Piluso G, Puca AA. Lack of replication of genetic associations with human longevity. *Biogerontology*. 2008;9:85–92. doi: 10.1007/s10522-007-9116-4.
19. Geesaman BJ, Benson E, Brewster SJ, Kunkel LM, Blanché H, Thomas G, Perls TT, Daly MJ, Puca AA. Haplotype-based identification of a microsomal transfer protein marker associated with the human lifespan. *Proc Natl Acad Sci U S A*. 2003;100:14115–14120. doi: 10.1073/pnas.1936249100.
20. Nebel A, Kleindorp R, Caliebe A, et al. A genome-wide association study confirms APOE as the major gene influencing survival in long-lived individuals. *Mech Ageing Dev*. 2011;132:324–330. doi: 10.1016/j.mad.2011.06.008.
21. Malovini A, Illario M, Iaccarino G, et al. Association study on long-living individuals from Southern Italy identifies rs10491334 in the CAMKIV gene that regulates survival proteins. *Rejuvenation Res*. 2011;14:283–291. doi: 10.1089/rej.2010.1114.
22. Spinetti G, Fortunato O, Cordella D, Portararo P, Kränkel N, Katare R, Sala-Newby GB, Richer C, Vincent MP, Alhenc-Gelas F, Tonolo G, Cherchi S, Emanueli C, Madeddu P. Tissue kallikrein is essential for invasive capacity of circulating proangiogenic cells. *Circ Res*. 2011;108:284–293. doi: 10.1161/CIRCRESAHA.110.236786.
23. Urbich C, Dimmeler S. Endothelial progenitor cells: characterization and role in vascular biology. *Circ Res*. 2004;95:343–353. doi: 10.1161/01.RES.0000137877.89448.78.
24. Kränkel N, Katare RG, Siragusa M, et al. Role of kinin B2 receptor signaling in the recruitment of circulating progenitor cells with neovascularization potential. *Circ Res*. 2008;103:1335–1343. doi: 10.1161/CIRCRESAHA.108.179952.
25. Urbich C, Dimmeler S. Endothelial progenitor cells functional characterization. *Trends Cardiovasc Med*. 2004;14:318–322. doi: 10.1016/j.tcm.2004.10.001.
26. Vecchione C, Patrucco E, Marino G, et al. Protection from angiotensin II-mediated vasculotoxic and hypertensive response in mice lacking PI3Kgamma. *J Exp Med*. 2005;201:1217–1228. doi: 10.1084/jem.20040995.
27. Vecchione C, Aretini A, Marino G, Bettarini U, Poulet R, Maffei A, Sbroggiò M, Pastore L, Gentile MT, Notte A, Iorio L, Hirsch E, Tarone G, Lembo G. Selective Rac-1 inhibition protects from diabetes-induced vascular injury. *Circ Res*. 2006;98:218–225. doi: 10.1161/01.RES.0000200440.18768.30.
28. Zacchigna L, Vecchione C, Notte A, et al. Emilin1 links TGF-beta maturation to blood pressure homeostasis. *Cell*. 2006;124:929–942. doi: 10.1016/j.cell.2005.12.035.
29. Andrault JB, Gaillard I, Giorgi D, Rouquier S. Expansion of the BPI family by duplication on human chromosome 20: characterization of the RY gene cluster in 20q11.21 encoding olfactory transporters/antimicrobial-like peptides. *Genomics*. 2003;82:172–184.
30. Vilchez D, Simic MS, Dillin A. Proteostasis and aging of stem cells. *Trends Cell Biol*. 2014;24:161–170. doi: 10.1016/j.tcb.2013.09.002.
31. Amanchy R, Periaswamy B, Mathivanan S, Reddy R, Tattikota SG, Pandey A. A curated compendium of phosphorylation motifs. *Nat Biotechnol*. 2007;25:285–286. doi: 10.1038/nbt0307-285.
32. Liu YC, Liu Y, Elly C, Yoshida H, Lipkowitz S, Altman A. Serine phosphorylation of Cbl induced by phorbol ester enhances its association with 14-3-3 proteins in T cells via a novel serine-rich 14-3-3-binding motif. *J Biol Chem*. 1997;272:9979–9985.
33. Zhang K, Kaufman RJ. Signaling the unfolded protein response from the endoplasmic reticulum. *J Biol Chem*. 2004;279:25935–25938. doi: 10.1074/jbc.R400008200.
34. Sato S, Fujita N, Tsuruo T. Regulation of kinase activity of 3-phosphoinositide-dependent protein kinase-1 by binding to 14-3-3. *J Biol Chem*. 2002;277:39360–39367. doi: 10.1074/jbc.M205141200.
35. Averna M, Stifanese R, De Tullio R, Passalacqua M, Salamino F, Pontremoli S, Melloni E. Functional role of HSP90 complexes with endothelial nitric-oxide synthase (eNOS) and calpain on nitric oxide generation in endothelial cells. *J Biol Chem*. 2008;283:29069–29076. doi: 10.1074/jbc.M803638200.
36. Puca AA, Carrizzo A, Ferrario A, Villa F, Vecchione C. Endothelial nitric oxide synthase, vascular integrity and human exceptional longevity. *Immun Ageing*. 2012;9:26. doi: 10.1186/1742-4933-9-26.
37. Zincarelli C, Soltys S, Rengo G, Rabinowitz JE. Analysis of AAV serotypes 1-9 mediated gene expression and tropism in mice after systemic injection. *Mol Ther*. 2008;16:1073–1080. doi: 10.1038/mt.2008.76.
38. Schiffrin EL. Reactivity of small blood vessels in hypertension: relation with structural changes. State of the art lecture. *Hypertension*. 1992;19(2 suppl):II1–9.
39. Welsh DG, Morielli AD, Nelson MT, Brayden JE. Transient receptor potential channels regulate myogenic tone of resistance arteries. *Circ Res*. 2002;90:248–250.
40. Carnevale D, Vecchione C, Mascio G, et al. PI3Kγ inhibition reduces blood pressure by a vasorelaxant Akt/L-type calcium channel mechanism. *Cardiovasc Res*. 2012;93:200–209. doi: 10.1093/cvr/cvr288.
41. Litteri G, Carnevale D, D'Urso A, et al. Vascular smooth muscle Emilin-1 is a regulator of arteriolar myogenic response and blood pressure. *Arterioscler Thromb Vasc Biol*. 2012;32:2178–2184. doi: 10.1161/ATVBAHA.112.254664.
42. OKAMOTO K, AOKI K. Development of a strain of spontaneously hypertensive rats. *Jpn Circ J*. 1963;27:282–293.
43. Rezzani R, Porteri E, De Ciuceis C, Bonomini F, Rodella LF, Paiardi S, Boari GE, Platto C, Pilu A, Avanzi D, Rizzoni D, Agabiti Rosei E. Effects of melatonin and Pycnogenol on small artery structure and function in

spontaneously hypertensive rats. *Hypertension*. 2010;55:1373–1380. doi: 10.1161/HYPERTENSIONAHA.109.148254.
44. Intengan HD, Thibault G, Li JS, Schiffrin EL. Resistance artery mechanics, structure, and extracellular components in spontaneously hypertensive rats: effects of angiotensin receptor antagonism and converting enzyme inhibition. *Circulation*. 1999;100:2267–2275.
45. Najjar SS, Scuteri A, Lakatta EG. Arterial aging: is it an immutable cardiovascular risk factor? *Hypertension*. 2005;46:454–462. doi: 10.1161/01.HYP.0000177474.06749.98.
46. Hoffmann J, Haendeler J, Aicher A, Rössig L, Vasa M, Zeiher AM, Dimmeler S. Aging enhances the sensitivity of endothelial cells toward apoptotic stimuli: important role of nitric oxide. *Circ Res*. 2001;89:709–715.
47. Asahara T, Murohara T, Sullivan A, Silver M, van der Zee R, Li T, Witzenbichler B, Schatteman G, Isner JM. Isolation of putative progenitor endothelial cells for angiogenesis. *Science*. 1997;275:964–967.
48. Emanueli C, Minasi A, Zacheo A, Chao J, Chao L, Salis MB, Straino S, Tozzi MG, Smith R, Gaspa L, Bianchini G, Stillo F, Capogrossi MC, Madeddu P. Local delivery of human tissue kallikrein gene accelerates spontaneous angiogenesis in mouse model of hindlimb ischemia. *Circulation*. 2001;103:125–132.
49. Emanueli C, Salis MB, Stacca T, Gaspa L, Chao J, Chao L, Piana A, Madeddu P. Rescue of impaired angiogenesis in spontaneously hypertensive rats by intramuscular human tissue kallikrein gene transfer. *Hypertension*. 2001;38:136–141.
50. Murohara T, Asahara T, Silver M, Bauters C, Masuda H, Kalka C, Kearney M, Chen D, Symes JF, Fishman MC, Huang PL, Isner JM. Nitric oxide synthase modulates angiogenesis in response to tissue ischemia. *J Clin Invest*. 1998;101:2567–2578. doi: 10.1172/JCI1560.
51. Willcox BJ, Donlon TA, He Q, Chen R, Grove JS, Yano K, Masaki KH, Willcox DC, Rodriguez B, Curb JD. FOXO3A genotype is strongly associated with human longevity. *Proc Natl Acad Sci U S A*. 2008;105:13987–13992. doi: 10.1073/pnas.0801030105.
52. Schächter F, Faure-Delanef L, Guénot F, Rouger H, Froguel P, Lesueur-Ginot L, Cohen D. Genetic associations with human longevity at the APOE and ACE loci. *Nat Genet*. 1994;6:29–32. doi: 10.1038/ng0194-29.
53. Flachsbart F, Caliebe A, Kleindorp R, Blanché H, von Eller-Eberstein H, Nikolaus S, Schreiber S, Nebel A. Association of FOXO3A variation with human longevity confirmed in German centenarians. *Proc Natl Acad Sci U S A*. 2009;106:2700–2705. doi: 10.1073/pnas.0809594106.
54. Sebastiani P, Timofeev N, Dworkis DA, Perls TT, Steinberg MH. Genome-wide association studies and the genetic dissection of complex traits. *Am J Hematol*. 2009;84:504–515. doi: 10.1002/ajh.21440.
55. Ferrario A, Villa F, Malovini A, Araniti F, Puca AA. The application of genetics approaches to the study of exceptional longevity in humans: potential and limitations. *Immun Ageing*. 2012;9:7. doi: 10.1186/1742-4933-9-7.
56. Hu Z, Xiong Y, Han X, Geng C, Jiang B, Huo Y, Luo J. Acute mechanical stretch promotes eNOS activation in venous endothelial cells mainly via PKA and Akt pathways. *PLoS One*. 2013;8:e71359. doi: 10.1371/journal.pone.0071359.

Novelty and Significance

What Is Known?

- The impaired production and release of nitric oxide (NO) from endothelial cells and the decline of vascular function are hallmarks of aging and predispose the development of cardiovascular diseases.
- Exceptionally long-living individuals share common genetic features associated with protection against the onset of cardiovascular illness. Thus, a study of their genetic code could shed light on new mechanisms that control aging and disease resistance.

What New Information Does This Article Contribute?

- Through the study of multiple populations of long-living individuals, we have identified the longevity-associated variant (LAV) of the gene BPIFB4 (bactericidal/permeability-increasing fold-containing family-B-member-4).
- The forced expression of LAV-BPIFB4 both in old mice and in animal model of hypertension reduced blood pressure and rescued age-related endothelial dysfunction stimulating endothelial nitric oxide synthase activation.
- In a mouse model of hindlimb ischemia, LAV-BPIFB4 facilitated reparative angiogenesis.

Identification and characterization of molecular regulators associated with longevity are important to develop new therapies aimed at reducing cardiovascular diseases. Based on a hypothesis-free genetic approach, we identified a novel exceptional longevity-associated variant of the gene BPIFB4, which was replicated in 3 independent populations. Moreover, we found that forced expression of LAV-BPIFB4 in cells activates stress response and proteostasis, 2 hallmarks of improved cellular homeostasis. Furthermore, in comparison with young controls, LAV-BPIFB4 expression was increased in cells from centenarian subjects, indicating its protective role. On phosphorylation by the stress kinase protein-kinase-R–like endoplasmic reticulum kinase, LAV-BPIFB4 modulates endothelial nitric oxide synthase activity through 14-3-3/heat shock protein 90 complex. Finally, in the hindlimb ischemia, LAV-BPIFB4 overexpression promotes the angiogenic reparative process and the recruitment of hematopoietic stem cells. These findings identify a new therapeutic target for preventing vascular aging and related cardiovascular diseases.

SUPPLEMENTAL MATERIAL

TABLE OF CONTENTS

ONLINE TABLES

SUPPLEMENTAL REFERENCES

DETAILED ONLINE METHODS

1. LLI populations

The Italian population (comprising 410 LLIs and 553 controls) is described extensively elsewhere.[1] The German sample comprised 1,628 LLIs (age range, 95–110 years; mean age, 98.8 years) and 1,104 younger controls (age range, 60–75 years old; mean age, 66.8 years), and was first described by Nebel et al.[2] The US-American study sample consisted of 1,461 LLIs with an age range of 91–119 years (mean age, 100.8 years) and 526 controls with an age range of 0–35 years (mean age, 28.2 years); these individuals were recruited by Elixir Pharmaceuticals, either directly or through the New England Centenarian Study.[3, 4]

2. Expression of BPIFB4 in different tissues

Expression PCR analysis was performed on a multiple tissue cDNA panel (Clontech) using the following primers for the amplification BPIFB4: fw:CCCAGTATATACCAACGGCAA; rev:ATTTCTCCAGGCTGCAGCT. Amplification results were visualized on an agarose gel with ethidium bromide staining.

3. BPIFB4 RT-PCR analysis in isolated endothelial mature and progenitor cells.

HUVECs were purchased from LONZA and cultured in endothelial basal medium (EBM) supplemented with growth factors (bullet kit) and 2% foetal bovine serum. Endothelial progenitor cells (EPCs) were culture selected from circulating mononuclear cells (MNCs) isolated from peripheral blood (PB) by centrifugation on Histopaque-1077 density medium (Sigma, St. Louis, USA) as we previously described.[5] $CD34^+$ cells were separated from PB-MNCs by magnetic bead-assisted cell sorting (MACS, Miltenyi Biotec, Germany) as we have previously described.[6]

RNA extraction for BPIFB4 gene expression was performed using miRNeasy mini kit (Qiagen) and cDNA synthesis with TaqMan Reverse Transcription Reagent (Applied Biosystems). The quality and concentration of total RNA was determined using the Nanodrop ND1000 Spectrophotometer (Thermo Scientific). PCR primers for gene expression were designed with Primer3 software (fw:GGATATCACCAATGGCATGTT; rev:ATCAGGGCTCCCAGTGTG).

4. Constructs

BPIFB4 cDNA codifies a 575 amino acid protein (identifier: P59827.2) erroneously referred to as an Ile229/Asn281/Phe488/Thr494-BPIFB4 isoform, which retains only the third and fourth amino acid substitutions of the M isoform.[7] The WT- and LAV-BPIFB4 in pRK5 were generated by direct mutagenesis following the manufacturer's instructions (Quik Change Site-Directed Mutagenesis Kit, Agilent Technologies). To obtain the WT isoform, a double nucleotide change was performed to gain Phe488Leu (fw: GACGTGGACACAGAACTCTTGGCCTCATTTTC, rev:GAAAATGAGGCCAAGAGTTCTGTGTCCACGTC) and Thr494Ile (fw:CTTGGCCTCATTTTCCATAGAAGGAGATAAGCTC, rev:GAGCTTATCTCCTTCTATGGAAAATGAGGCCAAG) amino acid shifts; to obtain the LAV-BPIFB4 isoform, a double nucleotide change was performed to achieve amino acid shifts Ile229Val (fw:AGTCTTATTGGCTTCCTGGACGTCGCAGTAGAAGTGAACATCA, rev:TGATGTTCACTTCTACTGCGACGTCCAGGAAGCCAATAAGACT) and Asn281Thr (fw:ATCTCGTGGACAATTTAGTGACCCGAGTCCTGGCCGACGTCCT, rev:AGGACGTCGGCCAGGACTCGGGTCACTAAATTGTCCACGAGAT). To introduce Ser75Ala in the PERK phosphorylation site on BPIFB4, two-step mutagenesis was carried out (fw1:GATCCTTGAGTCCGAGGGAGGCATCAGGGACCTCCGAAAC, rev1:GTTTCGGAGGTCCCTGATGCCTCCCTCGGACTCAAGGATC; fw2:ATCCTTGAGTCCGAGGGAGCCATCAGGGACCTCCGAAA, rev2:TTTCGGAGGTCCCTGATGGCTCCCTCGGACTCAAGGAT). Ser82Asn was introduced to destroy the atypical binding site of the 14-3-3 complex on BPIFB4 (fw:AGGGACCTCCGAAACAATGGCTATCGCAGTGCCG, rev:CGGCACTGCGATAGCCATTGTTTCGGAGGTCCCT). All constructs were sequenced for the BPIFB4 gene.

To obtain BPIFB4 constructs in pAAV2.1 TBG eGFP3 vector, BPIFB4 cDNA was PCR amplified on pRK5 vector[8] with the following primers: AAGCGGCCGCATGCTGCAGCAAAGTGATG for the insertion of

NotI site at 5'end; GCAAGCTTTCATGCGCTCAGCACCAAAAG for the insertion of HindIII site at 3'end. PCR products were purified with Wizard SV Gel and PCR Clean Up System (Promega), digested with NotI and HindIII, and cloned in pAAV2.1 TBG vector replacing the eGFP. All constructs were sequenced for the BPIFB4 gene.

5. Transcriptome analysis

HEK293T cells were grown in culture medium (DMEM, 10% fetal bovine serum, 2 mM L-glutamine, 100 U penicillin/0.1 mg/ml streptomycin) and transfected with pRK5 vector encoding WT-, LAV-, or RV-BPIFB4, or with an empty plasmid, using Lipofectamine 2000 (Life Technologies) according to the manufacturer's protocol, in triplicates. 24 hrs after transfection, cells were serum-starved for 18 hrs and then RNA extracted using the small RNA miRNeasy Mini Kit (Qiagen). The quantity of RNA was determined using a Nanodrop Spectrophotometer, and the quality of RNA, was evaluated by capillary electrophoresis on an Agilent Bioanalyzer 2100 using an RNA nano assay. 1000mg of RNA for each sample were retro-transcript to cDNA and then to cRNA and finally amplified using the Illumina Total Prep RNA amplification Kit (Life Technologies). 750 ng of cRNA of each sample were hybridized with BeadChipIllumina according to the manufacturer's protocol. The fluorescence signals were detected with Illumina iScan. Raw gene expression data were background-subtracted, normalized using the "Rank Invariant" algorithm provided by the Illumina software, and filtered on the basis of negative control beads. Probes were considered detected with p-values ≤ 0.05 in at least one of the samples collected for each cell population. An average expression value for each gene in each population was obtained by merging the values of probes corresponding to the same gene symbol. Complete transcriptome analysis datasets are available in Gene Expression Omnibus (GEO) database (www.ncbi.nlm.nih.gov/geo) in GSE63912.

6. Expression analysis by qPCR

RNA was extracted from cells using the small RNA miRNeasy Mini Kit (Qiagen) and quantified by Nanodrop Spectrophotometer. Genomic DNA was removed by DNase I treatment. Reverse transcription was performed on 1µg of total RNA. Real-time PCR was performed by using the following primers for HSPA6 (fw:GGGGGACAAATGTGAGAAAG; rev:AGAGACAGGGGAGCCACAT), HSPA7 (fw:GGTAAGGCTAACAAGATCACCAA; rev: GGCTTCATGAACCATCCTCT), HSP40 (fw:GGCCTACGACGTGCTCAG; rev: GTGTAGCTGAAAGAGGTACCATTG), HSPA1A (fw:GAAGAAGGTGCTGGACAAGTG; rev:GATGGGGTTACACACCTGCT), mVEGF (fw:TCTCCCAGATCGGTGACAGT; rev:GGGCAGAGCTGAGTGTTAGC), mSOD3 (fw:CCTTCTTGTTCTACGGCTTGC; rev:TCGCCTATCTTCTCAACCAGG), BPIFB4 (fw: GTGGGTGTCTACCTGAGCTTGTA; rev: ACAAGACCCAGCACCACATC), 18S (fw:GTAACCCGTTGAACCCCATT; rev:CCATCCAATCGGTAGTAGCG), with GoTaq PCR Master Mix (Promega), and the results determined with 7900 real-time detection system (Applied Biosystems). Reaction mixtures (15µl) included 10 ng of cDNA and 300 nM concentrations of primers in the reaction buffer and enzyme supplied by the manufacturer. All reactions were performed in triplicate, including negative control samples, which never showed significant threshold cycles (C_T). The relative amounts of the transcripts were determined with 18S rRNA as the reference gene ($[C_{T(\text{gene of interest})} - C_{T(16S)}] = \Delta C_T$).

7. Western blotting

Western blotting was performed on transfected HEK293T, pooled protein extracts from transfected perfused vessels, or from MNCs. Protein extracts were separated on 10% SDS-PAGE at 100V for 1 hr or on 4–12% SDS-PAGE at 100V for 2 hrs and then transferred to a nitrocellulose or PVDF membrane. The membranes were incubated overnight with the following primary antibodies: anti-phospho-EIF2S1 Ser51 (Abcam, rabbit mAb, 1:1000), antiEIF2-alpha (Santa Cruz Biotechnology, mouse mAb, 1:1000), anti-phospho-eNOS Ser1177 (Cell Signaling Technology, rabbit mAb, 1:1000), anti-eNOS (Cell Signaling Technology, mouse mAb, 1:800), anti-BPIFB4 (Abcam, rabbit pAb, 1:200), anti-beta-actin (Cell Signaling Technology, mouse mAb, 1:3000), anti-PKC-alpha phospho-T497 (Abcam, rabbit mAb, 1:10000), anti-PKC-alpha (Abcam, rabbit mAb, 1:1000), anti-SIRT1 phospho-S47 (ImmunoWay Biotechnology, rabbit pAb, 1:500), and anti-SIRT1 (Biorbyt, rabbit pAb, 1:200). After a triple wash, membranes were incubated for 1 or 2 hrs with the secondary antibody (Amersham Life Science, horseradish peroxidase-linked anti-rabbit IgG or anti-mouse IgG, 1:3000). The membranes were then washed four times and specific protein bands were detected with ECL Prime chemiluminescent agents (Amersham Life Science). Western-blot data were analyzed using

ImageJ software (developed by Wayne Rasband, National Institutes of Health, USA) to determine optical density (OD) of the bands. The OD readings of phosphorylated proteins were expressed as a ratio relative to total protein or to beta-actin. All other protein expressions were normalized to beta-actin to account for variations in loading.

A specific antibody for the phosphorylated form of BPIFB4 at serine 75 was generated in collaboration with Areta International (http://www.aretaint.com/), as follows: BalbC mice were immunized with the antigen peptide EGSIRDLRNC (phosphorylated on serine) from the protein BPIFB4 administered intraperitoneally together with Freund's adjuvant (Complete FA at first dose, Incomplete FA at second and third doses, pre-fusion dose without adjuvant). Three days after the pre-fusion dose, spleen cells were fused with myeloma cells (NS0 cells). After a 2-week incubation in hypoxanthine-aminopterin-thymidine selective medium, the hybridoma supernatants were screened for antibody binding activity by ELISA. 4G3 clone was identified as specific for the specific phosphorylated peptide. The 4G3 supernatant was used for our experiments to detect phospho-Ser75 BPIFB4.

8. Co-immunoprecipitation

Forty-eight hours post-transfection, HEK293T cells were harvested and solubilized in lysis buffer (20 mMTris-HCl, pH7.5, 650 mM sodium chloride, 500 mM EDTA, 250 mM EGTA, and Triton X-100). Treatment with GSK2606414 (0.6 μM), was performed for 2h before the harvesting. The cell lysates were cleared at 13,000 rpm for 20 min at 4ºC and the protein concentration of the supernatant was determined with the Bradford Protein Assay (Bio-Rad). 700 μg protein were incubated overnight with 2 μg of anti-GFP (Invitrogen, mouse mAb), anti-14-3-3 (Abcam, mouse mAb), anti-HSP90 (Abcam, mouse mAb), and anti-IgG (Millipore, mouse pAb) for control. The antibody–antigen complexes were precipitated with protein G-linked Sepharose (GE Healthcare) for 4 hr at 4°C and the beads were washed three times with lysis buffer. The denatured co-immunoprecipitation products were resolved with SDS-PAGE, electro-blotted onto PVDF membranes, and hybridized with anti-BPIFB4 (Abcam, rabbit pAb, 1:500).

9. Immunofluorescence and confocal microscopy

HeLa cells were grown in culture medium (DMEM supplemented with 10% fetal bovine serum, 2 mM L-glutamine, 100 U penicillin/0.1 mg/ml streptomycin) in multi-chamber slides and transfected with pRK5 vector encoding WT-, or LAV-BPIFB4, or with an empty plasmid, using Lipofectamine 2000 (Life Technologies) according to the manufacturer's protocol. 24 hr post-transfection, cells were serum-starved for 2 hr, fixed in 4% paraformaldehyde in PBS for 20 min, washed twice in PBS, and permeabilized for 5 min in 0.2% Triton X-100 in PBS. Fixed cells were treated as described.[9] Fixed cells were incubated with anti-14-3-3 (Cell Signaling Technology, rabbit pAb, 1:400) overnight and then with Alexa Fluor 546 secondary antibody (1:1000). Control staining was performed with 2 μg/mL of the vital dye Hoechst 33258 (Sigma Aldrich).

The λ of the two HeNe lasers was set at 543 and at 633 nm. Fluorescence emission was revealed by 560–615 band pass filter for Alexa Fluor 546. Double-staining immunofluorescence images were acquired separately in the red and infrared channels at a resolution of 1024 x 1024 pixels, with the confocal pinhole set to one Airy unit and then saved in TIFF format. Immunofluorescence analysis of 14-3-3 and BPIFB4 was executed under an Olympus BX51 epifluorescence microscope or a Fluoview BX 61 confocal microscope with confocal system FV50 with inserted filter wavelength filters for DAPI (λ_{exc} 405 nm), FITC (λ_{exc} 488 nm), and TRITC (λ_{exc} 546 nm). The fluorescence for the nuclear dye (DAPI channel) and that for the transfected protein (FITC channel) was measured at a single-cell level by a patented cell-segmentation software (Tissue Quest, Wien, Austria).

10. Isolation and characterization of mononuclear cells

DNA was extracted from peripheral blood of healthy subjects (QIAamp DNA blood midi kit, Qiagen) and was genotyped using Taqman probe rs2070325. MNCs were isolated from the peripheral blood of appropriate donors using a density gradient media (Histopaque-1077, Sigma-Aldrich), disrupted in lysis buffer charged with phosphatase inhibitor cocktails (Sigma-Aldrich), and the protein extracts analyzed by Western blotting.

11. EPC migration assay

MNCs were isolated and EPCs enriched as described previously.[10, 11] Antigenic profile was assessed using a FACS Canto flow cytometer and FACS Diva software (Becton, Dickinson and Company). Migration was

performed as described elsewhere.[10, 12, 13] Briefly, cells ($7.5x10^4$) were seeded in the upper chamber of 5 μm pore-size filter-equipped transwell chambers (Corning) coated with fibronectin and allowed to migrate toward SDF-1⟨ (R&D) (100 ng/mL) or vehicle control (bovine serum albumin 1%) for 12 hours at 37°C. Cells migrated to the lower side of filter were counted after nuclear staining with DAPI in 5 random fields at 20X magnification.

12. Ex vivo transfection of mouse vessels and evaluation of vascular reactivity

Second-order branches of the mesenteric arterial tree were removed from C57BL6 mice and transfected as described previously.[14] Briefly, vessels were placed in a Mulvany pressure system filled with Krebs solution supplemented with 20 μg of the pRK5 vector encoding either WT-BPIFB4, LAV-BPIFB4, LAV-$BPIFB4^{mutPERK}$, or LAV-$BPIFB4^{mut14\text{-}3\text{-}3}$, or with an empty plasmid as a negative control. Some vessels were transfected with a *BPIFB4*-siRNA or a scrambled control siRNA. All vessels were perfused at 100 mmHg for 1 hr and then at 60 mmHg for 5 hrs.

The mix of four siRNA (ON-TARGET plus SMART pool l-009125-02-0005, Human C20ORF186) was used in gene silencing. All these fragments are highly specific for human BPIFB4 and three of them map the region from 101 to 242 on BPIFB4 mRNA. There are no related genes in humans with high homology to BPIFB4 so the gene silencing was highly specific.

Vasoconstriction was assessed with 80 mM KCl or with increasing doses of phenylephrine (from 10^{-9} M to 10^{-6} M) in control conditions and after L-NAME exposure (300 μM), and the corresponding values are reported as the percentage of lumen diameter change after drug administration. Responses were tested before and after transfection. Endothelium-dependent and -independent relaxations were assessed by measuring the dilatory responses of mesenteric arteries to cumulative concentrations of acetylcholine (from 10^{-9} M to 10^{-5} M) or nitroglycerine (from 10^{-9} M to 10^{-5} M), respectively, in vessels pre-contracted with U46619 at a dose necessary to obtain a similar level of pre-contraction in each ring (80% of initial KCl-evoked contraction).[15] The maximal contraction evoked by U46619 was considered as the baseline for subsequent evoked vasorelaxations. Acetylcholine vasorelaxation was also tested in the presence of GSK2606414 (0.5 μM), a PERK inhibitor, and SNX5422 (400nM) (Selleckchem, USA), a HSP90 inhibitor. Caution was taken to avoid endothelial damage; functional integrity was reflected by the response to acetylcholine (10^{-6} M).[16]

13. Vector production and purification

Adeno-associated viral vectors were produced at the AAV vector facility of TIGEM, Italy. In brief, 10-layer cell stacks containing 2.2×10^9 of low passage 293 cells were triple-transfected by calcium phosphate with 1000 μg of pAd helper, that contains the adenovirus E2A, E4, and VA RNA helper genes,[17] 520 μg of pAAV2/9 packaging plasmid with AAV rep and cap genes,[18] and 520 μg of pAAVCis. Medium was changed the following day and cells were harvested 3 days after transfection.[19] Cell lysates were purified by two rounds of cesium chloride centrifugation.[20] For each viral preparation, physical titers (GCml-1) were determined by averaging the titer achieved by dot-blot analysis[21] and by PCR quantification using TaqMan[20] (Applied Biosystems, Carlsbad, CA, USA).

14. Infection of hypertensive rats with AAV and measurements of vascular function and blood pressure

Femoral arteries of male spontaneously hypertensive rats (SHR) weighing ~250g were analyzed in this study. The experimental protocol for this project was approved by the Istituto Neurologico Mediterraneo Neuromed, Italy, and complies with NIH guidelines for care and use of laboratory animals. The animals were placed individually in an induction chamber and anesthesia was induced with 5% isoflurane in 100% oxygen with a delivery rate of 5 L/min until loss of righting reflex. After induction, the animals were moved to a homeothermic blanket (N-HB101-S-402) and placed in dorsal recumbence. Anesthesia then was maintained with 1% isoflurane in 100% oxygen with a flow of 1.5 L/min administered by means of a facemask connected to a coaxial circuit (Fluovac anesthetic mask). The procedures replicated typical clinical practice when laboratory mice are anesthetized for surgical procedures. Body temperature was maintained at 37°C with a homeothermic blanket. Animals remained anesthetized for 1 h, after which all animals received 100% oxygen until recovery of righting reflex. Vascular surgery was performed with the aid of a microscope at 2–10X magnification. Femoral arteries were exposed and isolated circumferentially from the inguinal ligament to the knee; all side branches were ligated. To obtain an isolated arterial segment, the superficial femoral

artery was first controlled proximally with two microvascular clips. After temporary clamping of the proximal and distal femoral artery, either 100 µl of saline alone or saline plus AAV-GFP or AAV-LAV-BPIFB4 was infused into the femoral artery and incubated for 15 minutes. Viral titer was 1×10^{13} GC/kg for each experimental condition. After incubation, the distal femoral artery was permanently ligated, and clamps on the proximal femoral artery were removed to restore femoral blood flow. Animals were sacrificed at seven days after surgery and infection. Femoral arteries were excised and were placed on wire system[16] to perform vascular reactivity studies. Blood pressure was evaluated in another experimental series of spontaneously hypertensive rats (11-week-old) by tail-cuff plethysmography for one week as previously described.[16]

15. ELISA quantification of BPIFB4

Quantitative determination of BPIFB4 in serum of animals treated with AAV-LAV BPIFB4 and AAV-GFP was performed with ELISA (code: CSB-EL003694HU, CUSABIO).

16. Immunofluorescence analyses of mesenteric artery

Segments of the mesenteric artery were dissected free of fat and connective tissue from C57BL6 mice injected with AAV-LAV-BPIFB4 and frozen in OCT embedding medium. Frozen sections (10um) were treated with blocking solution (2% donkey serum, 1.5% BSA, 0.5% fish gelatin) for 45 min and immunostained overnight at 4 °C in blocking solution with antibodies anti-BPIFB4 (1:100; Abcam), anti-αSMA-eFluor570 (1:400; eBioscience), sheep anti-Von Willebrand (1:100; Abcam) and revealed with appropriate secondary antibodies (Rhodamine-Red anti-mouse IgG; Jackson ImmunoResearch; Alexa Fluor 488 anti-mouse and anti-sheep IgG; Molecular Probes, Invitrogen). Nuclei were counterstained with DAPI. The images were acquired using a fluorescence (Zeiss Axio Observer A1) microscope with 40X objective.

17. Immunohistochemical analysis from infected mice tissues

Brain, adipose tissue, liver and femur from C57BL6 mice infected with AAV-LAV-BPIFB4 were fixed with 4% PFA solution and routinely processed to paraffin blocks. Tissue slices (2,5 µm) were deparaffinized in xylene and rehydrated in solutions with decreasing alcohol content. Antigen retrieval was conducted by boiling the samples in citrate buffer (sodium citrate 10 mM, 0.05% Tween-20, pH 6) and the endogenous peroxidase activity was blocked with 3% H_2O_2 in methanol for 5 min. The sections were treated with blocking solution (2% donkey serum, 1.5% BSA, and 0.5% fish gelatin) for 45 min and immunostained 1hr at room temperature in blocking solution with primary antibodies anti-BPIFB4 (1:100; Abcam). Immunohistochemistry signals were revealed by incubating the sections with Dako REAL™ EnVision™/HRP, Rabbit/Mouse (ENV) for 25min at room temperature followed by a color reaction using Dako REAL™ DAB+ Chromogen for 5 minutes. The slides were counterstained with Mayer's hematoxylin for 1 min, dehydrated, cleared and mounted.

18. FACS analyses of mice infected vessels

Endohelial cells obtained from C57BL6 mice injected with AAV-GFP and AAV-LAV-BPIFB4 were stained with antibody anti-CD31-FITC (1:100, BD, Biosciences-Pharmigen) at 4°C for 20 min and then permeabilized with cytofix/cytoperm (BD, Biosciences-Pharmigen) at 4°C for 20 min. Subsequently, cells were incubated with primary antibody anti-BPIFB4 (1:100; Abcam) at 4°C for 1 hr and an APC-conjugated anti-mouse secondary antibody (1:200; BioLegend). Analyses of cell populations were performed using a FACS Canto II equipped with FACS Diva software (BD Biosciences).

19. Infection of hindlimb ischemia mice models with AAV and measurement of superficial blood flow and neovascularization

Experiments of this section involving live animals were performed in accordance with the Guide for the Care and Use of Laboratory Animals (The Institute of Laboratory Animal Resources, 1996) and with approval of the British Home Office and the University of Bristol.

Mice were separate to 3 groups and 10 µl $1x10^{11}$ Viral vectors (AAV219-EGFP1966, AAV-LAV- BPIFB4 and AAV-WT-BPIFB4) were injected through the tail vein 16 hours before limb ischemia (n=10 per group). Following anesthesia (2,2,2tribromo ethanol, 0.3mg/kg, i.p.), unilateral limb ischemia was induced in 7-8 weeks old male CD-1 mice (Harlan, UK), using a refined procedure which consists of ligation (with a 7-0 silk suture) in 2 points and electrocoagulation of the upper part of the femoral artery. Mice were then allowed to regain consciousness.

Foot blood flow was measured immediately after ischemia and then at 7, 14 and 21 days (n=10 mice/group) by using a laser Doppler perfusion imaging system (Moor Instrument, UK).
The occurrence of necrotic toes was assessed by daily inspection and recorded. Animals with necrosis extending to the whole foot were sacrificed with an excess of anesthesia.
At 21 days after ischemia, terminally anesthetized mice (n=7 at each time point) were perfused with 10ml PBS and then 10ml 4% paraformaldehyde. Muscle cryosections with thickness of 5μm were used for immunohistochemical analysis unless specified. The capillary and arteriole densities of ischemic adductor muscles were assessed using isolectin-B4 and α-smooth muscle actin (Sigma-Aldrich, UK) staining respectively. Counts of 10 random microscopic fields were averaged and expressed as the number of capillaries and arterioles per mm^2.

20. Evaluation of the modulation in recruitment of total, and short-term and long-term reconstituting LSK cells in the ischemic muscles of AAV injected mice.

In pilot experiments we found that day 3 corresponds to the peak homing time for LSK cells to home into ischemic muscle of mice subjected to femoral artery ligation. Three groups mice (n=5 per group) were injected with 10μl $1x10^{11}$ Viral vectors (AAV219-EGFP1966, AAV-WT-BPIFB4 and AAV-LAV-BPIFB4) through the tail vein, 16 hours before induction limb ischemia The relative abundance of LSK and $CD34^+$LSK cells in PB and ischemic adductor muscles was assessed by multicolor flow cytometry. The following preparatory protocols were applied:

Isolation: LSK cells were also enriched from adductor muscles of mice undergoing limb ischemia. Muscles were harvested, minced with fine scissors and placed into a digest solution of Collagenase A 100 μg/μl (Roche), Dispase II (1X) 2.4 U/ml (Roche), DNase I 10 mg/ml (Roche), $CaCl_2$ 50 mM, $MgCl_2$ 1 M in PBS at 37°C for 1 h, triturated through 40μm diameter nylon mesh, washed with 0.2% BSA + 0.1% DNAse I in PBS.

Analyses: mouse cells were fixed with 2% PFA 10 minutes and washed with ice-cold Hank balanced salt solution containing 0.5% bovine serum albumin and 0.02% sodium azide and blocked with Fc block (Fc, eBioscience anti mouse CD16/32) and stained with antibodies against the following markers: Lineage Mixture Alexa 488 1:100 (mouse CD3e, CD11b, CD45R, Ly-6C/G, TER119, Caltag), Ly6-A/E perCP cy5.5 1:300 (Sca-1, eBioscience), CD117 Alexa780 1:300 (c-Kit, eBioscience), and CD34 Alexa 647 1:100 (eBioscience). Analyses of antigenically defined cell populations were performed using a FACS Canto II equipped with FACS Diva software (BD Biosciences).

21. Statistical analyses

Genetics The reader may refer to Malovini A et al.[1] for details about the statistical methods and procedures applied to the analysis of data deriving from the genome-wide scan. Association tests within the replication cohorts were performed by logistic regression, assuming the genetic model hypothesized by the genome-wide scan. Logistic regression was implemented in the "base" package of the R statistical software[22] (http://www.R-project.org). Meta-analysis was performed by the *metabin* function implemented in the R package called "meta" (http://www.R-project.org, http://cran.rproject.org/web/packages/meta/index.html). Statistical power calculations were performed by the QUANTO software tool (http://biostats.usc.edu/Quanto.html), setting the prevalence of longevity trait in the general population as ~ 1/10,000, as reported by Ferrario et al.[23]

Haplotype analysis SNPs showing pairwise correlation $r^2<0.80$ in the Italian cohort were identified by the PLINK software tool[24] (command: --indep-pairwise 1500 150 0.8). Positional and functional annotations of the identified SNPs were performed by the SNPNexus on-line tool (http://www.snp-nexus.org/).

BPIFB4 RT-PCR analysis in isolated endothelial mature and progenitor cells Each Real time PCR reaction was performed in triplicate, and relative expression of mRNAs was calculated by the $2^{-\Delta\Delta Ct}$ method[25] using 18S ribosomal RNA as endogenous control. Statistical analysis was performed using Mann Whitney test. Data presented as mean±SEM.

EPC migration To assess migration to the chemoattractant (SDF-1⟨), number of migrated cells with or without SDF-1⟨ were compared using Student's t-test via GraphPad Prism Software, version 5.0. Values are expressed as mean ± SE.

Expression analyses Expression data are indicatedas mean ± SEM. One-way ANOVA statistics were calculated (GraphPad Prism Software, version 5.0).
Transcriptome and GO analysis Differential expression *P*-values for the detected transcripts were computed with a permutation-based test that builds a null distribution of the fold-change values by randomly shuffling the samples' labels.[26] Modulated genes were selected using a *P*-value cut off of 0.01. Enrichment of a priori-defined gene sets was performed with the hypergeometric test and enriched GO categories with FDR corrected *P*-values ≤ 0.01 were selected with statistical and bioinformatics functions implemented in the Orange Data Mining Suite (http://orange.biolab.si/).
Western Blotting analysis Densitometry data were analyzed with Student's t-test or two-way ANOVA, as appropriate, using a dedicated software (GraphPad Prism Software, version 5.0).
Colocalization data Unpaired Student's t-test was used to compare the percentage of co-localization among the three BPIFB4 variants and nuclear area stained by Hoechst 33258 and to compare the number of co-localizing pixels of the 14-3-3 protein and WT-, and LAV-BPIFB4 signals.
MNC data Unpaired Student's t-test was used to compare the mean (± SEM) of the OD data about the wild-type, homozygous and the heterozygous carriers of the rs2070325 variation.
Ex vivo data Vessel reactivity results are given as mean ± standard error of mean (SEM). Data were analyzed with Student's t-test or two-way ANOVA followed by Bonferroni post-hoc analysis, as appropriate, using a dedicated software (GraphPad Prism Software, version 5.0).
In vivo data Measurements of mice and rat blood pressure are given as mean ± SEM. Data were analyzed with ANOVA, using a dedicated software.
Unpaired Student's t-test was used to compare the amount of cell fractions in the ischemic muscles of AAV injected mice. Values are mean ± SE.
Values of blood flow recovery were compared using unpaired Student's t-test. Values are mean ± SE.
Capillary and arteriole density data were analysed using unpaired Student's t-test. Values are mean ± SE. (GraphPad Prism Software, version 5.0).
ELISA data Unpaired Student's t-test was used to compare the colorimetric values of enzymatic reaction of ELISA kit from controls and centenarians groups.

22. Declaration of ethical approval

The study protocol for the German population was approved by the Ethics Committee of University Hospital Schleswig–Holstein (Campus Kiel), Germany, and local data protection authorities. The US-American study samples were recruited by Elixir Pharmaceuticals, either directly or through the New England Centenarian Study. The study protocol was approved by the Boston Medical Center's Institutional Review Board and by the Western Institutional Review Board.

ONLINE TEXT

Online Text I. The Southern Italian Centenarian study

We tested nearly 298,714 SNPs in 410 LLIs (age range, 90–109 years; mean age, 96.6 years) and 553 young controls (age range, 18–48 years; mean age, 33.0 years), and found 67 potential longevity-associated variants (genomic control adjusted P <1x10^{-4} under allelic, dominant, or recessive genetic models).[1] One SNP (*CAMKIV*-rs10491334), already known to be associated with diastolic blood pressure, was chosen for further study and was found to be associated with longevity also in an independent replication cohort. The other variants remained to be validated.

Online Text II. German and US study populations

The German sample comprised 1,628 LLIs (age range, 95–110 years; mean age, 98.8 years) and 1,104 younger controls (age range, 60–75 years old; mean age, 66.8 years), and was first described by Nebel et al.[2] The study protocol was approved by the Ethics Committee of University Hospital Schleswig–Holstein (Campus Kiel), Germany, and local data protection authorities. The US-American study sample consisted of 1,461 LLIs with an age range of 91–119 years (mean age, 100.8 years) and 526 controls with an age range of 0–35 years (mean age, 28.2 years); these individuals were recruited by Elixir Pharmaceuticals, either directly or through the New England Centenarian Study.[3, 4] The study protocol was approved by the Boston Medical Center's Institutional Review Board and by the Western Institutional Review Board.

Online Text III. Meta-analysis of rs2070325 and statistical power calculations

rs2070325 did not deviate significantly from the Hardy–Weinberg equilibrium in the control populations (P >0.001). Genotype counts of rs2070325 stratified by case/control condition are reported in **Online Table II**.

No statistically significant heterogeneity between the ORs estimated for the two populations was detected (Q-statistic, P>0.05; heterogeneity index, I^2 = 0%). Effect sizes were then combined assuming a fixed effects model (3,060 LLIs and 1,609 controls: OR = 1.49; 95% CI = 1.22–1.81; P = 7.59 x 10^{-5}).

Finally, fixed effects meta-analysis of the screening and replication sets (Q-statistic, P = 0.12; heterogeneity index, I^2 = 52.6%) showed a significant association even after correction for multiple testing, based on the Bonferroni correction on 155,456 SNPs showing pairwise r^2<0.8 in the SICS cohort (3,464 LLIs and 2,160 controls; OR = 1.61; 95% CI = 1.34-1.92; P= 2.4 x 10^{-7}).

The significance threshold for identifying statistically significant associations when combining the effect sizes observed in the screening and replication cohorts was identified based on the Bonferroni correction on 155,456 SNPs showing pairwise r^2<0.8 in the SICS cohort (α = 0.05 / 155,456; P < 3.22 x 10^{-7}).

Power calculations were performed according to the following settings and scenarios.

- **Screening cohort.** Results from statistical power calculations showed that the screening analysis was sufficiently powered (>0.85) to detect the effect observed for rs2070325 in the SICS cohort (OR = 2.42), according to: i) the sample size defining the screening cohort (410 LLIs vs. 553 controls); ii) the significance threshold adopted (P<0.0001); iii) the genetic model tested (recessive); and iv) the MAF observed (MAF = 0.35). Results are graphically represented in **Online Figure I**.
- **Combined replication cohorts**. Similarly, our analysis had sufficient statistical power to detect the effects observed for rs2070325 when combining the effect sizes corresponding to the two replication cohorts (power >0.90 in detecting OR = 1.49; P = 7.59 x 10^{-5}, according to: i) the sample size reached by the replication cohorts combined [3,060 LLIs vs. 1,609 controls]; ii) the significance threshold adopted [P< 0.05]; iii) the genetic model tested [recessive]; and iv) the MAF observed [MAF = 0.35]).
- **Combined screening and replication cohorts**. Finally, the statistical power reached when combining the screening and the two replication cohorts (3,464 LLIs vs. 2,160 controls) was >0.80 in detecting OR = 1.6 observed for rs2070325, according to: i) the sample size defining the screening cohort (3,464 LLIs vs. 2,160 controls); ii) the significance threshold adopted (P < 3.22 x 10^{-7}); iii) the genetic model tested (recessive); and iv) the MAF observed (MAF = 0.35).

Online Text IV. Haplotype analyses of the *BPIFB4* locus

Analysis of the haplotype distribution in 960 Caucasian individuals revealed the presence of a major allele (allele frequency, 66%) carrying the combination AACT and codifying for the wild-type (WT) Ile229/Asn281/Leu488/Ile494-BPIFB4 isoform, and a minor allele (allele frequency, 29.5%) carrying the combination GCTC and codifying for the longevity associated variant (LAV) Val229/Thr281/Phe488/Thr494-BPIFB4 isoform. A rare variant (RV), found in <2% of chromosomes, harbored only the latter two substitutions.

Online Text V. Expression of BPIFB4 in different tissues

Further analysis of BPIFB4 gene expression was assessed with RT-PCR using a commercial panel of human cDNAs (Clontech) from different tissues. We found clear expression in testis and spleen. We also interrogated different tissues and cell lines, detecting BPIFB4 expression in endothelial progenitor cells (EPCs) cultured from MNCs on fibronectin, embryonic stem (ES) cells, induced pluripotent stem (iPS) cells (but not in their originating fibroblasts), and human hypertrophic heart (in which fetal genes are re-activated) and fetal (but not in adult) heart (**Online Figure II**).

We next analyzed human umbilical vein cells (HUVECs), EPCs, circulating $CD34^+$ cells, and total MNCs in LLIs. Of note, we found that EPCs and $CD34^+$ cells had enriched expression of BPIFB4 RNA (**Online Figure IIIA**).

Online Text VI. BPIFB4 isoforms activate adaptive stress responses and proteostasis

Genome-wide transcriptional profiling indicates that BPIFB4 induces the activation of heat shock factor (HSF)1-inducible heat-shock proteins (HSPs), such as HSPA6, HSPA7, HSP40, HSPA1A, HSPB1, and HSPA9, with an increment from 4 to 50 times (**Online Figure V** and **Online Tables III–VI**). We also observed significant up-regulation of the protein translation machinery and of ribosomal biogenesis (**Online Figure VIA** and **Online Tables VI, VII**). Among the many transcripts up-regulated by BPIFB4 isoform overexpression, there was a highly significant enrichment in H/ACA RNAs essential for ribosomal RNA pseudouridylation (snoRNAs) and of spliceosomal small nuclear RNAs (scaRNAs) (**Online Tables III–VI**). The most interesting among the up-regulated scaRNAs is scaRNA19, or TERC, the malfunctioning of which brings to telomere shortening and premature aging in congenital dyskeratosis.[27] Importantly, genes transcribing exosomal mRNAs released by stressed endothelial cells were significantly up-regulated by the different BPIFB4 isoforms[28] (**Online Figure VIA** and **Online Tables III–VI**). Thus, transcriptome analysis strengthens the notion of a role for BPIFB4 in stress adaptation *via* the exosomal machinery.

Online Text VII. LAV-BPIFB4 is more cytoplasmic and forms a complex with 14-3-3 more efficiently than WT-BPIFB4

HeLa cells, characterized by an abundant cytoplasm, were selected for colocalization experiments of the different BPIFB4 isoforms with subcellular compartments/organelles. A different pattern of nuclear/cytoplasmic distribution between WT- and LAV-BPIFB4 was the first, and most evident, difference. In cells expressing WT-BPIFB4, a high percentage of protein overlapped with the nuclear marker Hoechst 33258 (left panel, white arrows), LAV-BPIFB4 had a prevalent cytoplasmic distribution (right panel, red arrows), (**Online Figure VIIIA**). Images were supported by statistical analysis on % of GFP (i.e., BPIFB4) colocalizing with the nuclear stain Hoechst 33258 (**Online Figure VIIIB**).

The peculiar distribution of the BPIFB4 isoforms was also reflected in different profiles of colocalization with protein 14-3-3, whose expression is predominantly cytoplasmic. As clearly observable in highly magnified images (**Online Figure IXA**), BPIFB4 and 14-3-3 colocalized especially when HeLa cells were transfected with LAV-BPIFB4 (right panel). In agreement, co-immunoprecipitation experiments indicate the presence of a BPIFB4–14-3-3 complex when cells were transfected with LAV-BPIFB4, while no detectable co-immunoprecipitation was observed when cells were transfected with WT-BPIFB4 (**Online Figure IX**).

Online Text VIII. Effect of eNOS inhibition on the action of LAV-BPIFB4

Acetylcholine-evoked vasorelaxation in resistance vessels depends on the action of various mediators, such as eNOS, prostanoids and endothelium-derived-hyperpolarizing factor (EDHF); the effect of each of these factors can be restricted by higher amounts of another.[29] Based on this premise and on the above observations, we inhibited eNOS with N^G-nitro-L-arginine methyl ester (L-NAME) in order to clarify whether increased vasorelaxation was effectively due to eNOS-dependent NO production in LAV-BPIFB4-expressing vessels. We found that eNOS inhibition produced more pronounced reduction of acetylcholine-evoked vasorelaxation when LAV-BPIFB4 was expressed (**Online Figure X**). This effect could be explained by higher concentrations of NO reducing the availability of the other acetylcholine vasorelaxation mediators (**Online Figure X**).

Online Text IX. Characterization of AAV injection effects on LAV-BPIFB4 expression

Data from immunohistochemistry studies show localization of BPIFB4 in vascular endothelial and smooth muscle cells of mice injected with AAV-LAV-BPIFB4 (**Online Figure XVIII**). Additionally, we report new results on quantification of BPIFB4-positive vascular cells, indicating increased level of expression in $CD31^+$/endothelial cells of mice intra-arterially injected with AAV-LAV-BPIFB4 as compared to mice injected with AAV-GFP (12.7±3.8 vs. 3.7±0.5%; P=0.01). Furthermore, AAV-LAV-BPIFB4 infection induced BPIFB4 overexpression in femoral bone marrow, brain, adipose tissue, and endothelium, but not in liver as assessed by immunohistochemistry (**Online Figure XIXA**). No differences were detected in AAV-LAV-BPIFB4 versus AAV-GFP infected rat serum (507± 92 vs 551±56 pg/mL P=0.339) and MNCs (**Online Figure XIXB**) — as measured by ELISA and western blot, respectively. Thus, infection with AAV-LAV-BPIFB4 induced overexpression of the transgenic protein in endothelial cells of two and half-folds, as calculated by western blot densitometry analysis (**Figure 4 and 5**) as well as in different organs of the body. Similar to what observed with intra-arterial injection, intra-venous delivery of AAV-LAV-BPIFB4 increased the abundance of $CD31^+$/$BPIFB4^+$ endothelial cells as compared to AAV-GFP (11.0±3.1 vs. 5.3±2.9 %; P=0.08). We also measured the expression of the transgene in the limb ischemia model, where the vector was delivered through the tail vein. We found that the transgenic protein is localized in capillaries and small arterioles, but not in skeletal myocytes, suggesting that accelerated healing is driven by vascular expression of the transgene (**Online Figure XXVI**).

ONLINE FIGURES

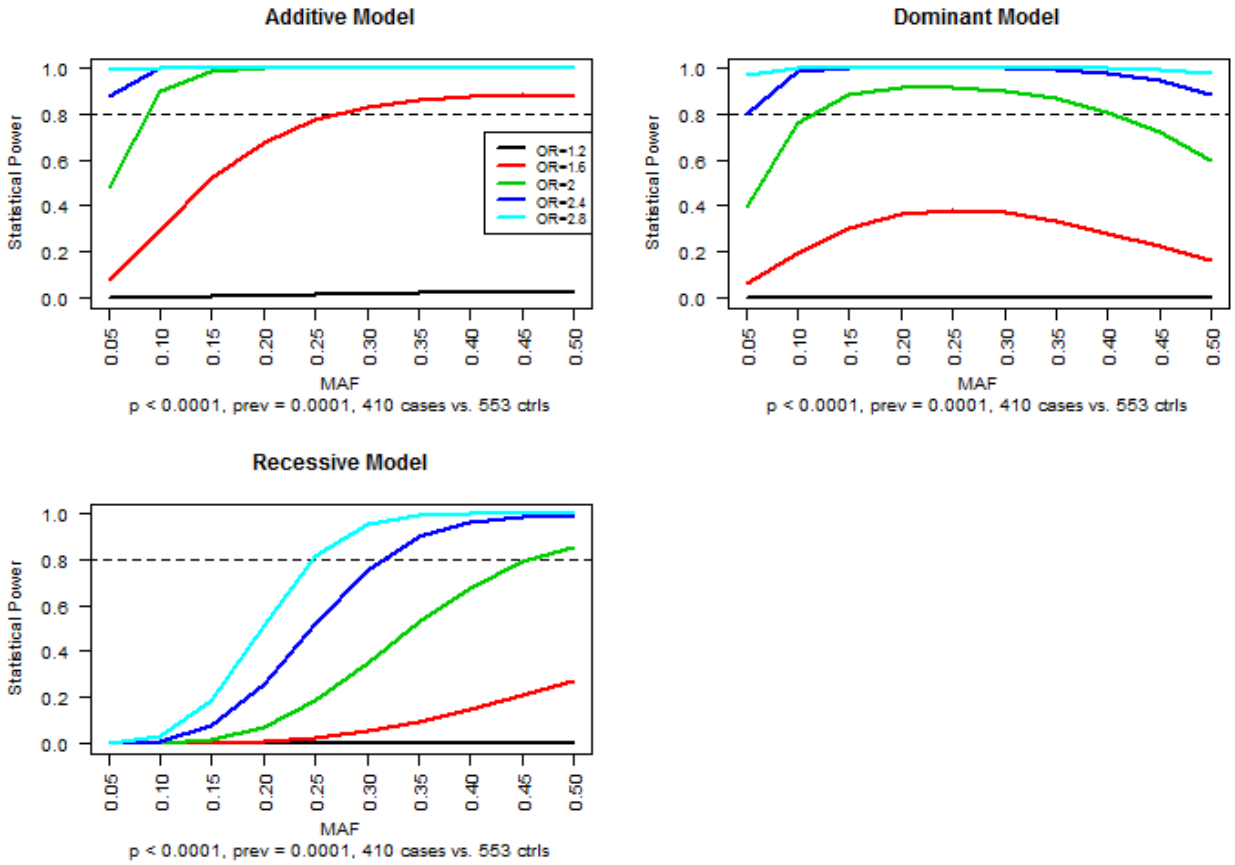

Online Figure I. Statistical power calculations for the screening set.
Each plot reports the results from statistical power calculations according to the additive, dominant and recessive models respectively. The x-axis of each plot reports the minor allele frequency, while the y-axis reports the corresponding statistical power defined according to different ORs (ranging from 1.2 to 2.8), and highlighted with different colors. The horizontal dashed line corresponds to statistical power = 0.8. Statistical power analyses were based on: i) the sample size defining the screening cohort (410 LLIs vs. 553 controls); ii) prevalence of longevity in the general population (~ 1/10,000)[23]; and iii) significance threshold (P<0.0001).

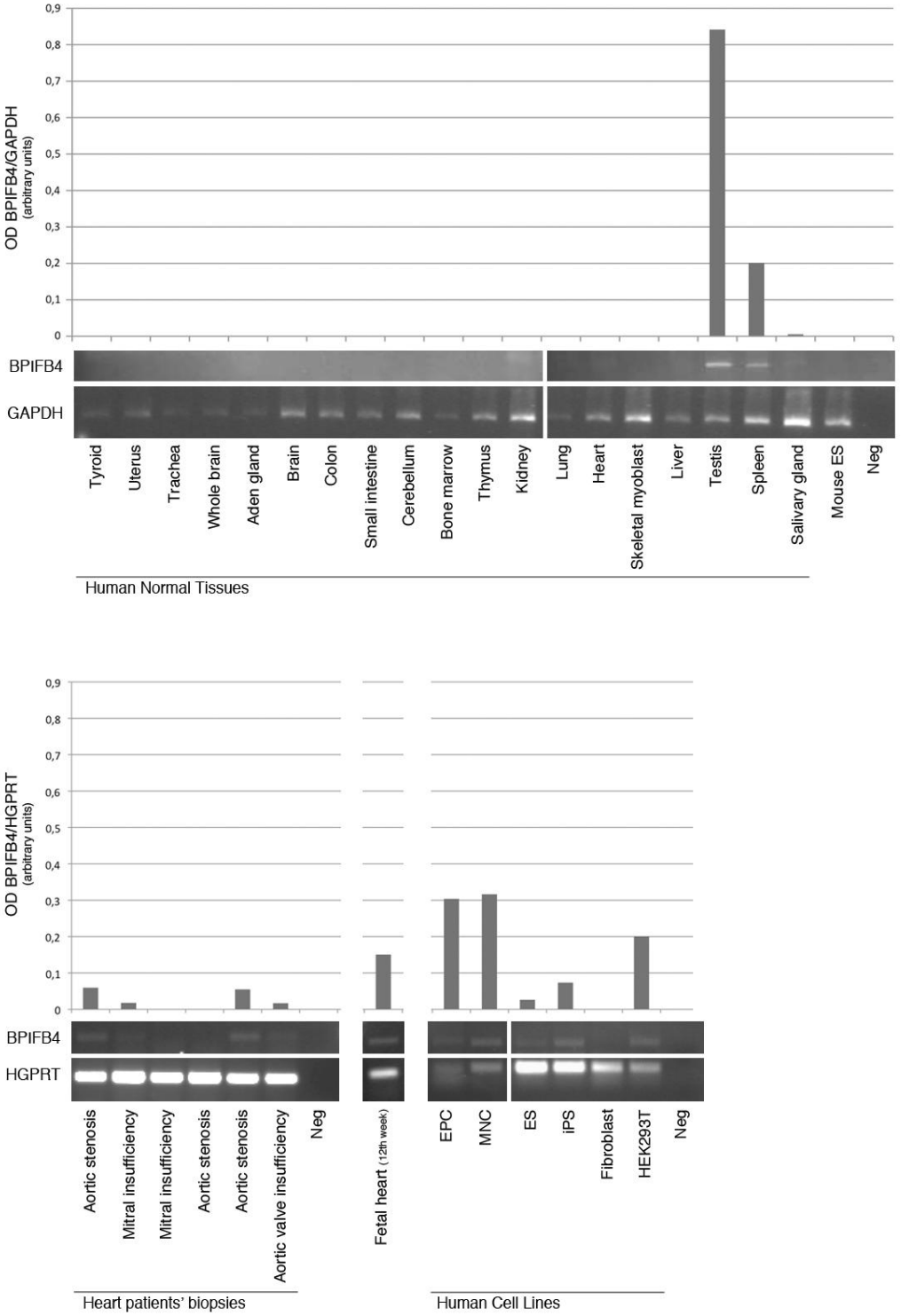

Online Figure II. Expression of BPIFB4 in different tissues.
The image shows the expression of *BPIFB4* and housekeeping genes (*GAPDH* or *HGPRT*) in different tissues (under physiological or pathological conditions) and cell lines by PCR amplification and visualization by agarose gel with ethidium bromide staining. Graphs show optical density values of BPIFB4 expression after normalization vs the housekeeping genes.

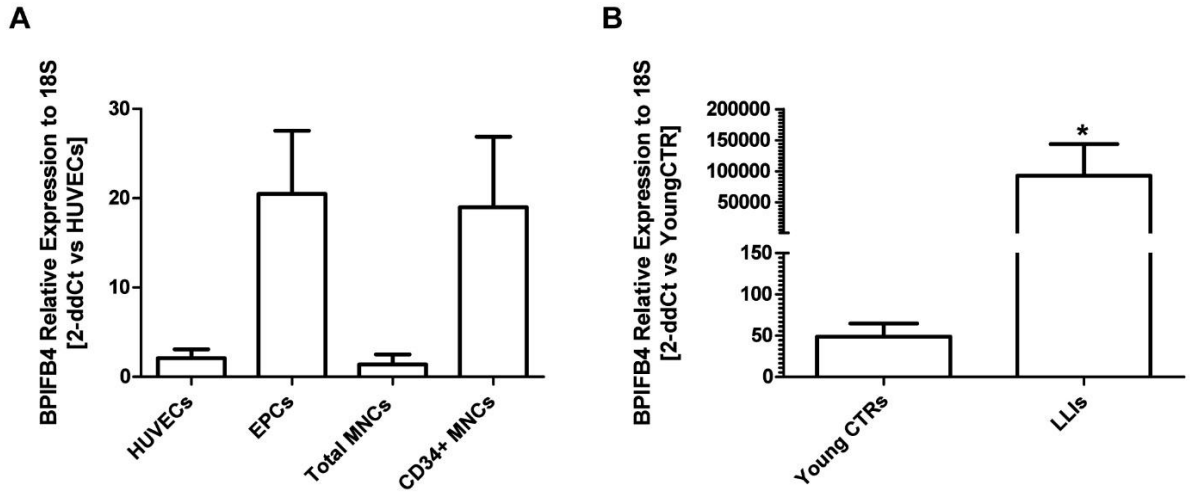

Online Figure III. *BPIFB4* is expressed by mature endothelial and progenitor cells
Graphs of average RT-PCR data showing BPIFB4 mRNA relative expression in **A,** human umbilical vein cells (HUVECs), culture-selected endothelial progenitor cells (EPCs), total peripheral blood mononuclear cells (Total MNCs), and magnetic bead-assisted sorted $CD34^+$ MNCs (N=3), and **B**, $CD34^+$ MNCs from young control volunteers (N=11, age=35±6 years) and LLIs (N=16, age=97±2 years). *, *P*=0.028 vs. CTRs (Mann Whitney test). Data presented as mean±SEM.

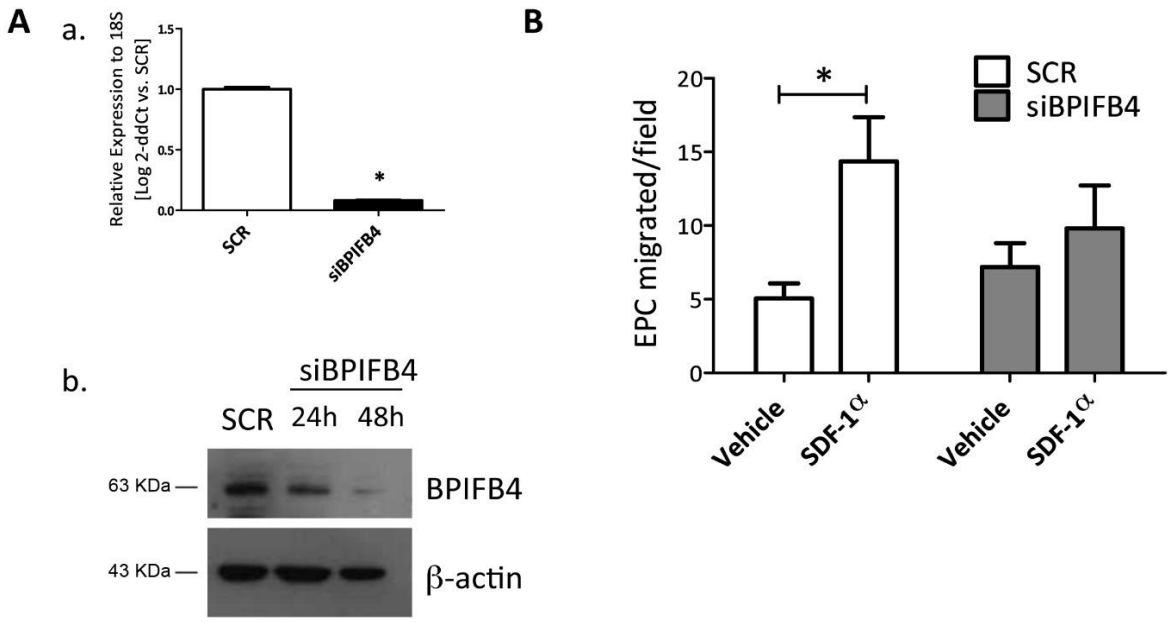

Online Figure IV. Silencing BPIFB4 inhibits *in vitro* migration of endothelial progenitor cells (EPCs). Human EPCs were enriched by selective culture on fibronectin from peripheral blood MNCs. Cells were transfected with siBPIFB4 or scramble (SCR) negative control (both from Dharmacon). **A) a,** BPIFB4 Real Time PCR PC after 48 hours siRNA transfection showing significant inhibition of RNA levels. Data are from one donor assayed in duplicate. * P<0.05 vs. SCR. **b,** Representative Western blot showing effective BPIFB4 protein silencing. **B)** EPCs treated for 48 hours with siBPIFB4 were tested *in vitro* for their ability to migrate along a gradient of the chemoattractant SDF-1 or vehicle. SCR-treated EPCs show significant migration that is blocked when BPIFB4 is silenced. Bar graph shows average migrated cells from 4 independent healthy donors assayed in duplicate wells ±SE. * P<0.05 vs. vehicle.

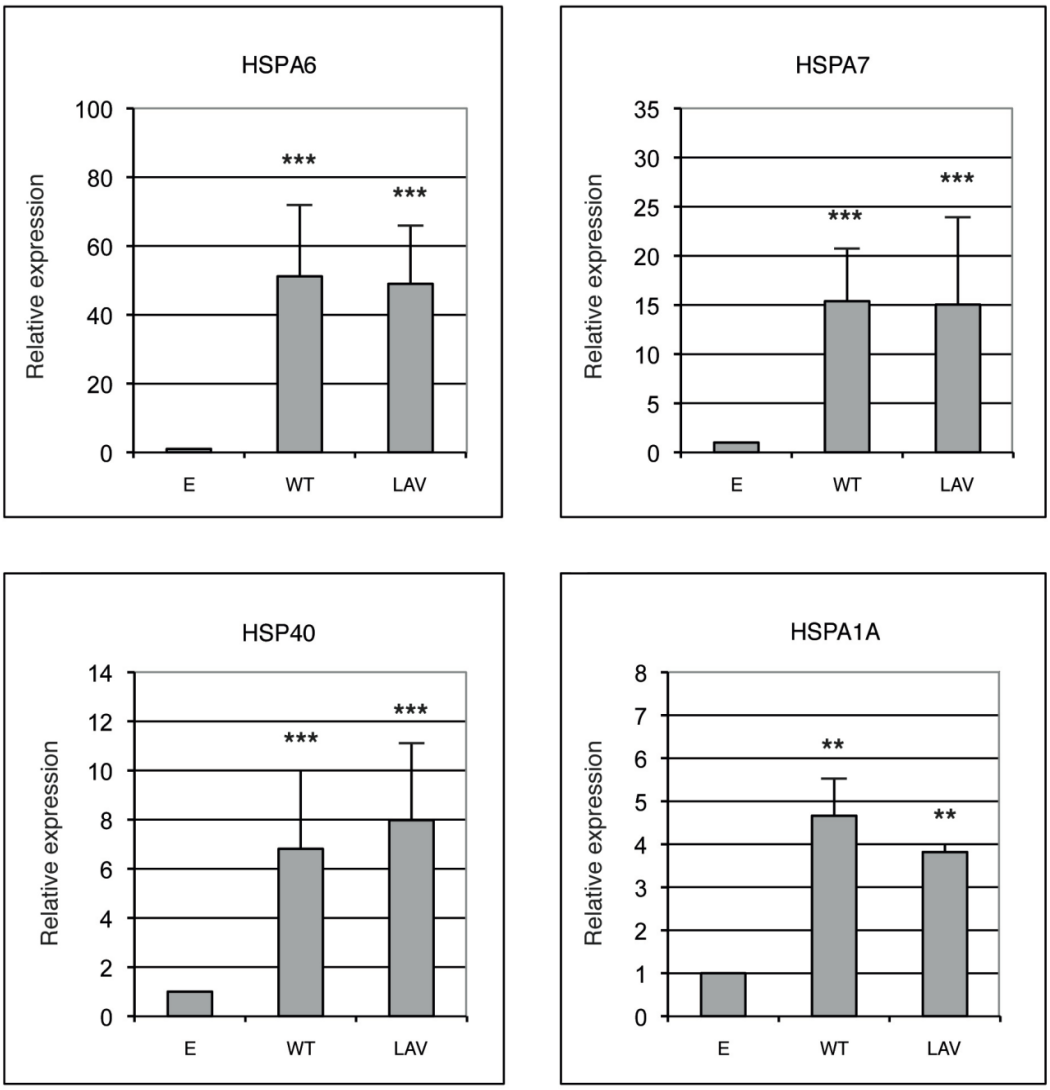

Online Figure V. Enhanced expression of heat shock proteins following forced expression of BPIFB4 isoforms.

Histograms of the relative expression of HSPs in HEK293T cells transfected with empty plasmid (E) or with plasmids carrying WT- or LAV-BPIFB4. Means±SEM; HSPA6 N=4; HSPA7 N=6; HSP40 N=6; HSPA1A N=3.**P<0.01; ***P<0.001 (ANOVA).

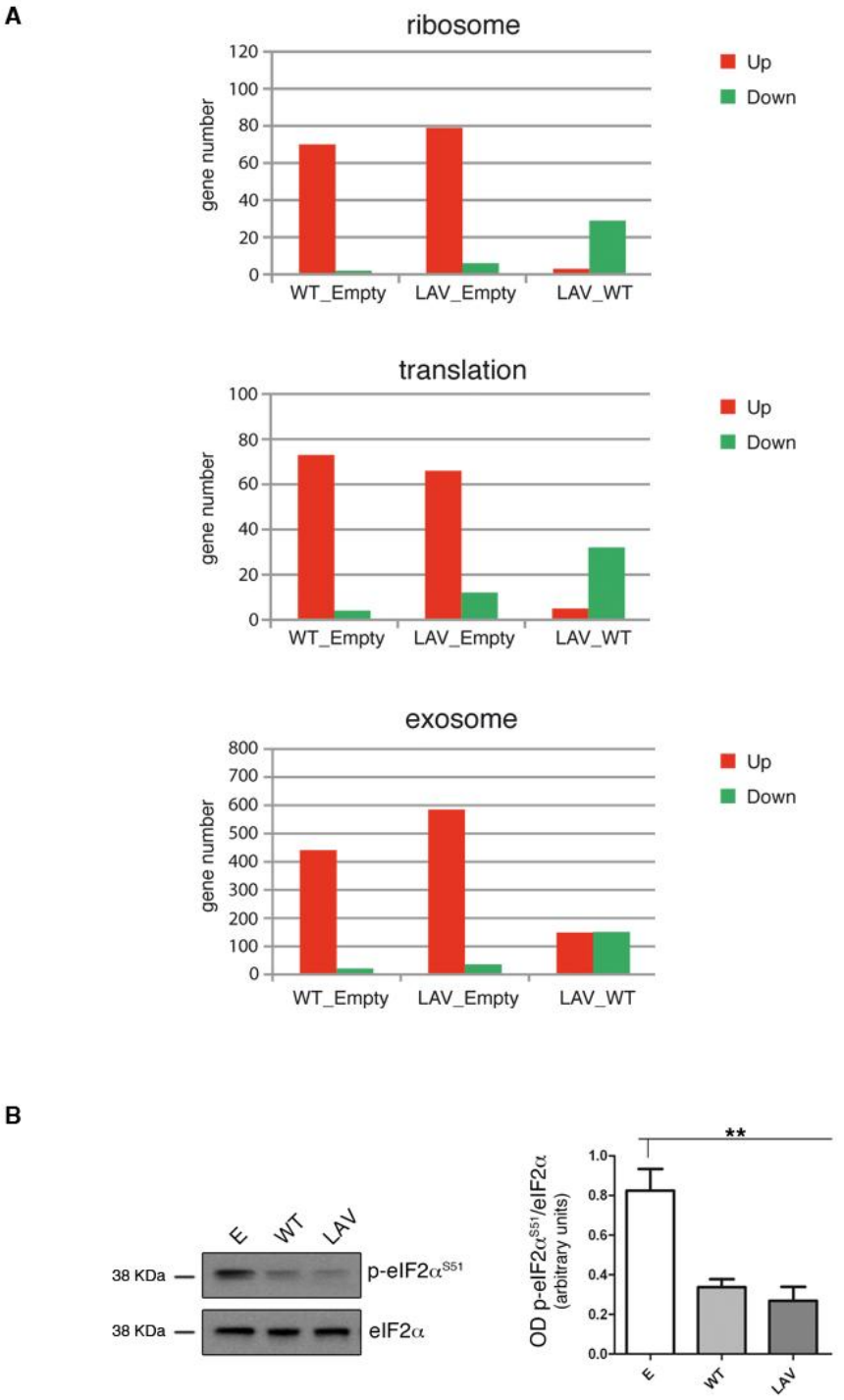

Online Figure VI. Transcriptional profiling and eIF2alpha analysis of cells transfected with BPIFB4 isoforms.

A, Graphs of Gene Ontology categories with the amount of differentially up-regulated (red bars) and down-regulated (green bars) genes in the indicated comparisons of expression profiles of HEK293T cells transfected with the different plasmids. Empty, empty vector; WT, wild-type BPIFB4; LAV, longevity-associated variant of BPIFB4. See **Online Table V** for statistics. **B,** Representative Western blot of the reduced phosphorylation of eIF2alpha at Ser51 after transfection with BPIFB4 isoforms. Right panel shows densitometry and statistical analyses (N=3, ANOVA; **, $P<0.01$).

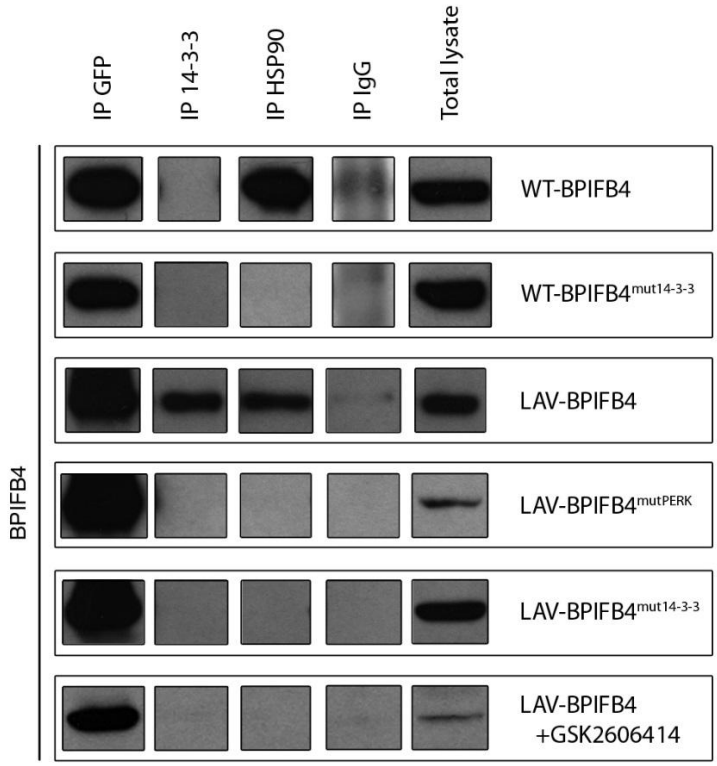

Online Figure VII. Co-immunoprecipitation of BPIFB4, 14-3-3 and HSP90 in HEK293T cells.
Co-immunoprecipitation of BPIFB4 with 14-3-3 and HSP90 in extracts of HEK293T cells transfected with plasmids carrying WT-BPIFB4, WT-BPIFB4 with a Ser82Asn (WT-BPIFB4$^{mut14\text{-}3\text{-}3}$) variation, LAV-BPIFB4, or LAV-BPIFB4 with a Ser75Ala (LAV-BPIFB4^{mutPERK}) or a Ser82Asn (LAV-BPIFB4$^{mut14\text{-}3\text{-}3}$) variation, or LAV-BPIFB4 treated with PERK inhibitor GSK2606414. Co-immunoprecipitation with anti-GFP indicates the presence of BPIFB4 because the plasmids encoded for fusion proteins. IgG and total lysate lanes were used as controls.

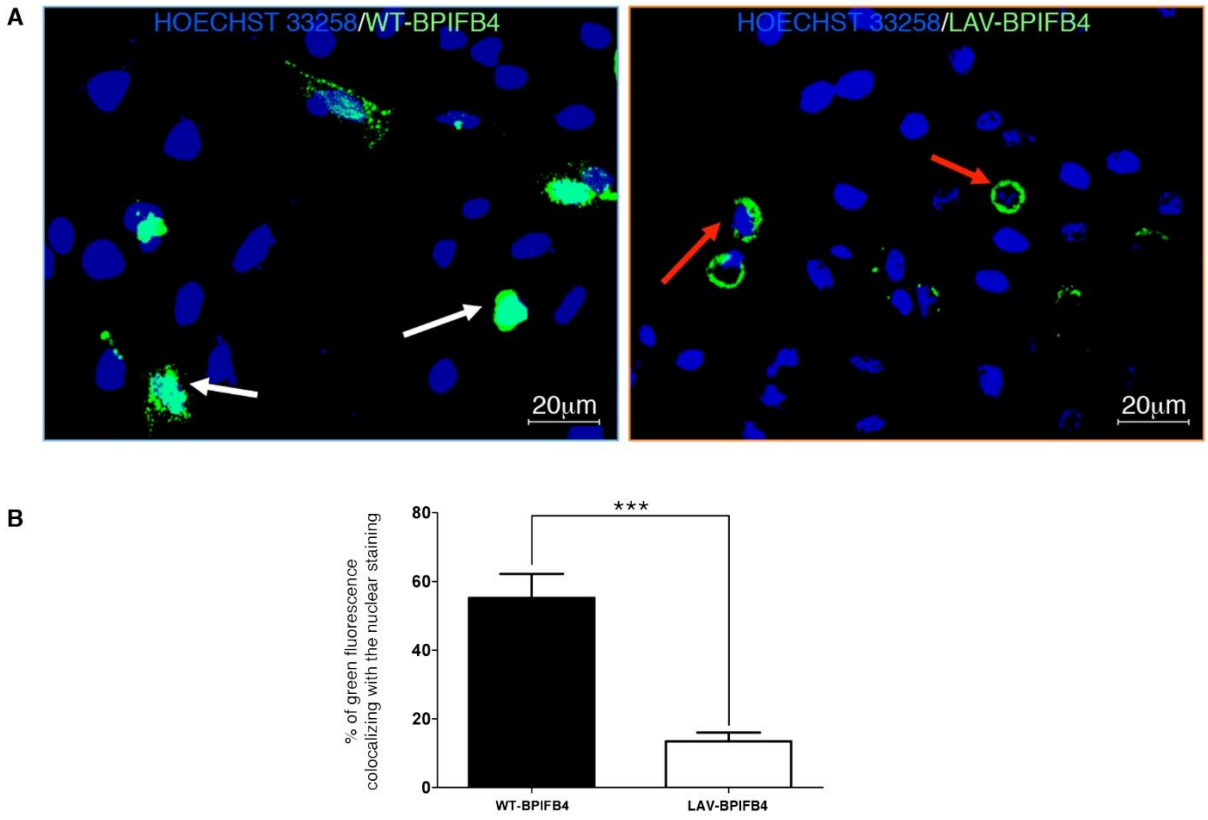

Online Figure VIII. Subcellular localization of BPIFB4 and its isoforms in transfected HeLa cells.
A, Representative panels showing: in light green the profile of expression of WT-BPIFB4 (left) and LAV-BPIFB4 (right); in blue the nuclear marker Hoechst 33258. White arrows indicate nuclear distribution of BPIFB4 protein, while red arrows indicate cytoplasmic distribution. **B**, Histogram of percentage co-localization between the nuclear marker Hoechst 33258 and WT- and LAV-BPIFB4. Data are expressed as mean ± SEM; N=18. ***P*<0.01; ****P*<0.001 (Student's t-test). Overall, these images point to a shift in the localization of BPIFB4 from mainly nuclear (WT isoform) to cytoplasmic (LAV isoform).

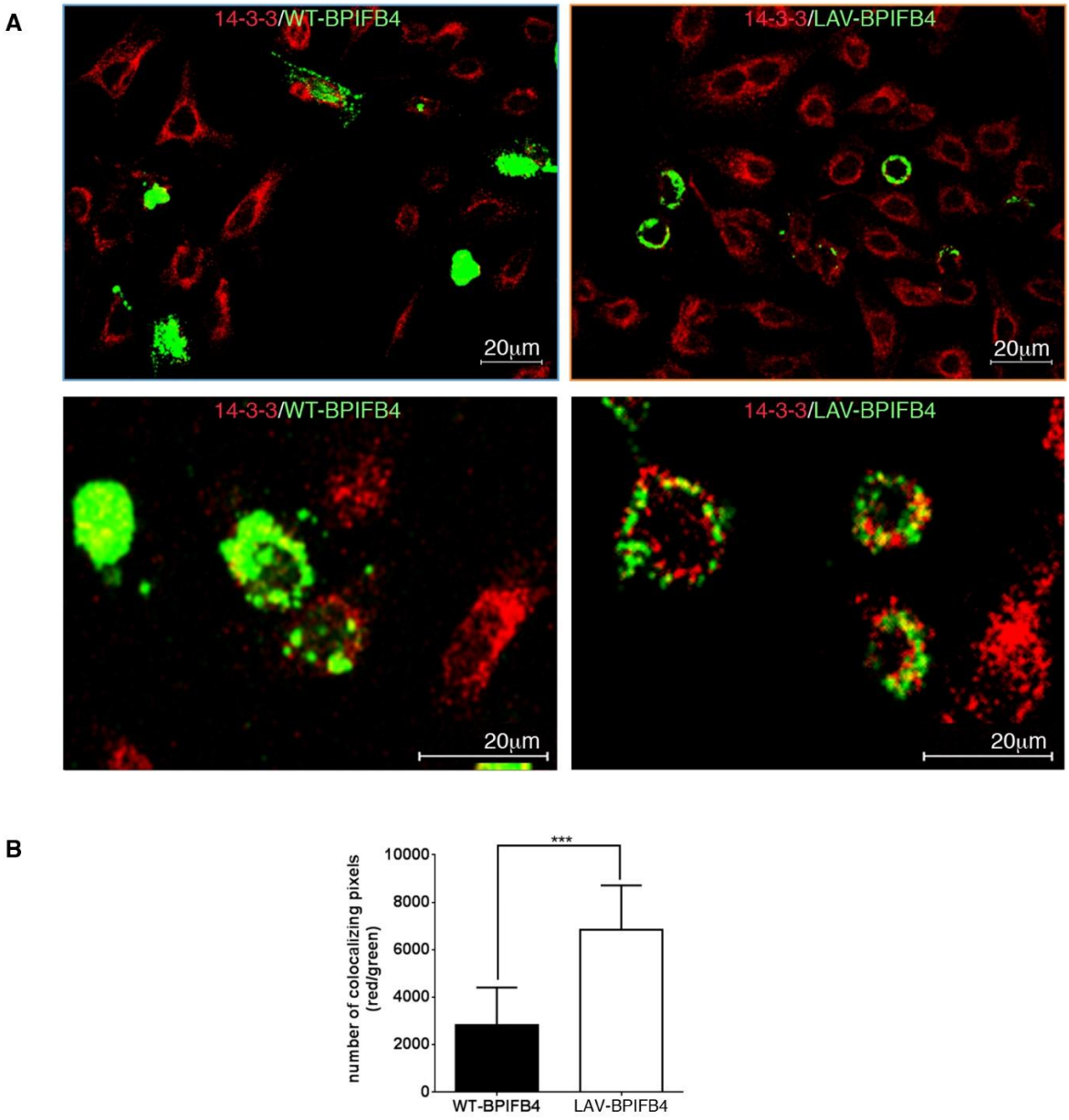

Online Figure IX. Co-localization of BPIFB4 and its mutated form with 14-3-3.
A, Representative merged immunostaining images of the signal from the BPIFB4 isoforms (green) and that from 14-3-3 protein (red). The LAV-BPIFB4 signal co-localizes with that of 14-3-3 (yellow signal). **B**, Histogram of number of co-localizing pixels of the 14-3-3 protein signal and WT- and LAV-BPIFB4 signals. Data are expressed as mean ± SEM; N=12. ***P<0.001 (Student's t-test).

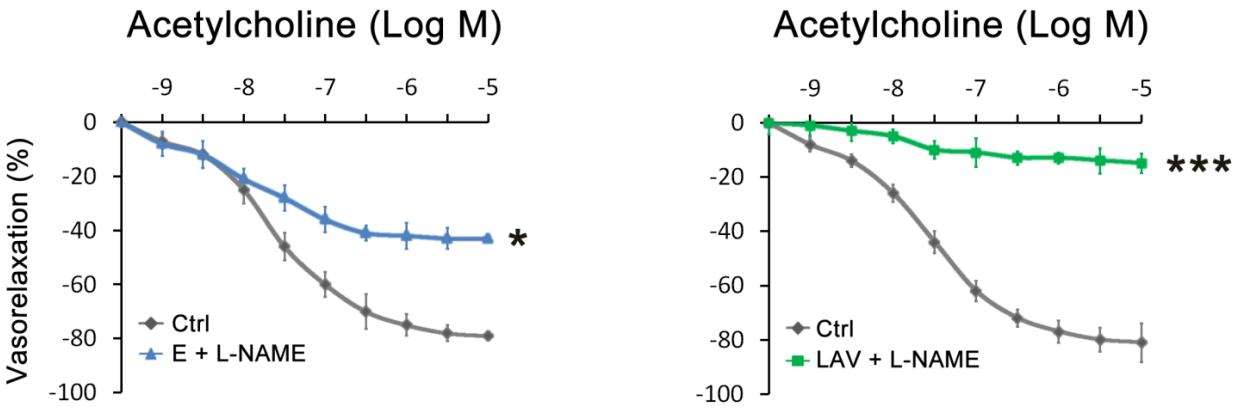

Online Figure X. L-NAME inhibits acetylcholine-induced vasorelaxation of LAV-BPIFB4-transfected vessels.

Dose–response curve to acetylcholine in *ex vivo* C57BL/6 mouse mesenteric arteries untreated (Ctrl) or treated with N^G-nitro-L-arginine methyl ester (L-NAME, 300μM), an eNOS inhibitor, and transfected with empty vector (E, on the left) or with LAV-BPIFB4 plasmid (on the right). The blockade of NO production by L-NAME in LAV-BPIFB4-expressing vessels evoked a more pronounced inhibition of acetylcholine-mediated vasorelaxation compared with that of vessels transfected with an empty plasmid, indicating the presence of a higher NO concentration in the former. Values given as mean ± SEM. N=7; **P* <0.05; ****P* <0.001 (Student's t-test).

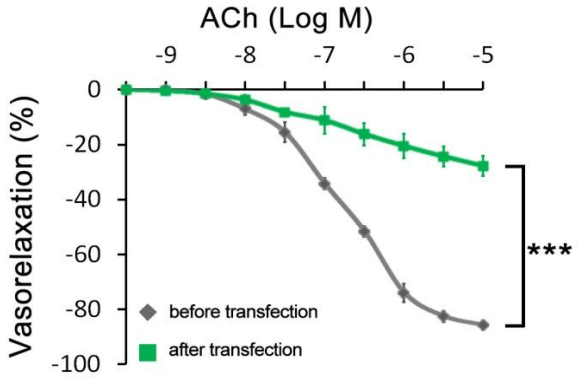

Online Figure XI. Mutation at serine 82 of wild type BPIFB4 (WT-BPIFB4$^{mut14\text{-}3\text{-}3}$) inhibits acetylcholine-mediated vasorelaxation.
The vascular response of *ex vivo* mouse mesenteric arteries to acetylcholine (ACh), before (◆—) and after (■) transfection with WT-BPIFB4$^{mut14\text{-}3\text{-}3}$. Values given as means ± SEM. N=4 experiments per group. *** $P<0.001$ (ANOVA).

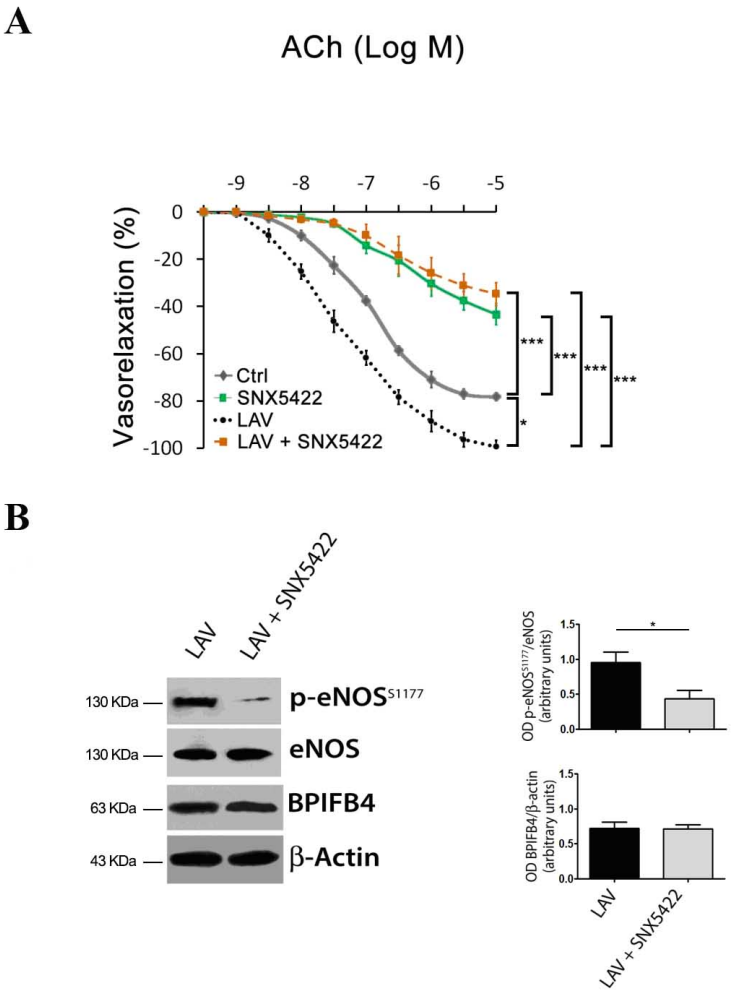

Online Figure XII. The HSP90 inhibitor SNX5422 blunts LAV-BPIFB4-mediated enhancement of vasorelaxation and eNOS activation in mesenteric arteries.

A, The vascular response of *ex vivo* mouse mesenteric arteries to acetylcholine (ACh), before transfection ( ), after treatment with SNX5422 (400nM) ( ), after transfection with LAV-BPIFB4 (••) and after transfection with LAV-BPIFB4 plus SNX5422 ( ). Values are given as mean ± SEM. N=4 experiments per group. **P*<0.05; ****P*<0.001 (ANOVA). **B,** Western blot of four pooled experiments on mesenteric arteries of *ex vivo* mouse transfected with LAV-BPIFB4 or LAV-BPIFB4 plus SNX5422. Right graphs show quantification of eNOS phosphorylation and BPIFB4. Values are means±SEM, N=2 pools of experiments. Statistic was performed using ANOVA; ***P* <0.01.

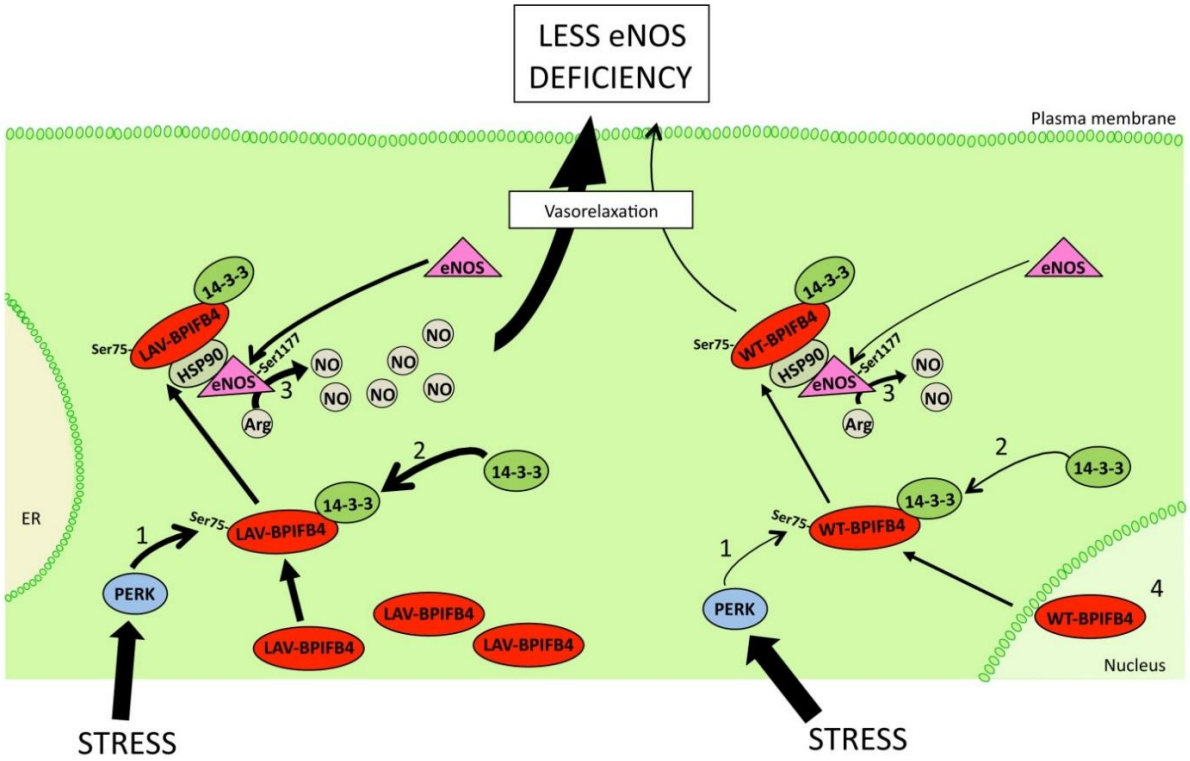

Online Figure XIII. Schematic representation of the hypothetical mechanism of action of LAV-BPIFB4 (on the left) and of WT-BPIFB4 (on the right).
Cellular stress, such as mechanical stress, induces protein kinase RNA-like endoplasmic reticulum kinase (PERK) phosphorylation of both LAV- and WT-BPIFB4, with more efficiency for the LAV-isoform (1). LAV-BPIFB4 binds to 14-3-3 more efficiently than WT-BPIFB4 (2). Endothelial nitric oxide synthase (eNOS) is activated by BPIFB4/14-3-3/heat shock protein (HSP)90-mediated mechanisms to increase the production of nitric oxide (NO) from L-arginine (Arg) (3). Increased NO production enhances endothelial function, which is lost during aging. WT-BPIFB4, which is less phosphorylated, show less 14-3-3 affinity, is more nuclear (4), and is therefore less efficient in activating eNOS as compared with LAV-BPIFB4.

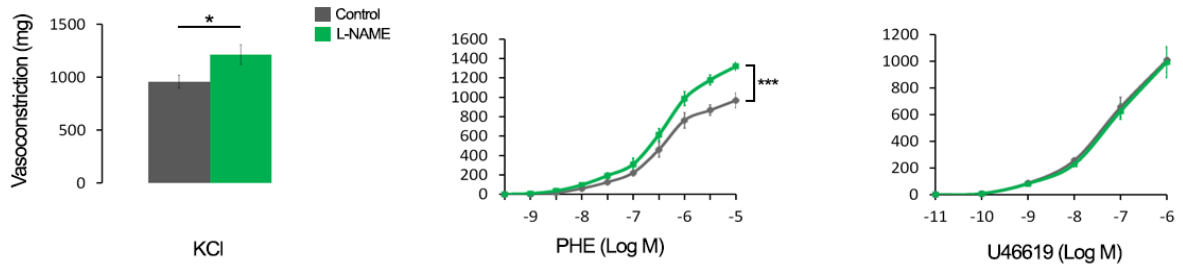

Online Figure XIV. Effect of L-NAME on potassium, phenylephrine and U46619 vasoconstriction in mice mesenteric arteries.

Graphs show, from left to right, the vascular response of *ex vivo* mouse mesenteric arteries to potassium (80mM KCl), and the dose–responses to phenylephrine (PE), and thromboxane agonist U46619. The vascular responses are measured before (◆) and after L-NAME (300µM) exposure (■). Values are means±SEM. N=5 experiments per group. Statistics was performed using ANOVA; **P*<0.05; ****P*<0.001, before vs. after L-NAME.

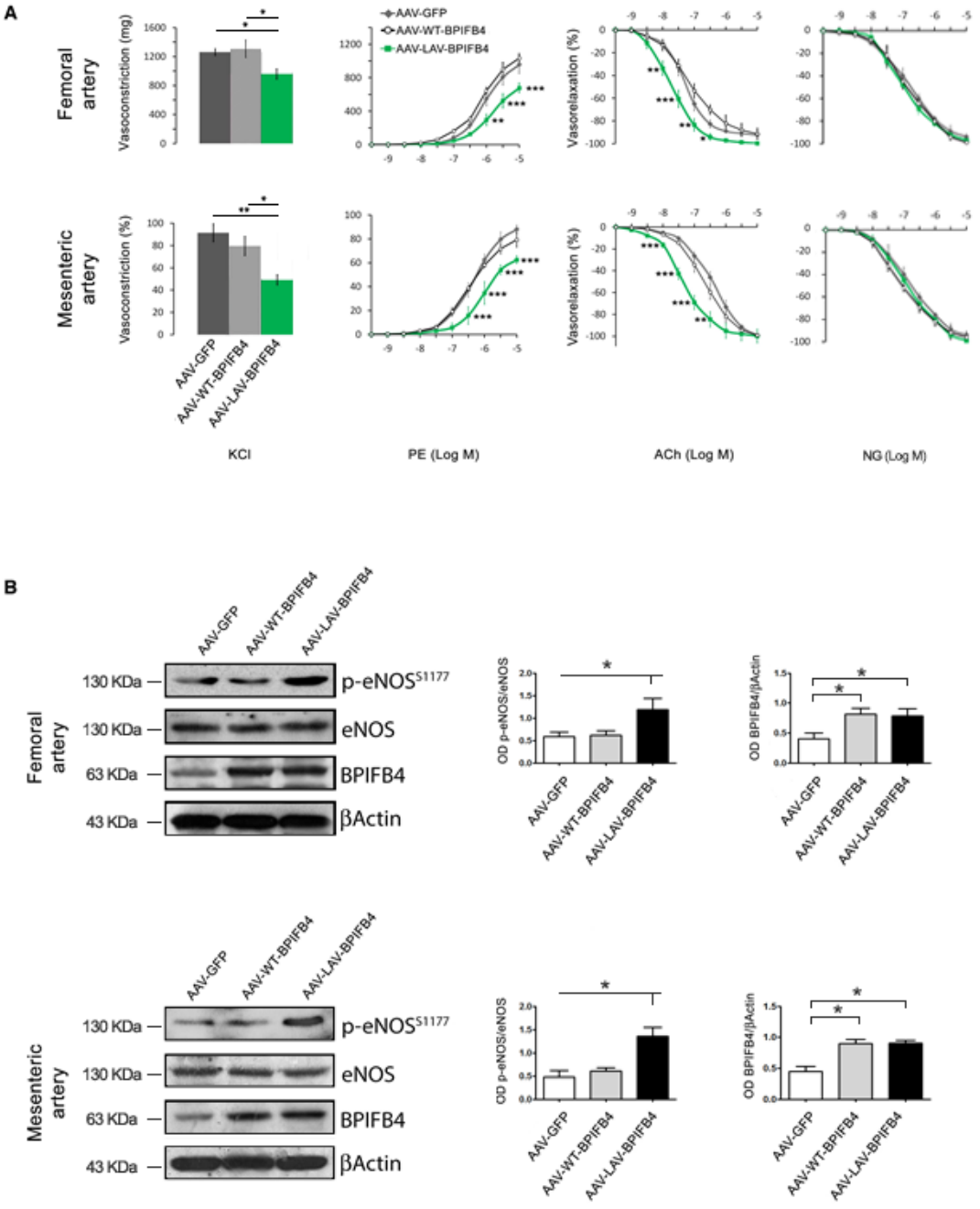

Online Figure XV. Expressional and vascular responses of vessels from mice infected with AAV-LAV-BPIFB4.

A, The graphs show, from the left to the right, the vascular response of femoral (first row) and mesenteric (second row) arteries to potassium (80mM KCl), and the dose–response to phenylephrine (PE), acetylcholine (ACh) and nitroglycerine. For these ex vivo studies, vessels were harvested from mice injected with AAV-GFP (◆), AAV-WT-BPIFB4 (○) or AAV-LAV-BPIFB4 (■). Values are means±SEM. N=4 experiments per group.*, $P<0.05$; **$P<0.01$; ***$P<0.001$ (ANOVA). **B,** Western blot of four pooled experiments on *ex vivo* femoral (first row) and mesenteric (second row) arteries from mice injected with AAV-GFP, AAV-WT-BPIFB4 or AAV-LAV-BPIFB4. Right graphs show quantification of eNOS

phosphorylation and BPIFB4. Values are means±SEM, N=2 pools of experiments. Statistic was performed using ANOVA; *P<0.05.

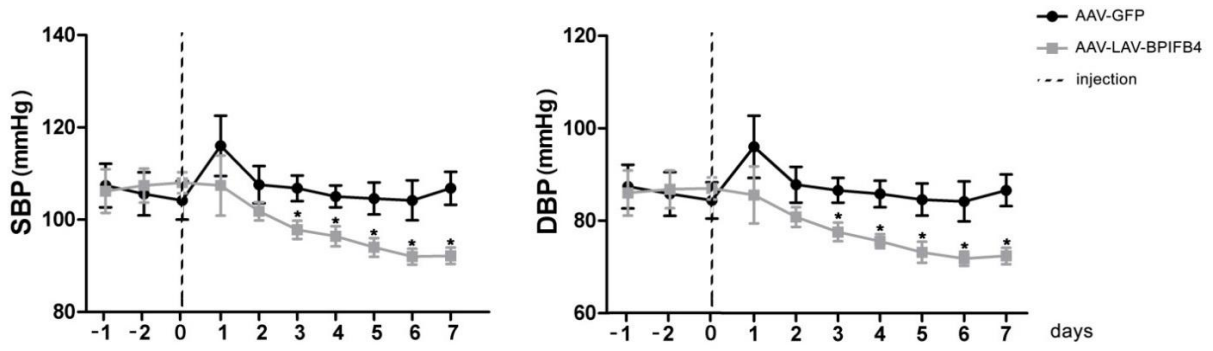

Online Figure XVI. Effect of AAV-LAV-BPIFB4 on blood pressure levels in normotensive mice.
Systolic (SBP, on the left) and diastolic blood pressure (DBP, on the right) in C57BL/6 mice treated with AAV-GFP (●) or AAV-LAV-BPIFB4 (■) (N=5/group). Measurements conducted before injection (reported on the x axis) were considered as basal values. Data are given as mean±SEM. **P*<0.05 vs. AAV-GFP (unpaired t-test).

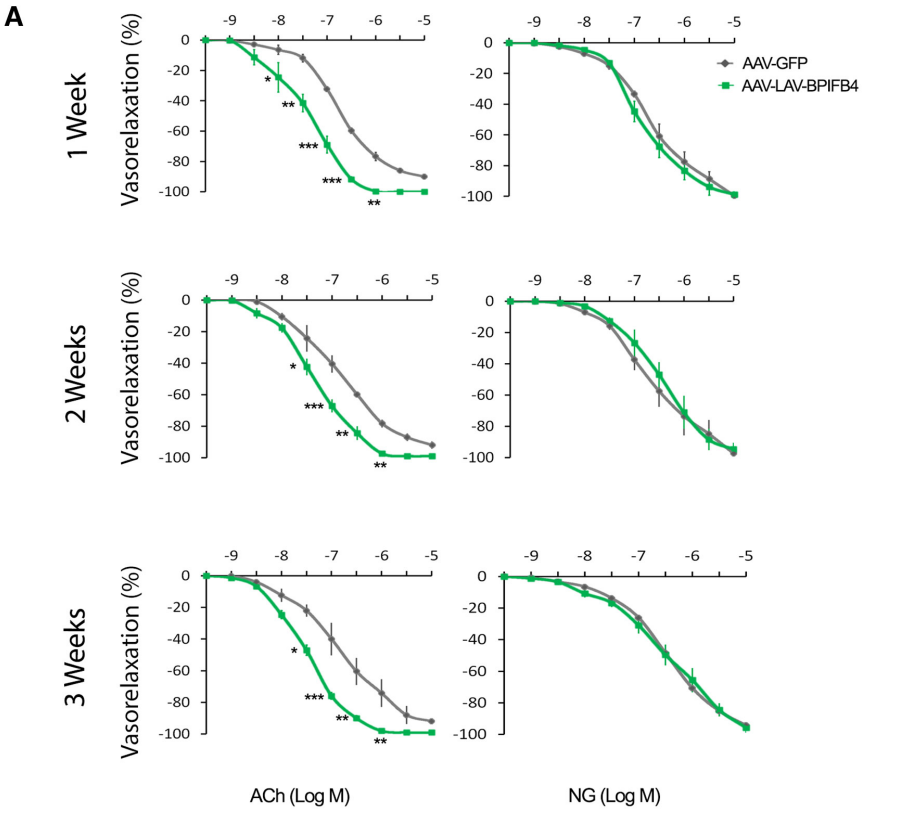
A
1 Week
2 Weeks
3 Weeks
Vasorelaxation (%)
AAV-GFP
AAV-LAV-BPIFB4
ACh (Log M)
NG (Log M)

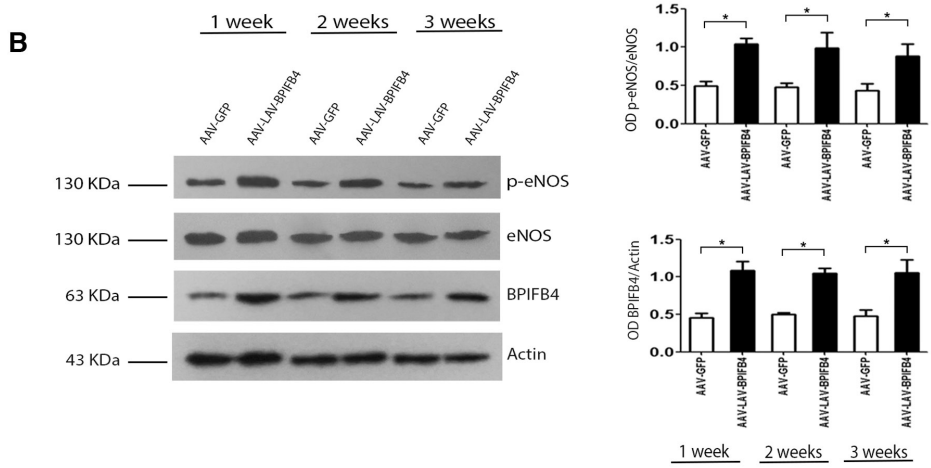
B
1 week
2 weeks
3 weeks
AAV-GFP
AAV-LAV-BPIFB4
130 KDa
p-eNOS
eNOS
63 KDa
BPIFB4
43 KDa
Actin
OD p-eNOS/eNOS
OD BPIFB4/Actin

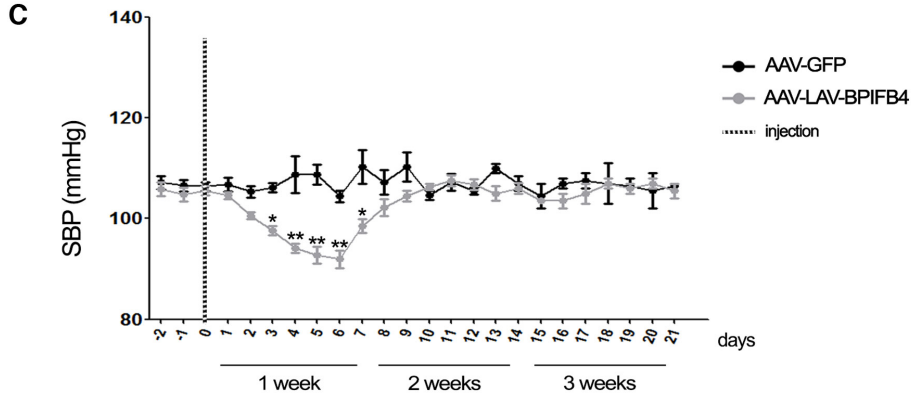
C
SBP (mmHg)
AAV-GFP
AAV-LAV-BPIFB4
injection
days
1 week
2 weeks
3 weeks

Online Figure XVII. Durability of transgene expression and vascular responses following AAV-LAV-BPIFB4 delivery in normotensive mice.

A, Graphs show the dose-response curves of *ex vivo* mesenteric arteries, from mice injected with AAV-GFP(◆) or AAV-LAV-BPIFB4(■), to acetylcholine (ACh) and nitroglycerin (NG). Experiments were performed at 1 (first row), 2 (second row) and 3 weeks (third row) after gene delivery. Values are means±SEM. N=5 experiments per group. Statistics was performed using ANOVA; **P*<0.05; ***P*<0.01; ****P*<0.001. **B,** Representative Western blot for eNOS phosphorylation and BPIFB4 levels in mesenteric arteries of mice injected with AAV-GFP or AAV-LAV-BPIFB4. The right graph gives the quantification of eNOS phosphorylation and BPIFB4 level of three independent experiments. **C,** Systolic blood pressure (SBP) in mice treated with AAV-GFP (● ; *n*=5) or AAV-LAV-BPIFB4 (● ; *n*=5). Values are means±SEM. Statistics was performed using ANOVA; **P*<0.05; ***P*<0.01; ****P*<0.001.

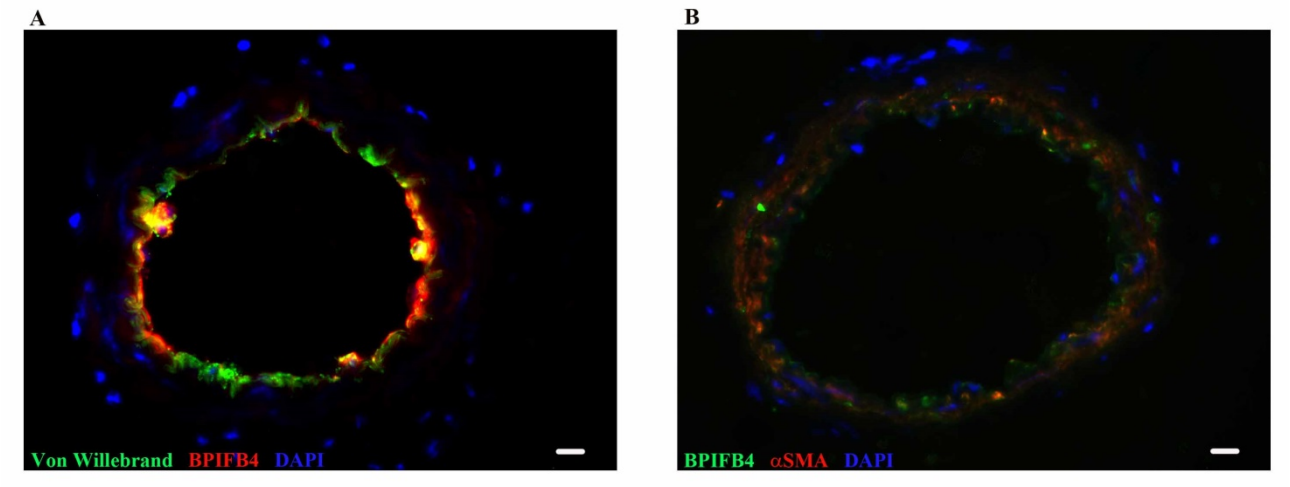

Online Figure XVIII. Immunostaining analysis of BPIFB4 in mesenteric artery of mice infected with AAV-LAV-BPIFB4.
The BPIFB4 signal co-localizes (yellow signal) with Von Willebrand signal in endothelial cells (A) and with α-SMA signal in smooth muscle vessel wall (B). Bar= 100um.

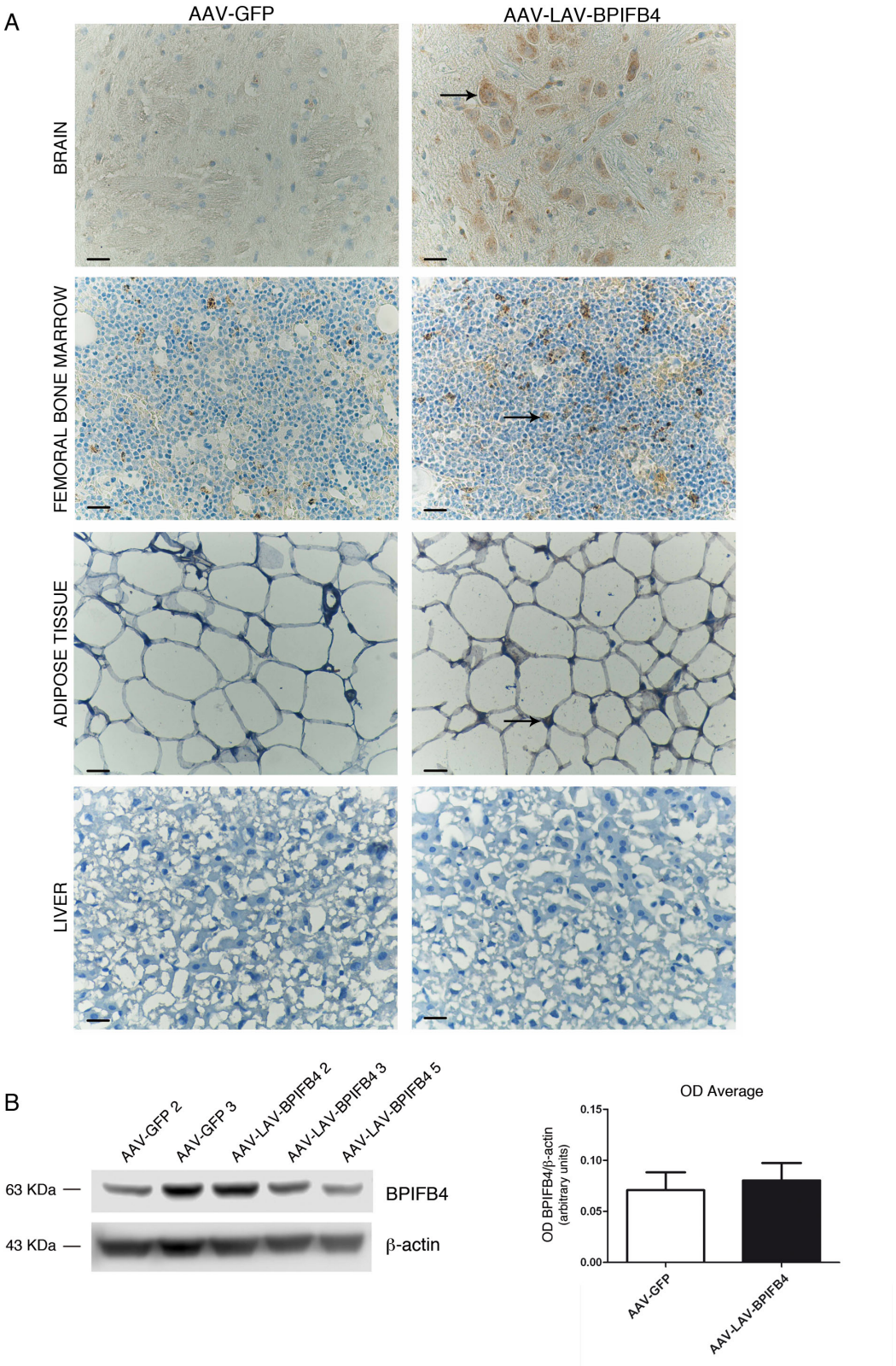

Online Figure XIX. BPIFB4 expression in tissues of infected mice and MNCs from infected rats.
A, Immunohistochemical analysis of BPIFB4 in different tissues of mice infected with AAV-GFP or AAV-LAV-BPIFB4. BPIFB4 overexpression (brown signals indicated by arrows) was detected in brain, femoral bone marrow and adipose tissue, but not in the liver of mice injected with AAV-LAV-BPIFB4. Bar = 40μm. **B,** Representative Western blot of BPIFB4 expression in MNCs of rats injected with AAV-

GFP (N=2) or AAV-LAV-BPIFB4 (N=3) on the left. The right graph gives the average quantification of BPIFB4 vs. β-actin. No significant difference between two groups was detected (unpaired t-test). Values are means±SEM.

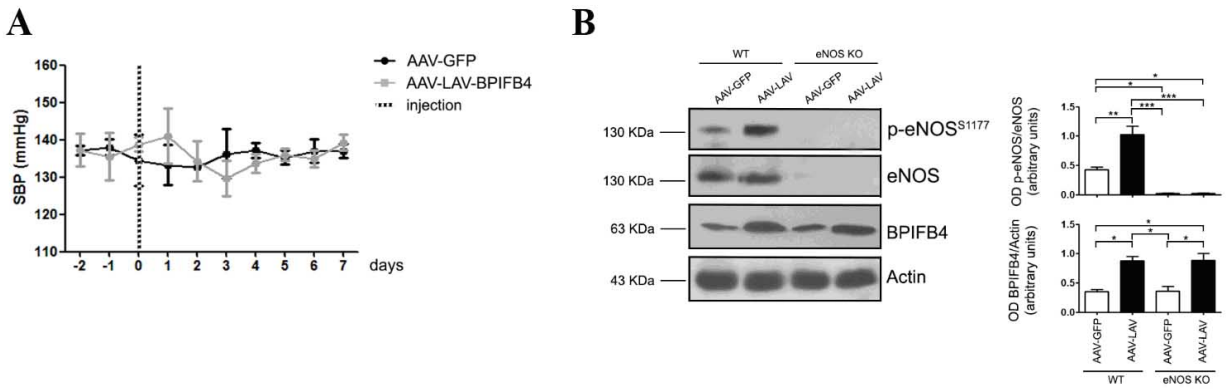

Online Figure XX. Effects of AAV-LAV-BPIFB4 in eNOS knockout mice.
A, Systolic blood pressure (SBP)in eNOS knockout mice treated with AAV-GFP (● ; *n*=5) or AAV-LAV-BPIFB4 (■ ; *n*=5).Values are means±SEM. **B**, Representative Western blot for eNOS phosphorylation and BPIFB4 levels in mesenteric arteries of eNOS knockout mice injected with AAV-GFP or AAV-LAV-BPIFB4. The right graph gives the quantification of eNOS phosphorylation and BPIFB4 levels of three experiments. Statistics was performed using ANOVA; **P*<0.05; ***P*<0.01; ****P*<0.001.

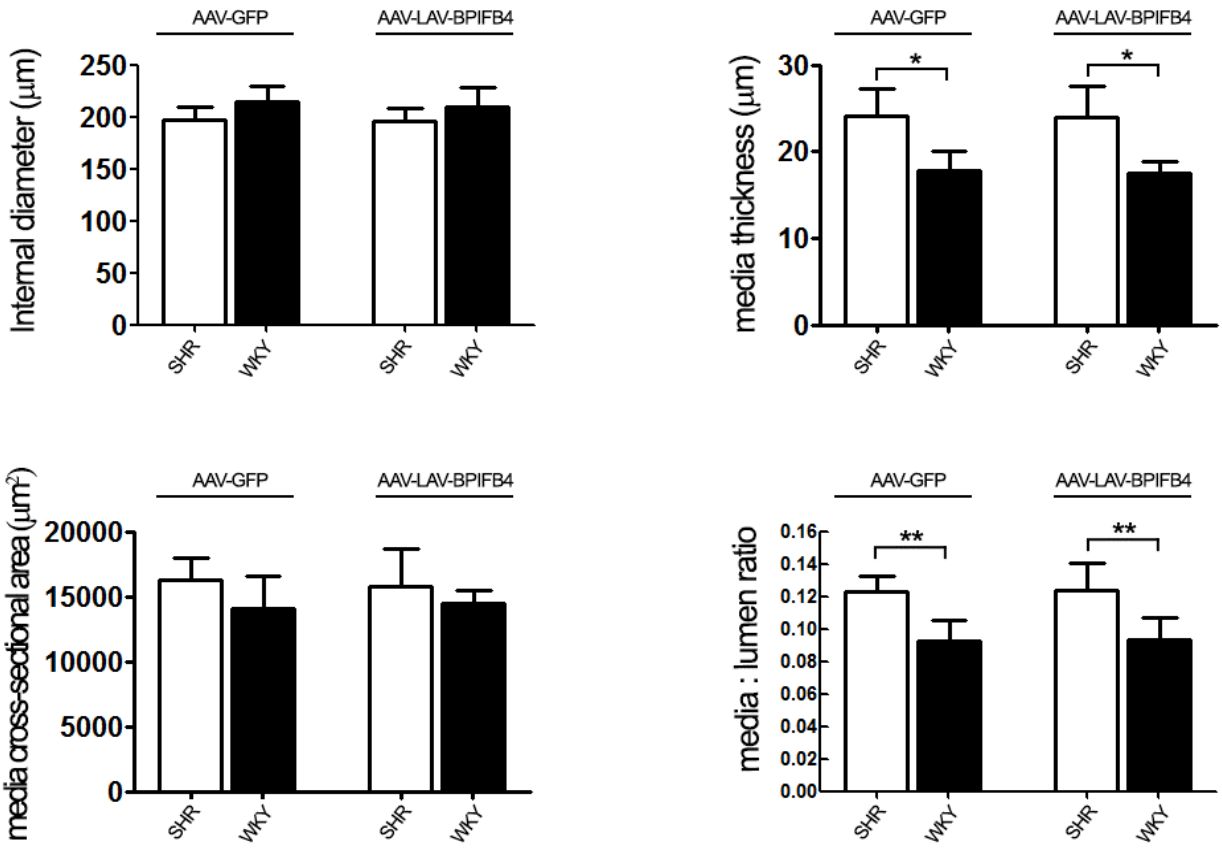

Online Figure XXI. Vascular remodeling in SHR and Wistar rats injected with AAV-LAV-BPIFB4. Bar graphs demonstrate morphological characteristics of small mesenteric arteries in SHRs (N=5) and their normotensive controls (WKY rats; N=5) injected with AAV-GFP or AAV-LAV-BPIFB4. Statistics was performed using ANOVA; **P*<0.05, ***P*< 0.01.

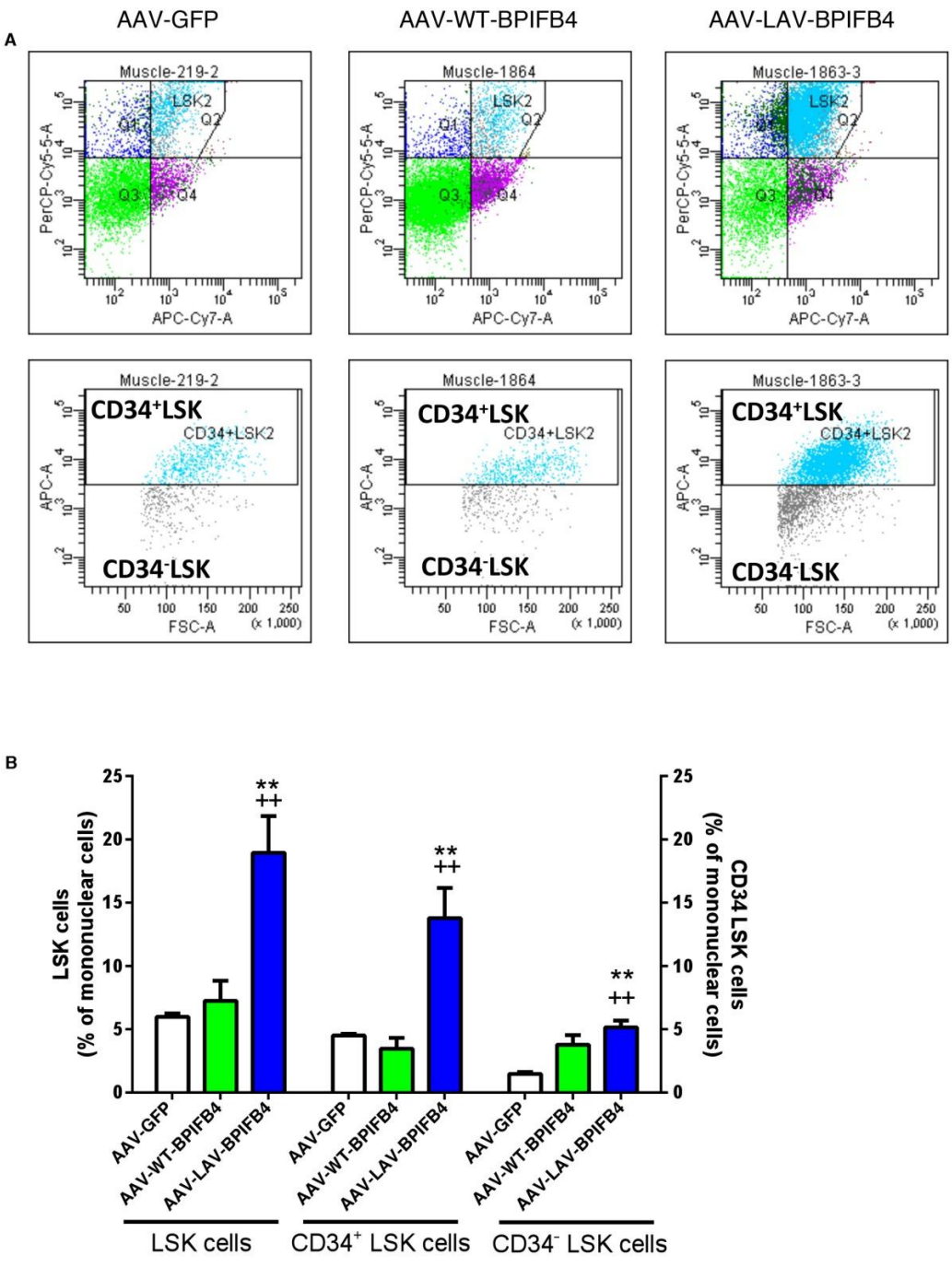

Online Figure XXII. Homing of stem cells to ischemic muscles.
Mice were infected systemically with AAV-WT-BPIFB4, AAV-LAV-BPIFB4 or received vehicle (AAV-GFP) through the tail vein before induction of femoral artery occlusion. Samples were collected 3 days post-ischemia. **A,** representative gating strategy for LSK and CD34/ LSK fractions. **B,** bar graphs showing average values in ischemic muscles. Data are mean (SE). $^{**}P<0.01$ vs vehicle, $^{++}P<0.01$ vs WT.

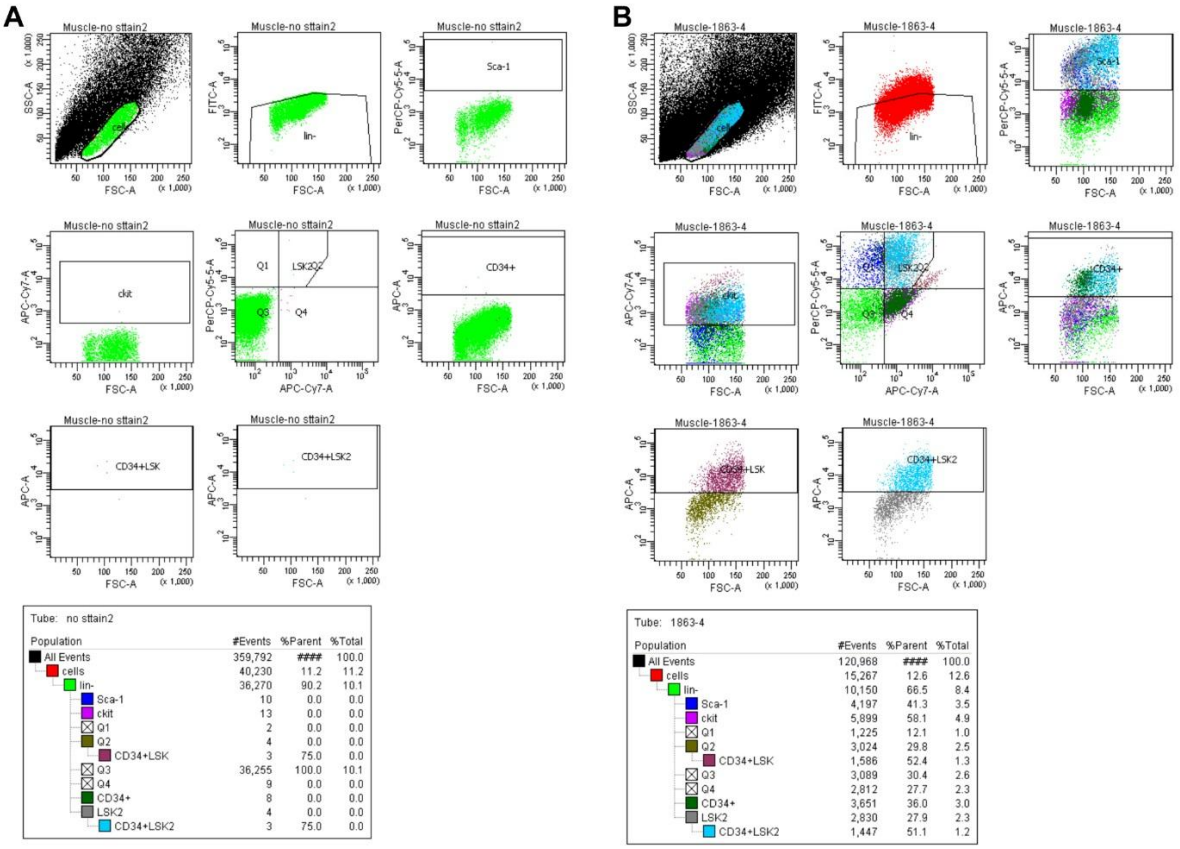

Online Figure XXIII. Gating strategy of LSK cells.
A, Gating of control samples in which the antibody was omitted. **B,** gating of samples showing initial identification of cells followed by definition of lineage negative elements and then definition of Sca-1 and cKit populations. Among the LSK cells, the two sub-fractions of CD34 positive and negative progenitor cells were finally distinguished.

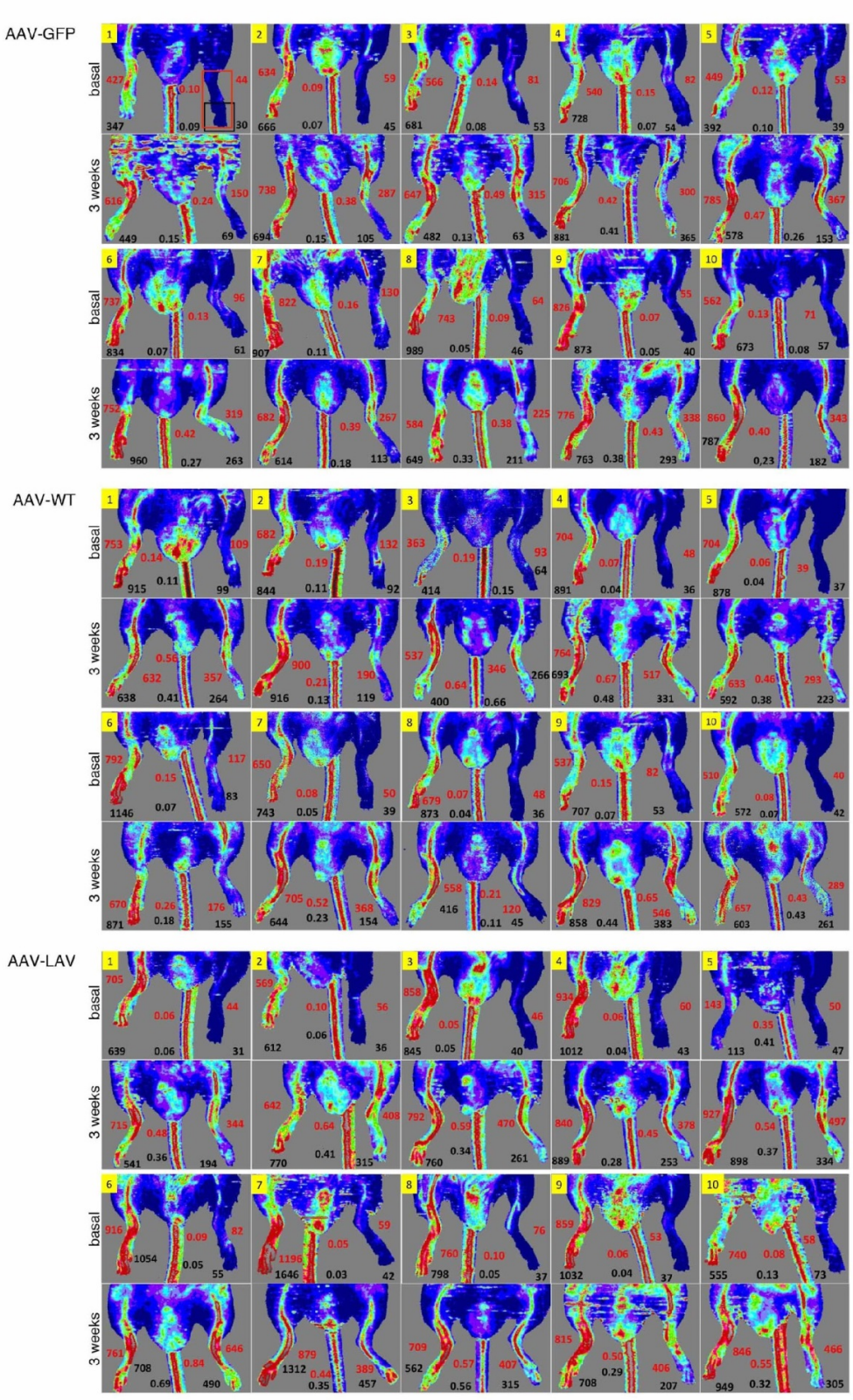

Online Figure XXIV. Effect of LAV-BPIFB4 on post-ischemic recovery of superficial blood flow.
Images of laser Doppler flowmetry captured at 0 and 21 days after induction of limb ischemia. Values represent arbitrary blood flow units taken at the level of the foot (black font) and whole limb (red font). The ratio of ischemic to contralateral side is also shown between each side values. N=10 in each group.

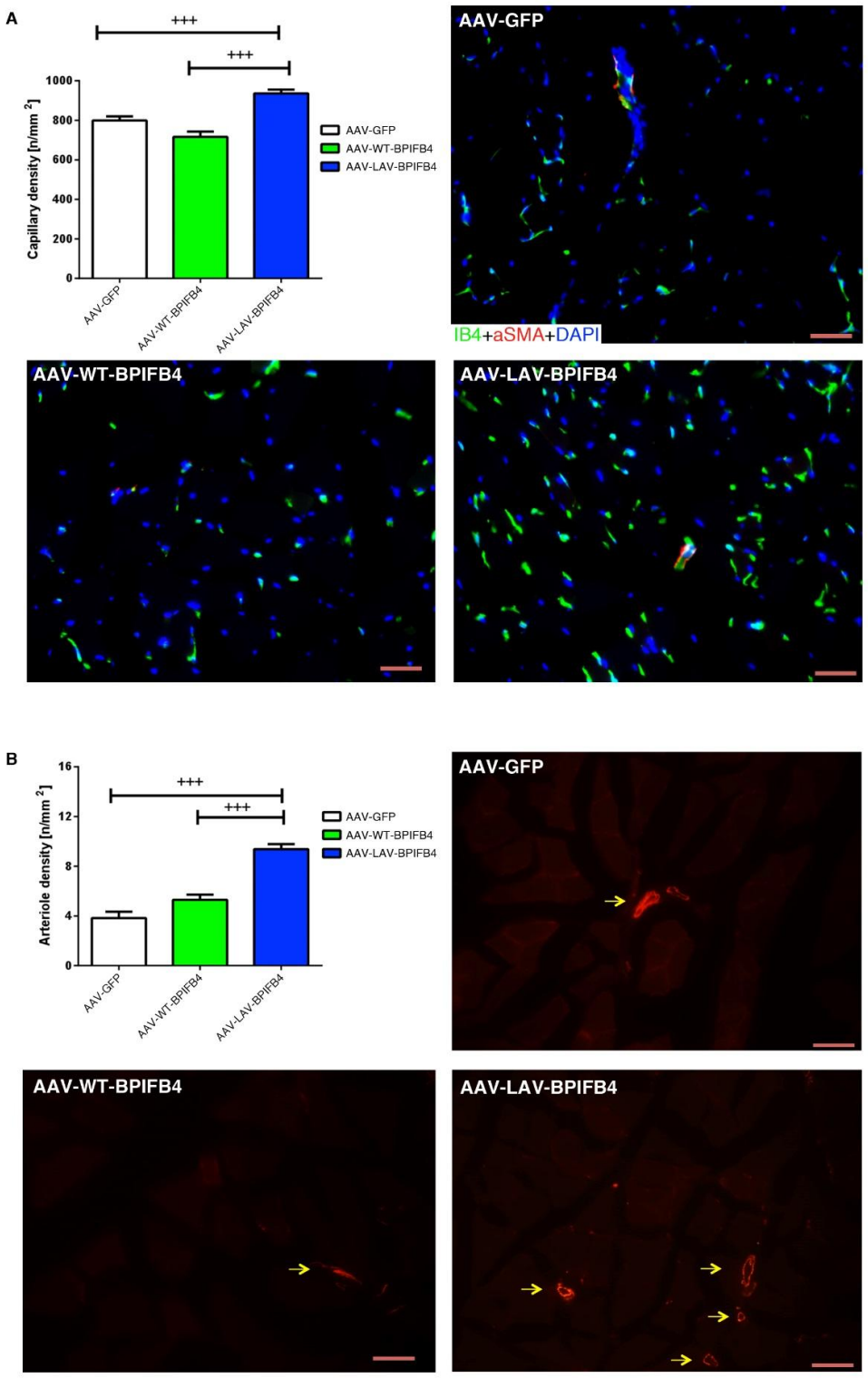

Online Figure XXV. Revascularization effect of LAV-BPIFB4 in mouse model of hindlimb ischemia. **A**, capillary density and **B**, arteriole density, as assessed 3 weeks post-ischemia. Values are mean±SEM of N=7–10 in each group. Bar = 50 μm.

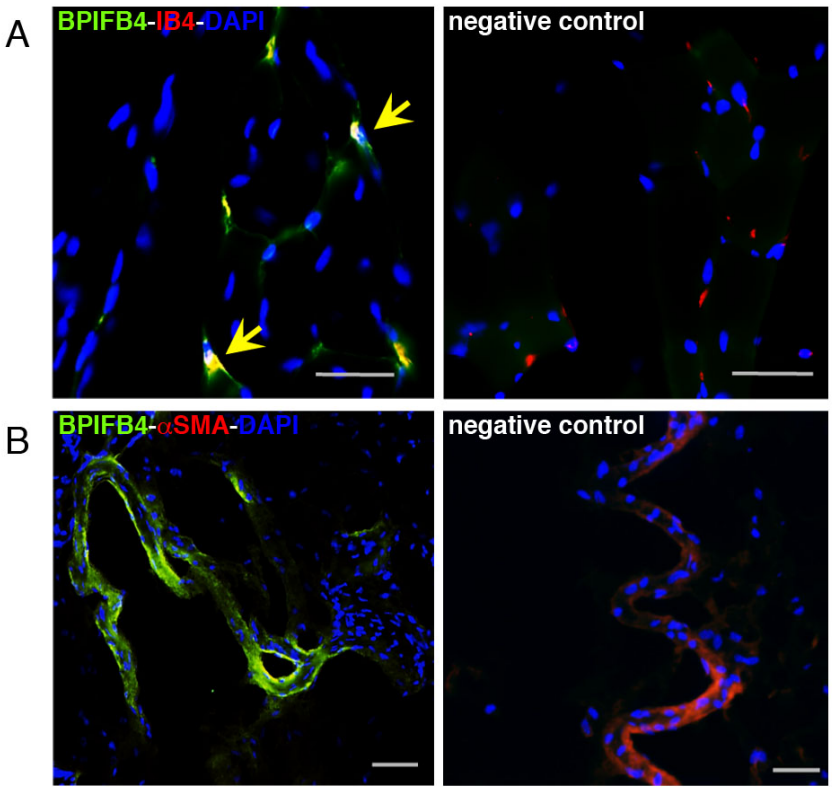

Online Figure XXVI. Immunofluorescence microscopy images showing transgene expression at 3 weeks after AAV-LAV-BPIFB4 intravenous injection and induction of limb ischemia. Ischemic adductor muscle sections were stained with anti-BPIFB4, IB4/a-SMA and DAPI. **A**, IB4 positive capillary endothelial cells and **B**, alpha-SMA positive arterioles from muscles of mice injected with AAV-LAV-BPIFB4 express abundantly the transgene. Yellow arrows indicate co-localization between BPIFB4 and IB4 signals. Bar=50um.

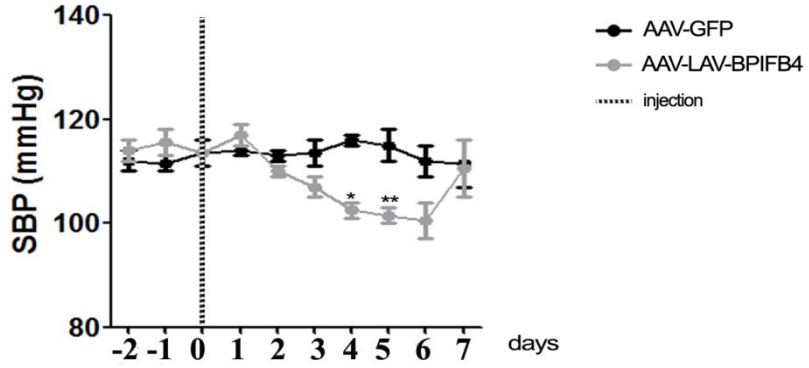

Online Figure XXVII. Effect of AAV-LAV-BPIFB4 on mice systolic blood pressure after vein injection. Systolic blood pressure (SBP) in mice treated with AAV-GFP (● ; *n*=5) or AAV-LAV-BPIFB4 (● ; *n*=5). Values are means ± SEM. Statistics was performed using ANOVA; *, $p<0.05$; **, $p<0.01$.

ONLINE TABLES

Online Table I. Association Tests Results in the Screening Set and Replication Cohorts.

SNP	Assoc. Model	Cohort	a/A	MAF	Allele or Genotype	No. (%) of Alleles/Genotypes		*P*-value	OR (95%CI)
						LLIs	Controls		
rs7583529	RM	SICS-scr	A/G	0.21	AA	37 (9)	17 (3)	$6.45x10^{-5}$	3.15 (1.75–5.68)
		GLS-rep	A/G	0.22	AA	83 (5)	53 (5)	0.69	1.07 (0.75–1.53)
		USA-rep	-- Not tested --						
rs571391	DM	SICS-scr	G/A	0.43	GG/GA	241 (59)	399 (72)	$1.39x10^{-5}$	0.55 (0.42–0.72)
		GLS-rep	G/A	0.34	GG/GA	903 (57)	623 (57)	0.93	0.99 (0.85–1.16)
		USA-rep	-- Not tested --						
rs285097	AM	SICS-scr	G/T	0.08	G	43 (5)	116 (10)	$3.79x10^{-5}$	0.47 (0.33–0.68)
		GLS-rep	G/T	0.07	G	195 (6)	150 (7)	0.26	0.88 (0.71–1.10)
		USA-rep	-- Not tested --						
rs2070325	RM	SICS-scr	G/A	0.30	GG	57 (14)	35 (6)	$5.98x10^{-5}$	2.42 (1.56–3.77)
		GLS-rep	G/A	0.36	GG	225 (14)	112 (10)	0.0036	1.43 (1.12–1.80)
		USA-rep	G/A	0.35	GG	196 (13)	46 (9)	0.0063	1.60 (1.14–2.24)

SNP, dbSNP ID; Assoc. Model, associated genetic model (AM = allelic model, DM = dominant model, RM = recessive model); Cohort, analysed cohort (SICS-scr = Southern Italian Centenarian Study screening cohort, GLS-rep = German Longevity Study replication cohort, USA-rep = United States-American replication cohort); a/A, minor allele/major allele based on whole sample; MAF, minor allele frequency; No. (%) Alleles/Genotypes, number and percentage of reference alleles/genotypes in long-living individuals (LLIs) and control individuals (controls); OR, odds ratio; 95% CI, 95% confidence interval.

Online Table II. Genotype counts.

Cohort	CHR	SNP	m	M	LLIs	CTRLs
SICS-scr	20	rs2070325	G	A	57/146/201	35/250/266
GLS-rep	20	rs2070325	G	A	225/715/659	112/545/432
USA-rep	20	rs2070325	G	A	196/648/617	46/242/232

Cohort, analysed cohort; Chr, Chromosome; m, minor allele; M, major allele; LLIs, number of mm/mM/MM genotypes in cases; CTRLs, number of mm/mM/MM genotypes in controls SICS-scr, Italian screening set; GLS-rep, German replication set; USA-rep, American replication set.

Online Table III. Comparison of HEK293T cell transcriptional profiles after transfection with WT-BPIFB4 or empty vector

Gene	WT.AVG_Signal	Empty.AVG_Signal	FC	*P*-value	Regulation	Exosome
HSPA6	11384.717	625.217	4.187	<0.001	Up	no
HSPA7	3907.633	288.367	3.76	<0.001	Up	no
LOC652750	1699	144.433	3.556	<0.001	Up	no
TCEAL7	962.833	129.1	2.899	<0.001	Up	no
HSPA1A	559.4	136.1	2.039	<0.001	Up	no
DNAJB1	5896.7	1485.233	1.989	<0.001	Up	no
HS.543887	1011.633	333.2	1.602	<0.001	Up	no
RNU1-3	970	353.033	1.458	<0.001	Up	yes
ZFAND2A	1495.133	570.9	1.389	<0.001	Up	no
RNU1-5	1162.2	452.267	1.362	<0.001	Up	yes
PPIL2	378.7	148.967	1.346	<0.001	Up	no
RNU1G2	824.4	338.467	1.284	<0.001	Up	yes
HS.579631	20786.367	8670.467	1.261	<0.001	Up	no
MIR1974	589.2	248.567	1.245	<0.001	Up	yes
SCARNA8	1005.6	424.967	1.243	<0.001	Up	no
RN5S9	1421.2	610.4	1.219	<0.001	Up	yes
BAG3	3604.067	1551.067	1.216	<0.001	Up	no
MUM1	512.2	226.133	1.18	<0.001	Up	no
HSPA1B	22851.5	10136.333	1.173	<0.001	Up	no
SNORD83B	798.133	356.433	1.163	<0.001	Up	no
RNU4ATAC	382.867	172.033	1.154	<0.001	Up	no
PPP1R15A	1626.667	732.833	1.15	<0.001	Up	no
SNORA79	1026.833	468.367	1.132	<0.001	Up	no
SNORD15B	404.033	185.933	1.12	<0.001	Up	no
RNU1F1	631	291.533	1.114	<0.001	Up	yes
RNU1A3	1156.467	541.533	1.095	<0.001	Up	yes
HSPB1	3392.8	1656	1.035	<0.001	Up	yes
SCARNA14	466.6	231.567	1.011	<0.001	Up	no
BCYRN1	3007.433	1501.1	1.003	<0.001	Up	yes
LOC388796	2132.833	1071.933	0.993	<0.001	Up	no
NBPF20	1448.6	2974.55	-1.038	<0.001	Down	yes
LOC440092	144.1	308.9	-1.1	<0.001	Down	no
SNORA71C	681.2	1534.4	-1.172	<0.001	Down	no

WT.AVG_Signal: average of fluorescence signals of HEK293T transfected with vector encoding for WT-BPIFB4 (n=3); Empty. AVG_Signal: average of fluorescence signals of HEK293T transfected with empty vector (n=3); FC: fold change; Exosome: RNA detected by de Jong et al.[28] in exosomes produced by endothelial cells under stress conditions. Only genes with *P*-value < 0.001 are indicated.

Online Table IV. Comparison of HEK293T cell transcriptional profiles after transfection with LAV-BPIFB4 or empty vector

Gene	LAV.AVG_Signal	Empty.AVG_Signal	FC	*P*-value	Regulation	Exosome
HSPA7	5512.1	288.367	4.257	<0.001	Up	no
HSPA6	10394	625.217	4.055	<0.001	Up	no
LOC652750	1522.833	144.433	3.398	<0.001	Up	no
TCEAL7	892.933	129.1	2.79	<0.001	Up	no
HSPA1A	835.167	136.1	2.617	<0.001	Up	no
HS.543887	1532.6	333.2	2.202	<0.001	Up	no
MIR1974	1029.433	248.567	2.05	<0.001	Up	yes
DNAJB1	6058.167	1485.233	2.028	<0.001	Up	no
RN5S9	2194.433	610.4	1.846	<0.001	Up	yes
SCARNA8	1439.133	424.967	1.76	<0.001	Up	no
SNORD15B	606.1	185.933	1.705	<0.001	Up	no
RNU1G2	1070	338.467	1.661	<0.001	Up	yes
RNU1-3	1113.7	353.033	1.657	<0.001	Up	yes
ZFAND2A	1769.933	570.9	1.632	<0.001	Up	no
RNU1-5	1373.3	452.267	1.602	<0.001	Up	yes
PPIL2	443.183	148.967	1.573	<0.001	Up	no
SCARNA14	685.433	231.567	1.566	<0.001	Up	no
SNORA79	1362.733	468.367	1.541	<0.001	Up	no
RNU4ATAC	493.167	172.033	1.519	<0.001	Up	no
SNORD83B	995.333	356.433	1.482	<0.001	Up	no
LOC100130516	10136.8	3635.233	1.479	<0.001	Up	yes
SCARNA23	551.133	199.267	1.468	<0.001	Up	no
BCYRN1	4118.2	1501.1	1.456	<0.001	Up	yes
RNY1	607.7	236.333	1.363	<0.001	Up	yes
FLJ36131	5761.433	2291.833	1.33	<0.001	Up	yes
SNORA12	1746.067	700.133	1.318	<0.001	Up	no
CATSPER2	8787.5	3526.733	1.317	<0.001	Up	yes
RNU1A3	1348.133	541.533	1.316	<0.001	Up	yes
LOC648852	1625.567	654.567	1.312	<0.001	Up	yes
BAG3	3808.633	1551.067	1.296	<0.001	Up	no
SCARNA18	572.833	234.867	1.286	<0.001	Up	no
SNORD13	642.833	265.5	1.276	<0.001	Up	yes
RNU1F1	693.633	291.533	1.251	<0.001	Up	yes
TRK1	503.633	218.433	1.205	<0.001	Up	no
SNORA42	409.9	182.067	1.171	<0.001	Up	no
PPP1R15A	1604.067	732.833	1.13	<0.001	Up	no
HS.579631	18840.5	8670.467	1.12	<0.001	Up	no
HS.129244	320.5	147.6	1.119	<0.001	Up	no
TRQ1	347.333	160.167	1.117	<0.001	Up	no
MIR1978	6763.4	3140	1.107	<0.001	Up	yes
HS.25892	4475.233	2083.5	1.103	<0.001	Up	no
LOC100132585	2751.167	1280.533	1.103	<0.001	Up	yes
SNORA27	386.5	180.8	1.096	<0.001	Up	no
LOC388796	2274.2	1071.933	1.085	<0.001	Up	no
RNU86	643.767	303.767	1.084	<0.001	Up	no
SCARNA13	2019.2	957.4	1.077	<0.001	Up	no
SCARNA16	661.833	313.933	1.076	<0.001	Up	no
E2F2	1587.733	757.467	1.068	<0.001	Up	no
SNORD4A	812.967	390.567	1.058	<0.001	Up	no

HS.163752	1896.833	932.633	1.024	<0.001	Up	no
SNORD3D	801.6	399.067	1.006	<0.001	Up	yes
SNORD38A	474.133	237.1	1	<0.001	Up	no
DYNLT3	352.9	709.067	-1.007	<0.001	Down	no
TULP4	152.733	308.883	-1.016	<0.001	Down	no
NBPF20	1442.15	2974.55	-1.044	<0.001	Down	yes
SNORA71C	700.167	1534.4	-1.132	<0.001	Down	no
LOC440092	136.8	308.9	-1.175	<0.001	Down	no

LAV.AVG Signal: average of fluorescence signals of HEK293T transfected with vector encoding for LAV-BPIFB4 (n=3); Empty. AVG Signal: average of fluorescence signals of HEK293T transfected with empty vector (n=3); FC: fold change; Exosome: RNA detected by de Jong et al.[28] in exosomes produced by endothelial cells under stress conditions. Only genes with *P*-value < 0.001 are indicated in the table.

Online Table V. Comparison of HEK293T cell transcriptional profiles after transfection with LAV-BPIFB4 or WT-BPIFB4

Gene	LAV.AVG_Signal	WT.AVG_Signal	FC	*P*-value	Regulation	Exosome
LOC648852	1625.567	793.333	1.035	<0.001	Up	yes
MIR1974	1029.433	589.2	0.805	<0.001	Up	yes
LOC100132673	8167.1	4837.867	0.755	<0.001	Up	yes
HS.163752	1896.833	1141.267	0.733	<0.001	Up	no
LOC100131713	6172.983	10548.7	-0.773	<0.001	Down	yes

LAV.AVG Signal: average of fluorescence signals of HEK293T transfected with vector encoding for LAV-BPIFB4 (n=3); WTAVG Signal: average of fluorescence signals of HEK293T transfected with vector encoding for WT-BPIFB4 (n=3); FC: fold change; Exosome: RNA detected by de Jong et al.[28] in exosomes produced by endothelial cells under stress conditions. Only genes with *P*-value < 0.001 are indicated in the table.

Online Table VI. *P*-values generated by the comparison of the transcriptional profiles for ribosomal, translational, and exosomal categories.

Comparison	Total # genes	Ribosome		Translation		Exosome	
		# genes	*P*-value	# genes	*P-value*	# genes	*P*-value
WT_Empty	1558	72	2.00E-14	77	4.83E-07	462	<1.00E-11
LAV_Empty	2291	85	2.87E-09	78	0.02	621	<1.00E-11
LAV_WT	816	32	7.50E-05	37	0.001	300	<1.00E-11

Total # genes: total number of modulated genes for the respective comparison; # genes: number of modulated genes for the respective comparison in the indicated category.

Online Table VII. GO categories for ribosome and translation

ribosome	
ribosomal small subunit biogenesis	biological_process
organellar large ribosomal subunit	cellular_component
organellar ribosome	cellular_component
cytosolic ribosome	cellular_component
large ribosomal subunit	cellular_component
structural constituent of ribosome	molecular_function
mature ribosome assembly	biological_process
ribosome biogenesis	biological_process
mitochondrial ribosome	cellular_component
ribosome	cellular_component
cytosolic small ribosomal subunit	cellular_component
small ribosomal subunit	cellular_component
cytosolic large ribosomal subunit	cellular_component
mitochondrial large ribosomal subunit	cellular_component
ribosomal subunit	cellular_component
organellar small ribosomal subunit	cellular_component
mitochondrial small ribosomal subunit	cellular_component
ribosomal large subunit biogenesis	biological_process

translation	
translational elongation	biological_process
translation	biological_process
translational initiation	biological_process
cotranslational protein targeting to membrane	biological_process
translational termination	biological_process
SRP-dependent cotranslational protein targeting to membrane	biological_process

Online Table VIII. Capillary density values

Vehicle											
section	**cage number (sequence mouse number)**										
	E1 (1)	**E2 (2)**	**E3 (3)**	**E4 (4)**	**E5 (5)**	**I3 (8)**	**I5 (10)**				
1	933.927	417.526	629.501	940.498	1253.421	784.378	1189.772				
2	534.76	492.348	725.97	491.27	990.123	904.101	893.83				
3	847.806	492.248	424.717	1014.139	1284.985	297.734	356.245				
4	858.771	745.385	467.191	432.308	1178.67	976.358	895.904				
5	733.411	674.779	785.207	131.423	1015.569	1061.318	1422.481				
6	589.335	374.643	699.76	533.982	855.53	1516.8	979.191				
7	252.7	735.34	600.003	918.48	1061.758	829.71	1092.182				
8	263.139	394.141	751.368	409.022	908.463	1197.117	1782.812				
9	204.725	457.735	827.846	840.393	853.476	1429.76	1543.926				
10	272.293	703.798	639.359	1526.879	721.679	979.313	933.409	**Mean**			
Means	549.087	548.794	655.092	723.839	1012.367	997.659	1108.975	**799.402**			

WT											
section	**cage number (sequence mouse number)**										
	G1 (1)	**G2 (2)**	**G3 (3)**	**G4 (4)**	**G5 (5)**	**K1 (6)**	**K2 (7)**	**K3 (8)**	**K4 (9)**	**K5 (10)**	
1	1075.372	778.469	633.559	1350.421	353.931	1277.027	920.691	368.298	399.242	645.129	
2	720.259	780.805	1177.509	711.703	722.327	552.915	753.504	749.555	515.065	666.64	
3	537.545	1227.233	506.912	782.636	606.483	560.957	642.205	350.027	220.406	80.861	
4	1286.197	1166.881	537.01	902.349	868.445	443.815	165.807	249.114	217.04	229.63	
5	1066.642	1156.438	1018.822	784.955	752.892	486.189	744.027	267.334	522.417	243.26	
6	1397.316	757.3	924.569	1212.149	559.027	556.119	976.956	290.216	565.096	420.109	
7	1095.653	770.232	1090.49	780.961	541.665	323.417	745.826	721.242	547.289	500.105	
8	905.076	675.261	845.47	697.009	933.395	760.706	479.028	404.003	595.461	546.625	
9	988.7	585.762	587.485	664.291	1082.285	1074.752	1001.76	1033.55	610.825	671.359	
10	772.944	775.836	951.611	706.367	741.237	1066.436	989.688	858.085	505.245	527.463	**Mean**
Means	984.570	867.422	827.344	859.284	716.169	710.233	741.95	529.143	469.809	453.118	**715.904**

LAV											
section	**cage number (sequence mouse number)**										
	F1 (1)	**F2 (2)**	**F5 (5)**	**J1 (6)**	**J2 (7)**	**J3 (8)**	**J5 (10)**				
1	417.329	1496.725	812.613	927.834	926.475	1048.525	904.747				
2	518.349	1023.32	957.99	474.512	813.301	1051.325	988.506				
3	589.384	1428.239	995.801	771.618	564.556	854.102	1271.395				
4	443.706	1150.827	780.886	1062.171	882.959	1046.717	959.946				
5	806.646	1268.649	715.626	1105.729	737.713	826.769	865.552				
6	1227.058	1132.843	826.744	775.295	803.885	591.252	1132.997				
7	1206.071	901.684	1015.68	1018.394	1251.181	758.848	1186.716				
8	867.688	932.133	1085.473	968.39	1044.566	423.642	1026.097				
9	699.105	1138.702	823.984	1279.175	718.023	956.728	1055.469				
10	970.825	1356.429	675.182	1228.665	650.524	1253.381	1038.567	**Mean**			
Means	774.616	1182.955	868.998	961.178	839.318	881.129	1042.999	**935.885**			

Online Table IX. Arteriole density values

Vehicle											
section	**cage number (sequence mouse number)**										
	E1 (1)	**E2 (2)**	**E3 (3)**	**E4 (4)**	**E5 (5)**	**I3 (8)**	**I5 (10)**				
1	9.019	4.45	11.66	4.071	1.95	4.765	15.19				
2	2.962	6.047	1.667	4.476	4.237	8.408	4.488				
3	0	0	3.136	5.161	6.258	5.607	1.427				
4	0	8.021	1.795	8.307	0	3.57	0				
5	3.732	1.46	0	8.735	4.396	3.387	4.185				
6	3.363	4.15	1.401	0	0	0	0				
7	1.762	8.027	2.789	0	0	1.594	5.609				
8	1.598	9.516	2.978	3.144	4.025	3.607	4.145				
9	1.482	6.014	6.406	0	0	6.567	0				
10	9.861	7.984	1.745	1.904	5.364	5.269	4.837	**Mean**			
Means	3.378	5.567	3.358	3.58	2.623	4.277	3.988	**3.824**			

WT											
section	**cage number (sequence mouse number)**										
	G1 (1)	**G2 (2)**	**G3 (3)**	**G4 (4)**	**G5 (5)**	**K1 (6)**	**K2 (7)**	**K3 (8)**	**K4 (9)**	**K5 (10)**	
1	3.045	0	4.709	2.734	5.924	4.624	4.523	5.335	1.474	17.356	
2	8.943	0	5.59	0	6.327	3.253	0	15.343	6.466	7.215	
3	8.932	1.65	9.28	0	2.687	2.934	0	14.382	2.964	16.612	
4	1.693	4.708	3.428	4.144	0	0	3.903	10.826	9.908	15.262	
5	0	0	5.379	5.039	4.573	8.175	6.609	13.606	0	13.998	
6	0	0	6.354	0	2.924	0	1.426	7.805	1.662	16.325	
7	3.438	1.747	2.933	0	4.567	0	0	6.625	7.691	13.454	
8	3.514	5.373	6.305	4.038	4.625	14.507	0	16.188	8.738	18.848	
9	1.79	7.879	5.186	8.568	7.72	7.427	1.886	7.345	8.584	2.974	
10	1.842	0	6.04	3.8	5.877	4.858	1.775	2.762	9.061	1.182	**Mean**
Means	3.32	2.136	5.521	2.832	4.522	4.578	2.012	10.022	5.655	12.321	**5.292**

LAV											
section	**cage number (sequence mouse number)**										
	F1 (1)	**F2 (2)**	**F5 (5)**	**J1 (6)**	**J2 (7)**	**J3 (8)**	**J5 (10)**				
1	0	16.222	8.408	3.926	13.774	18.986	8.379				
2	4.8	10.908	3.608	3.372	13.798	17.836	5.772				
3	0	11.916	7.325	1.651	14.563	6.918	3.069				
4	0	27.964	4.693	0	13.041	20.533	3.144				
5	2.284	25.598	9.725	6.883	6.615	21.306	1.369				
6	0	16.696	8.896	11.526	17.138	19.01	3.005				
7	3.521	11.54	7.019	3.519	5.566	23.049	3.99				
8	4.497	19.325	7.641	0	11.134	20.743	1.475				
9	6.751	21.024	8.254	6.691	13.355	6.056	6.76				
10	0	21.127	13.043	7.628	13.612	7.565	6.563	**Mean**			
Means	2.185	18.232	7.861	4.519	12.26	16.2	4.353	**9.373**			

SUPPLEMENTAL REFERENCES

1. Malovini A, Illario M, Iaccarino G, Villa F, Ferrario A, Roncarati R, Anselmi CV, Novelli V, Cipolletta E, Leggiero E, Orro A, Rusciano MR, Milanesi L, Maione AS, Condorelli G, Bellazzi R, Puca AA. Association study on long-living individuals from Southern Italy identifies rs10491334 in the CAMKIV gene that regulates survival proteins. *Rejuvenation Res.* 2011;14:283-291.

2. Nebel A, Kleindorp R, Caliebe A, Nothnagel M, Blanche H, Junge O, Wittig M, Ellinghaus D, Flachsbart F, Wichmann HE, Meitinger T, Nikolaus S, Franke A, Krawczak M, Lathrop M, Schreiber S. A genome-wide association study confirms APOE as the major gene influencing survival in long-lived individuals. *Mech Ageing Dev.* 2011;132:324-330.

3. Novelli V, Viviani Anselmi C, Roncarati R, Guffanti G, Malovini A, Piluso G, Puca AA. Lack of replication of genetic associations with human longevity. *Biogerontology.* 2008;9:85-92.

4. Geesaman BJ, Benson E, Brewster SJ, Kunkel LM, Blanche H, Thomas G, Perls TT, Daly MJ, Puca AA. Haplotype-based identification of a microsomal transfer protein marker associated with the human lifespan. *Proc Natl Acad Sci U S A.* 2003;100:14115-14120.

5. Spinetti G, Fortunato O, Caporali A, Shantikumar S, Marchetti M, Meloni M, Descamps B, Floris I, Sangalli E, Vono R, Faglia E, Specchia C, Pintus G, Madeddu P, Emanueli C. MicroRNA-15a and microRNA-16 impair human circulating proangiogenic cell functions and are increased in the proangiogenic cells and serum of patients with critical limb ischemia. *Circ Res.*112:335-346.

6. Spinetti G, Cordella D, Fortunato O, Sangalli E, Losa S, Gotti A, Carnelli F, Rosa F, Riboldi S, Sessa F, Avolio E, Beltrami AP, Emanueli C, Madeddu P. Global remodeling of the vascular stem cell niche in bone marrow of diabetic patients: implication of the microRNA-155/FOXO3a signaling pathway. *Circ Res.* 2013;112:510-522.

7. Bingle CD, Seal RL, Craven CJ. Systematic nomenclature for the PLUNC/PSP/BSP30/SMGB proteins as a subfamily of the BPI fold-containing superfamily. *Biochem Soc Trans.* 2011;39:977-983.

8. Andrault JB, Gaillard I, Giorgi D, Rouquier S. Expansion of the BPI family by duplication on human chromosome 20: characterization of the RY gene cluster in 20q11.21 encoding olfactory transporters/antimicrobial-like peptides. *Genomics.* 2003;82:172-184.

9. Cali G, Gentile F, Mogavero S, Pallante P, Nitsch R, Ciancia G, Ferraro A, Fusco A, Nitsch L. CDH16/Ksp-cadherin is expressed in the developing thyroid gland and is strongly down-regulated in thyroid carcinomas. *Endocrinology.* 2012;153:522-534.

10. Spinetti G, Fortunato O, Cordella D, Portararo P, Krankel N, Katare R, Sala-Newby GB, Richer C, Vincent MP, Alhenc-Gelas F, Tonolo G, Cherchi S, Emanueli C, Madeddu P. Tissue kallikrein is essential for invasive capacity of circulating proangiogenic cells. *Circ Res.* 2011;108:284-293.

11. Urbich C, Dimmeler S. Endothelial progenitor cells: characterization and role in vascular biology. *Circ Res.* 2004;95:343-353.

12. Urbich C, Dimmeler S. Endothelial progenitor cells functional characterization. *Trends Cardiovasc Med.* 2004;14:318-322.

13. Krankel N, Katare RG, Siragusa M, Barcelos LS, Campagnolo P, Mangialardi G, Fortunato O, Spinetti G, Tran N, Zacharowski K, Wojakowski W, Mroz I, Herman A, Manning Fox JE, MacDonald PE, Schanstra JP, Bascands JL, Ascione R, Angelini G, Emanueli C, Madeddu P. Role of kinin B2 receptor signaling in the recruitment of circulating progenitor cells with neovascularization potential. *Circ Res.* 2008;103:1335-1343.

14. Vecchione C, Patrucco E, Marino G, Barberis L, Poulet R, Aretini A, Maffei A, Gentile MT, Storto M, Azzolino O, Brancaccio M, Colussi GL, Bettarini U, Altruda F, Silengo L, Tarone G, Wymann MP, Hirsch E, Lembo G. Protection from angiotensin II-mediated vasculotoxic and hypertensive response in mice lacking PI3Kgamma. *J Exp Med.* 2005;201:1217-1228.

15. Vecchione C, Aretini A, Marino G, Bettarini U, Poulet R, Maffei A, Sbroggio M, Pastore L, Gentile MT, Notte A, Iorio L, Hirsch E, Tarone G, Lembo G. Selective Rac-1 inhibition protects from diabetes-induced vascular injury. *Circ Res.* 2006;98:218-225.

16. Zacchigna L, Vecchione C, Notte A, Cordenonsi M, Dupont S, Maretto S, Cifelli G, Ferrari A, Maffei A, Fabbro C, Braghetta P, Marino G, Selvetella G, Aretini A, Colonnese C, Bettarini U, Russo G, Soligo S, Adorno M, Bonaldo P, Volpin D, Piccolo S, Lembo G, Bressan GM. Emilin1 links TGF-beta maturation to blood pressure homeostasis. *Cell.* 2006;124:929-942.

17. Zhang Y, Chirmule N, Gao G, Wilson J. CD40 ligand-dependent activation of cytotoxic T lymphocytes by adeno-associated virus vectors in vivo: role of immature dendritic cells. *J Virol.* 2000;74:8003-8010.

18. Gao G, Vandenberghe LH, Alvira MR, Lu Y, Calcedo R, Zhou X, Wilson JM. Clades of Adeno-associated viruses are widely disseminated in human tissues. *J Virol.* 2004;78(12):6381-6388.

19. Auricchio A, Hildinger M, O'Connor E, Gao GP, Wilson JM. Isolation of highly infectious and pure adeno-associated virus type 2 vectors with a single-step gravity-flow column. *Hum Gene Ther.* 2001;12:71-76.

20. Doria M, Ferrara A, Auricchio A. AAV2/8 vectors purified from culture medium with a simple and rapid protocol transduce murine liver, muscle, and retina efficiently. *Hum Gene Ther Methods.* 2013;24:392-398.

21. Nelson DM, Wahlfors JJ, Chen L, Onodera M, Morgan RA. Characterization of diverse viral vector preparations, using a simple and rapid whole-virion dot-blot method. *Hum Gene Ther.* 1998;9:2401-2405.

22. R Development Core Team. *R: A language and environment for statistical computing*. Vienna, Austria: R Foundation for Statistical Computing; 2009.

23. Ferrario A, Villa F, Malovini A, Araniti F, Puca AA. The application of genetics approaches to the study of exceptional longevity in humans: potential and limitations. *Immun Ageing.* 2012;9:7.

24. Purcell S, Neale B, Todd-Brown K, Thomas L, Ferreira MA, Bender D, Maller J, Sklar P, de Bakker PI, Daly MJ, Sham PC. PLINK: a tool set for whole-genome association and population-based linkage analyses. *Am J Hum Genet.* 2007;81:559-575.

25. Schmittgen TD, Livak KJ. Analyzing real-time PCR data by the comparative C(T) method. *Nat Protoc.* 2008;3:1101-1108.

26. Tusher VG, Tibshirani R, Chu G. Significance analysis of microarrays applied to the ionizing radiation response. *Proc Natl Acad Sci U S A.* 2001;98:5116-5121.

27. Kiss T, Fayet-Lebaron E, Jady BE. Box H/ACA small ribonucleoproteins. *Mol Cell.*37:597-606.

28. de Jong OG, Verhaar MC, Chen Y, Vader P, Gremmels H, Posthuma G, Schiffelers RM, Gucek M, van Balkom BW. Cellular stress conditions are reflected in the protein and RNA content of endothelial cell-derived exosomes. *J Extracell Vesicles.*1.

29. Sekiguchi F, Nakahira T, Kawata K, Sunano S. Responses to endothelium-derived factors and their interaction in mesenteric arteries from Wistar-Kyoto and stroke-prone spontaneously hypertensive rats. *Clin Exp Pharmacol Physiol.* 2002;29:1066-1074.

Chapter 3. Discussion

3.1 Summary

In this thesis, I show that the polymorphic variant rs2070325 (Ile229Val) in bactericidal/permeability-increasing fold-containing-family-B-member-4 (*BPIFB4*) associates with exceptional longevity, under a recessive genetic model, in three independent populations. Moreover, the expression of BPIFB4 is instrumental to maintenance of cellular and vascular homeostasis through regulation of protein synthesis. In isolated vessels, BPIFB4 is up-regulated by mechanical stress, and its knock-down inhibits endothelium-dependent vasorelaxation. In hypertensive rats and as well as old mice, gene transfer of longevity associated variant (LAV) of BPIFB4 restores eNOS signaling, rescues endothelial dysfunction, and reduces blood pressure levels. Furthermore, BPIFB4 is implicated in vascular repair: in a murine model of peripheral ischemia, systemic gene therapy with LAV-BPIFB4 promotes the recruitment of hematopoietic stem cells, reparative vascularization, and reperfusion of the ischemic muscle. Ultimately, LAV-BPIFB4 may represent a novel therapeutic tool to fight endothelial dysfunction and promote vascular reparative processes.

3.2 Conclusions

Recent landmark studies have significantly improved our understanding of the genetic determinants of slow aging.[1-3] Unfortunately, only apolipoprotein E (APOE) ε4 has reached the

penalizing genome-wide threshold of significance to date.[4] Therefore, in order to identify genes and genetic variants that influence human health through interaction with environmental factors, alternative approaches are needed, such as multistage study designs aimed at reducing the statistical penalty.[4-7] In line with this, the present study adopted a combination of a multistage genetic and functional approach to investigate if a candidate gene, i.e., BPIFB4, is associated with exceptional longevity. Our findings strongly indicate the pivotal role of BPIFB4 in preserving the ability to activate an adaptive stress response and proteostasis, two physiological processes negatively affected by aging.[8]

BPIFB4 belongs to the superfamily of bactericidal BPI/PLUNC proteins, which are central to the host innate immune response against bacteria in regions of significant bacterial exposure, like the mouth, nose and lungs. The expression of the activity-enhanced polymorphic variant LAV-BPIFB4 might initially produce privileged survival through better resistance to infectious diseases. The variant may offer additional advantages because of its ability to activate the NO-releasing enzyme eNOS. NO and peroxynitrite, which is generated by the interaction of NO with $O2^{-}$ during the respiratory burst, are mediators of the bactericidal effects of macrophages through inactivation of heme-containing enzymes, including cytochrome oxidases and cytochrome P450. Interestingly, development and refining of this prosurvival mechanism has facilitated exceptional longevity by ensuring better adaptation to stress conditions through improved function of ribosomal biogenesis, protein synthesis and cardiovascular homeostasis.

Data from gene arrays of HEK293T cells indicate that BPIFB4 activates adaptive stress responses and proteostasis, two key aspects for improved organism survival,[9] as well as stem cell maintenance.[10] Analysis of BPIFB4's sequence revealed a phosphorylation site for PERK, which is a further link between BPIFB4 and the stress response. A key element that makes LAV-BPIFB4 uniquely suited to confer physiological advantages is its peculiar ability to be superiorly phosphorylated by PERK and, thereby recruit the eNOS-activating factor HSP90. Although both LAV-BPIFB4 and WT-BPIFB4 can form an activated complex with HSP90, only LAV-BPIFB4 is capable of making this complex more productive for eNOS activation through post-transcriptional modulation by 14-3-3. In this regard, BPIFB4 sequence analysis revealed an atypical 14-3-3 binding site. Thus, 14-3-3 may modulate BPIFB4-mediated cell signaling by binding and retaining the latter within the cytoplasm on the basis of its phosphorylation status at serine 75. In fact, immunoprecipitation and confocal microscopy studies showed the LAV-BPIFB4 complexes efficiently with 14-3-3, a phenomenon that apparently did not occur with WT-BPIFB4. In support of the importance of PERK-mediated phosphorylation at serine 75, and of serine 82 for LAV-BPIFB4's binding to 14-3-3, LAV-BPIFB4$^{mut14\text{-}3\text{-}3}$, LAV-BPIFB4^{mutPERK} or LAV-BPIFB4 with GSK2606414 (PERK inhibitor) failed to immunoprecipitate 14-3-3.

A landmark finding of this study is the recognition that BPIFB4 plays a crucial role in maintenance of vascular homeostasis and that LAV-BPIFB4 exerts extra-protection. We show that biomechanical stress due to increased arterial pressure upregulates BPIFB4 expression, and

that BPIFB4 silencing induces eNOS/endothelial dysfunction. Moreover, we found that LAV-BPIFB4 potentiated eNOS signaling in mouse vessels. In line with cellular data, studies in isolated vessels showed that the LAV-BPIFB4/HSP90 complex was dependent on PERK phosphorylation and 14-3-3 binding, with endothelial dysfunction ensuing upon transfection of vessels with LAV-BPIFB4$^{mut14\text{-}3\text{-}3}$, LAV-BPIFB4^{mutPERK} or LAV-BPIFB4 with GSK2606414. Similarly, WT-BPIFB4 binds to HSP90 and modulates endothelial function through a 14-3-3-mediated mechanism, as shown by mutagenesis of serine 82 (WT-BPIFB4$^{mut14\text{-}3\text{-}3}$). However, LAV-BPIFB4 may have a more potent vasculoprotective effect because of its increased ability to bind 14-3-3.

Endothelial dysfunction is a systemic pathological state characterized by a reduction in the bioavailability of and/or responsiveness to vasodilators, and altered vascular wall metabolism. Because of its major causal role in cardiovascular diseases, such as hypertension and ischemia, therapeutic agents that restore endothelial function are of clinical interest. In this context, a body of evidence pinpoints eNOS as a major player in blood pressure homeostasis and eNOS downregulation as a hallmark of cardiovascular disease.[11] Hence, we evaluated the effect of LAV-BPIFB4 in a rat model of essential hypertension characterized by impaired endothelial function. The *in vivo* administration of LAV-BPIFB4 normalized blood pressure levels and endothelial function in genetically hypertensive rats, without influencing vascular remodeling.

It is well known that cardiovascular risk is markedly increased in aged individuals. Our results show the association of dysfunctional endothelial-dependent vasorelaxation, reduced eNOS phosphorylation and BPIFB4 downregulation in old mice. Importantly, we also newly demonstrate that forced BPIFB4 expression by AAV-LAV-BPIFB4 restores endothelium-dependent vasorelaxation, eNOS phosphorylation and reduces blood pressure levels in old mice.

These results strongly candidate LAV-BPIFB4 as new therapeutic agent able to enhance endothelial NO release and reduce high blood pressure levels. We also recorded the higher expression of *BPIFB4* in the $CD34^+$ cells of LLIs and the absence of migration ability in EPCs after SDF-1 stimulation in the absence of BPIFB4. Thus, high levels of BPIFB4 could protect LLIs by improving revascularization, a process dependent on the migration ability of EPCs.[12] In line, in a mouse model of hindlimb ischemia, LAV-BPIFB4 exerted a beneficial effect, significantly increasing homing of progenitor cells, enhancing blood flow and spontaneous revascularization in the affected limb. Of note, only the LAV isoform confers substantial protection from acute ischemia through potentiation of vascular repair, which is associated with activation of VEGF and SOD3 in ischemic skeletal muscles, suggesting a role of pro-angiogenic and ROS scavenging mechanisms. More studies are needed to clarify the role of the effect of blood pressure lowering on this vascular phenotype.

In conclusion, BPIFB4 is a multitasking protein involved in processes that are important for cellular and organism homeostasis, and whose role in modulating eNOS is potentiated by the variations harbored by

the LAV isoform. We have unraveled the molecular determinants linking functional vasculature responses, endothelial function and a specific genetic trait, and have identified BPIFB4 as a potential tool for innovative therapeutic strategies for aging, vascular repair and endothelial dysfunction.

Finally, we have found that genetic traits enriched in centenarians might be exploited to combat and attenuate cardiovascular disease at earlier stages of life. Thus, investigating exceptional longevity could bestow us with new knowledge instrumental to extending a clinical benefit to the population at large.

3.3 Future perspectives

The way toward a pharmacology of aging still follows the perception of the discovery of a drug mimetic of dietary restriction (DR). Many populations have healthy food behaviors with a correct intake of nutritional elements. Where this concept of nutrition is unknown, it could be important to develop a substance able to perturb metabolism and cellular homeostasis and induce effects similar to the ones we encountered in our study. The final goal could be the extension of life span, but this could be considered a side effect. The real goal, instead, is the achievement of the old age through an healthy ageing process.

In 2009 a report of Harrison et al.[13] it's been showed that rapamycin was able to extend the life span of mice and this result was achieved in study with different animal models and different rapamycin protocols or similar drugs, called rapalogs. Rapamycin has a specific pharmacological target: the inhibition of mTORC1.[14, 15] mTORC1

controls protein translation and autophagy and rapamycin is able to reduce the first and increase the second, in cells or multicellular organisms.[16]

The improvement of lifespan in vivo, studied in experiment with *Drosophila* and mice, is linked to the inhibition of the downstream effector p70-S6K.[17, 13]

Another important molecule with an effect on life span is Metformin. This is an antidiabetic drug that has been shown to extend life span in *C. elegans* and mice, but not in *Drosophila*.[18] The increment in life span is associated with a reduction of cholesterol levels (total cholesterol and LDL), an improvement of glucose tolerance an increment of antioxidant defense, and a reduction of markers of inflammation. The molecular studies on metformin effects showed that this drugs perturb AMPK pathway, with an activation profile similar to that observed in animals under DR.[19]

The healthy aging could be achieved also through antioxidant treatments. It has been shown that molecules that promotes stress resistance, and in particular oxidative stress resistance, could also increase life span, for example in *C. elegans* where *sod-2* modulation[20, 21] are been measured.

In the last years, the studies about the research of a DR mimetic converged on a plant derived molecule: resveratrol. It's a stress-response lipophilic polyphenol obtainable from grapevine plants and its derivates, such as wine, and it's responsible for a wide-range of health-promoting benefits.[22-24] The resveratrol molecular pathway involved Sirtuins, a group of histone deacetylases responsible for the control of gene expression[23, 25] that is activated by resveratrol with a

life-span increasing effect in *C. elegans* and in mice treated with a high caloric diet.[26] Recently studies suggest that resveratrol might have some beneficial effects on healthy ageing.[25, 27]

Until today, none of the known antiaging therapy is been tested in human, except for caloric restriction. Also in our case, we are interested in healthspan more than lifespan. Indeed, speaking about a therapy against the age-related diseases, it's important to understand when it's better to start a treatment that could reduce or delay the effects of ageing on a particular body district. For this point, the anamnestic analysis of subject and his family is fundamental, but these data should be crossed with the knowledge on the statistic of age of onset of age-related disturbs. On the basis of these data (risk factor) the subject could begin a particular treatment or more than one. Indeed, in these last years, a group of scientists have projected a "polypill" composed by different drugs able to fight against aging or maybe only against the symptoms generated by age-related disorders. They proposed the combination of a cholesterol lowering drug (a statin), three drugs for the treatment of blood pressure (each at half-standard dose), folic acid and aspirin.[28-30]

The incredible results obtained through the administration of Adeno-Associated Viral vectors carrying the LAV isoform of BPIFB4 in mouse and rat models encourage and force us to walk the very important and very expensive step toward the clinical trials. Viral mediated gene therapy could represent a realistic and nearby achievement and maybe it's suitable for a longer and more performing solution of age-related diseases. The road to the administration and the perfecting of the recombinant protein is better for a pharmacological

and industrial aspect but it requires an enormous technical and economic support.

References

1. Willcox BJ, Donlon TA, He Q, Chen R, Grove JS, Yano K et al. FOXO3A genotype is strongly associated with human longevity. Proc Natl Acad Sci U S A. 2008;105(37):13987-92. doi:10.1073/pnas.0801030105.

2. Schachter F, Faure-Delanef L, Guenot F, Rouger H, Froguel P, Lesueur-Ginot L et al. Genetic associations with human longevity at the APOE and ACE loci. Nat Genet. 1994;6(1):29-32. doi:10.1038/ng0194-29.

3. Flachsbart F, Caliebe A, Kleindorp R, Blanche H, von Eller-Eberstein H, Nikolaus S et al. Association of FOXO3A variation with human longevity confirmed in German centenarians. Proc Natl Acad Sci U S A. 2009;106(8):2700-5. doi:10.1073/pnas.0809594106.

4. Nebel A, Kleindorp R, Caliebe A, Nothnagel M, Blanche H, Junge O et al. A genome-wide association study confirms APOE as the major gene influencing survival in long-lived individuals. Mech Ageing Dev. 2011;132(6-7):324-30. doi:10.1016/j.mad.2011.06.008.

5. Novelli V, Viviani Anselmi C, Roncarati R, Guffanti G, Malovini A, Piluso G et al. Lack of replication of genetic associations with human longevity. Biogerontology. 2008;9(2):85-92. doi:10.1007/s10522-007-9116-4.

6. Sebastiani P, Timofeev N, Dworkis DA, Perls TT, Steinberg MH. Genome-wide association studies and the genetic dissection of complex traits. Am J Hematol. 2009;84(8):504-15. doi:10.1002/ajh.21440.

7. Ferrario A, Villa F, Malovini A, Araniti F, Puca AA. The application of genetics approaches to the study of exceptional longevity in humans: potential and limitations. Immun Ageing. 2012;9(1):7. doi:1742-4933-9-7 [pii] 10.1186/1742-4933-9-7.

8. Rando TA. Stem cells, ageing and the quest for immortality. Nature. 2006;441(7097):1080-6. doi:nature04958 [pii] 10.1038/nature04958.

9. Nisoli E, Tonello C, Cardile A, Cozzi V, Bracale R, Tedesco L et al. Calorie restriction promotes mitochondrial biogenesis by inducing the expression of eNOS. Science. 2005;310(5746):314-7. doi:10.1126/science.1117728.

10. Vilchez D, Simic MS, Dillin A. Proteostasis and aging of stem cells. Trends Cell Biol.24(3):161-70. doi:S0962-8924(13)00154-2 [pii] 10.1016/j.tcb.2013.09.002.

11. Hu Z, Xiong Y, Han X, Geng C, Jiang B, Huo Y et al. Acute mechanical stretch promotes eNOS activation in venous endothelial cells mainly via PKA and Akt pathways. PLoS One. 2013;8(8):e71359. doi:10.1371/journal.pone.0071359.

12. Asahara T, Murohara T, Sullivan A, Silver M, van der Zee R, Li T et al. Isolation of putative progenitor endothelial cells for angiogenesis. Science. 1997;275(5302):964-7.

13. Harrison DE, Strong R, Sharp ZD, Nelson JF, Astle CM, Flurkey K et al. Rapamycin fed late in life extends lifespan in genetically heterogeneous mice. Nature. 2009;460(7253):392-5. doi:nature08221 [pii] 10.1038/nature08221.

14. Wullschleger S, Loewith R, Hall MN. TOR signaling in growth and metabolism. Cell. 2006;124(3):471-84. doi:S0092-8674(06)00108-5 [pii] 10.1016/j.cell.2006.01.016.

15. Zoncu R, Efeyan A, Sabatini DM. mTOR: from growth signal integration to cancer, diabetes and ageing. Nat Rev Mol Cell Biol.12(1):21-35. doi:nrm3025 [pii] 10.1038/nrm3025.

16. Bjedov I, Partridge L. A longer and healthier life with TOR down-regulation: genetics and drugs. Biochem Soc Trans.39(2):460-5. doi:BST0390460 [pii] 10.1042/BST0390460.

17. Bjedov I, Toivonen JM, Kerr F, Slack C, Jacobson J, Foley A et al. Mechanisms of life span extension by rapamycin in the fruit fly

Drosophila melanogaster. Cell Metab.11(1):35-46. doi:S1550-4131(09)00374-X [pii] 10.1016/j.cmet.2009.11.010.

18. Slack C, Foley A, Partridge L. Activation of AMPK by the putative dietary restriction mimetic metformin is insufficient to extend lifespan in Drosophila. PLoS One.7(10):e47699. doi:10.1371/journal.pone.0047699 PONE-D-12-18554 [pii].

19. Martin-Montalvo A, Mercken EM, Mitchell SJ, Palacios HH, Mote PL, Scheibye-Knudsen M et al. Metformin improves healthspan and lifespan in mice. Nat Commun.4:2192. doi:ncomms3192 [pii] 10.1038/ncomms3192.

20. Cabreiro F, Ackerman D, Doonan R, Araiz C, Back P, Papp D et al. Increased life span from overexpression of superoxide dismutase in Caenorhabditis elegans is not caused by decreased oxidative damage. Free Radic Biol Med.51(8):1575-82. doi:S0891-5849(11)00473-4 [pii] 10.1016/j.freeradbiomed.2011.07.020.

21. Van Raamsdonk JM, Hekimi S. Deletion of the mitochondrial superoxide dismutase sod-2 extends lifespan in Caenorhabditis elegans. PLoS Genet. 2009;5(2):e1000361. doi:10.1371/journal.pgen.1000361.

22. Chachay VS, Kirkpatrick CM, Hickman IJ, Ferguson M, Prins JB, Martin JH. Resveratrol--pills to replace a healthy diet? Br J Clin Pharmacol.72(1):27-38. doi:10.1111/j.1365-2125.2011.03966.x.

23. de Cabo R, Carmona-Gutierrez D, Bernier M, Hall MN, Madeo F. The search for antiaging interventions: from elixirs to fasting regimens. Cell.157(7):1515-26. doi:S0092-8674(14)00679-5 [pii] 10.1016/j.cell.2014.05.031.

24. Timmers S, Auwerx J, Schrauwen P. The journey of resveratrol from yeast to human. Aging (Albany NY).4(3):146-58. doi:100445 [pii].

25. Novelle MG, Wahl D, Dieguez C, Bernier M, de Cabo R. Resveratrol supplementation: Where are we now and where should we go? Ageing Res Rev.21:1-15. doi:S1568-1637(15)00004-5 [pii] 10.1016/j.arr.2015.01.002.

26. Baur JA, Pearson KJ, Price NL, Jamieson HA, Lerin C, Kalra A et al. Resveratrol improves health and survival of mice on a high-calorie diet. Nature. 2006;444(7117):337-42. doi:nature05354 [pii] 10.1038/nature05354.

27. Park EJ, Pezzuto JM. The pharmacology of resveratrol in animals and humans. Biochim Biophys Acta.1852(6):1071-113. doi:S0925-4439(15)00023-X [pii] 10.1016/j.bbadis.2015.01.014.

28. Gems D. What is an anti-aging treatment? Exp Gerontol.58:14-8. doi:S0531-5565(14)00208-3 [pii] 10.1016/j.exger.2014.07.003.

29. Le Couteur DG, McLachlan AJ, Quinn RJ, Simpson SJ, de Cabo R. Aging biology and novel targets for drug discovery. J Gerontol A Biol Sci Med Sci.67(2):168-74. doi:glr095 [pii] 10.1093/gerona/glr095.

30. Wald NJ, Law MR. A strategy to reduce cardiovascular disease by more than 80%. BMJ. 2003;326(7404):1419. doi:10.1136/bmj.326.7404.1419 326/7404/1419 [pii].

Publications

Serum BPIFB4 levels predict health status in long-living individuals
Villa F, Malovini A, Carrizzo A, Spinelli CC, Ferrario A, Maciąg A, Madonna M, Bellazzi R, Milanesi L, Vecchione C, Puca AA.
Immun Ageing - submitted

Genetic Analysis Reveals a Longevity-Associated Protein Modulating Endothelial Function and Angiogenesis.
Villa F, Carrizzo A, Spinelli CC, Ferrario A, Malovini A, Maciąg A, Damato A, Auricchio A, Spinetti G, Sangalli E, Dang Z, Madonna M, Ambrosio M, Sitia L, Bigini P, Calì G, Schreiber S, Perls T, Fucile S, Mulas F, Nebel A, Bellazzi R, Madeddu P, Vecchione C, Puca AA.
Circ Res. 2015 Jul 31;117(4):333-45. doi: 10.1161/CIRCRESAHA.117.305875. Epub 2015 Jun 1.
PMID:26034043

Exome sequencing of a family with lone, autosomal dominant atrial flutter identifies a rare variation in ABCB4 significantly enriched in cases.
Maciąg A, **Villa F**, Ferrario A, Spinelli CC, Carrizzo A, Malovini A, Torella A, Montenero C, Parisi A, Condorelli G, Vecchione C, Nigro V, Montenero AS, Puca AA.
BMC Genet. 2015 Feb 11;16:15. doi: 10.1186/s12863-015-0177-0.
PMID: 25888430

A G613A missense in the Hutchinson's progeria lamin A/C gene causes a lone, autosomal dominant atrioventricular block.
Villa F, Maciąg A, Spinelli CC, Ferrario A, Carrizzo A, Parisi A, Torella A, Montenero C, Condorelli G, Vecchione C, Nigro V, Montenero AS, Puca AA.
Immun Ageing. 2014 Nov 26;11(1):19. doi: 10.1186/s12979-014-0019-3. eCollection 2014.
PMID: 25469153

Polymorphisms of the antiapoptotic protein bag3 may play a role in the pathogenesis of tako-tsubo cardiomyopathy.
Citro R, d'Avenia M, De Marco M, Giudice R, Mirra M, Ravera A, Silverio A, Farina R, Silvestri F, Gravina P, **Villa F**, Puca AA, De Windt L, De Laurenzi V, Bossone E, Turco MC, Piscione F.

Int J Cardiol. 2013 Sep 30;168(2):1663-5. doi: 10.1016/j.ijcard.2013.03.050. Epub 2013 Apr 11. No abstract available.
PMID: 23582692

Vascular ageing: the role of oxidative stress.
Puca AA, Carrizzo A, **Villa F**, Ferrario A, Casaburo M, Maciąg A, Vecchione C.
Int J Biochem Cell Biol. 2013 Mar;45(3):556-9. doi: 10.1016/j.biocel.2012.12.024. Epub 2013 Jan 7. Review.
PMID: 23305730

Endothelial nitric oxide synthase, vascular integrity and human exceptional longevity.
Puca AA, Carrizzo A, Ferrario A, **Villa F**, Vecchione C.
Immun Ageing. 2012 Nov 15;9(1):26. doi: 10.1186/1742-4933-9-26.
PMID: 23153280

The application of genetics approaches to the study of exceptional longevity in humans: potential and limitations.
Ferrario A, **Villa F**, Malovini A, Araniti F, Puca AA.
Immun Ageing. 2012 Apr 23;9(1):7. doi: 10.1186/1742-4933-9-7.
PMID: 22524405

Association study on long-living individuals from Southern Italy identifies rs10491334 in the CAMKIV gene that regulates survival proteins.
Malovini A, Illario M, Iaccarino G, **Villa F**, Ferrario A, Roncarati R, Anselmi CV, Novelli V, Cipolletta E, Leggiero E, Orro A, Rusciano MR, Milanesi L, Maione AS, Condorelli G, Bellazzi R, Puca AA.
Rejuvenation Res. 2011 Jun;14(3):283-91. doi: 10.1089/rej.2010.1114. Epub 2011 May 25.
PMID: 21612516

Association of the FOXO3A locus with extreme longevity in a southern Italian centenarian study.
Anselmi CV, Malovini A, Roncarati R, Novelli V, **Villa F**, Condorelli G, Bellazzi R, Puca AA.
Rejuvenation Res. 2009 Apr;12(2):95-104. doi: 10.1089/rej.2008.0827.
PMID: 19415983